Fouling Dependency of Air in Dairy Processing

by

Erik Lorin

Department of Chemical Engineering
Lund University

May 2018

Supervisor: **PhD Anton Sellberg**
Co-supervisor at Tetra Pak: **PhD Tomas Skoglund**
Examiner: **Professor Bernt Nilsson**

Picture on front page: Armfield modular UHT overview. Photo by Erik Lorin

Postal address	**Visiting address**	**Telephone**
P.O. Box 124	Naturvetarvägen 14	+46 46-222 82 85
SE-221 00 Lund, Sweden		+46 46-222 00 00
Web address		**Telefax**
www.chemeng.lth.se		+46 46-222 45 26

Preface

This master thesis project was performed as a collaboration between Lunds Tekniska Högskola and Tetra Pak. Most of the time was spent on site at Tetra Pak Råbyholm either at the anchoring point of the department Research & Technology (R&T) or at the Product Development Center (PDC) where all runs were conducted.

Initially I would like to thank my examiner Professor Bernt Nilsson at the Department of Chemical Engineering, to whom I without a doubt took my master thesis studies when finding the project. I would also like to thank my supervisor PhD Anton Sellberg and take the time to congratulate him to the newly acquired academic degree.

The department of Research & Technology should receive a thank you for all the good times during the coffee breaks and the warm atmosphere when welcoming a new colleague. A special thanks to my supervisor at Tetra Pak for taking time at any time assisting me throughout my work, PhD Tomas Skoglund who seem to know anything about everything. Also, a big thank you to PhD Anders Göransson who is the platform manager of fouling and cleaning where this project was present.

All employees at the Product Development Center deserve a thank you for the help with welding, ordering and handling of milk and assisting me with process issues. Tetra Pak has got me to appreciate milk again, a product I have not indulged in since high school.

Finally, I would like to thank my partner Anna Fältman for always supporting me during late nights in school or at work and our son, Sixten, for giving me motivation and perspective in life.

Abstract

In this master thesis project, the formation of fouling on heat exchanger surfaces in dairy processing and mainly the influence of air was examined. Based on prior experimental findings regarding the influence of air bubbles in combination with calculations based on solubility properties of air in milk, a hypothesis was stated. Milk can enter the processing system without any undissolved air, with altered equilibrium due to change in temperature and pressure the solubility can decrease. From this phenomenon, air bubbles can be created which are simultaneously filled with steam at the corresponding steam pressure. Assuming the steam is evaporated from the boundary layer of the bubble a local increase in TS would be present, creating a fouling footprint. The influence of dissolved air and processing pressure on the fouling rate was examined in the thesis and the reason behind the creation of fouling is assumed to be drying.

A lab scale tubular heat exchanger UHT was used in the experiments and a part of the thesis is focused on the instrumentation of the machine. The results points in two directions. While processing milk entering with a high level of dissolved air, an increased process pressure led to a decreased initial fouling rate and prolonged induction period. The results from processing milk with low level of dissolved oxygen were inconclusive. Either a point of low enough oxygen level and high enough pressure was reached for nil creation of bubbles, or the milk properties were changed from the preprocessing which intended to lower the oxygen level.

Sammanfattning

I detta examensarbete undersöktes luftens inverkan vid skapandet av fouling på värmeväxlarytor i värmebehandling av mjölk. Baserat på tidigare experimentella upptäckter gällande inverkan av luftbubblor samt beräkningar baserade på löslighetskonstanter av luft i mjölk fastställdes en hypotes. Mjölk kan presenteras i systemet utan olöst luft, med förändrat jämviktstillstånd på grund av nytt tryck och temperatur kan lösligheten minska. Utifrån denna förändring kan luftbubblor skapas som parallellt fylls med ånga vid korresponderande ångtryck. Under antagandet att ångan evaporerar från bubblans gränsskikt ökar torrsubstansen här vilket skapar ett foulingavtryck. Inverkan från löst luft och tryck i processen undersöktes i arbetet och orsaken till skapandet av fouling antogs vara uttorkning.

En tubvärmeväxlare i labbskala ämnad för UHT processing användes för experimenten och delar av rapporten fokuserar på instrumentering av denna maskin. Resultaten pekar i två riktningar. När mjölk med hög löst syrehalt behandlades, bidrog ett ökat processtryck till minskad initial foulinghastighet samt en förlängd induktionstid. Resultaten från körningar med låg löst syrehalt var ofullständiga. Antingen nåddes en punkt då tillräckligt låg syrehalt och tillräckligt högt tryck bidrog till ett obefintligt skapande av bubblor, eller så förändrades mjölken på något sätt på grund av den värmande förbehandlingen som skulle sänka syrehalten.

Table Of Contents

1 Introduction

1.1 Heat treatment of milk

Milk has not always been an as obvious choice for a nutritional beverage as it is considered today. Since it is almost an optimal environment conducive for the growth of microorganisms, without proper processing several pathogenic organisms can be found in milk. Raw milk has been known to contain pathogens like *Salmonella, E. coli, Listeria* and *Campylobacter* [1] and historically, raw milk was a common source of spreading diseases like tuberculosis, typhus and scarlet fever [2, p. 87].

To kill the harmful substances milk is heated to a certain temperature for a certain time, called pasteurization. It was from the work performed by Louis Pasteur in the 19th century regarding the lethal effect heat has on microbes the process today commemorates his name [2, p. 87]. The kind of processing this thesis deals with is called Ultra High Temperature (pasteurization) performed in Tubular Heat Exchangers, denoted simply UHT and THE. UHT is performed in the temperature range of 135-140 °C for a couple of seconds.

1.2 Fouling

Fouling in general is a wide concept considered to be the formation of unwanted material on a solid surface [3]. In the sense of the dairy processing industry fouling is mainly the buildup of precipitated proteins [2, p. 97] and partly mineral deposits on the hot heat exchanger surfaces [4] [5]. Some of the many factors affecting the fouling rate are the temperature difference between the milk and the heating side, the milk quality and composition, the air content of the product and the operating pressure of the heat exchanger [2, p. 98] [6].

The negative impact air content in milk, dissolved and undissolved, has on the fouling formation has been a long-recognized fact [2] [4] [5] [7]. However, the exact reason why and the phenomenon occurring has not been determined. Bennett [8], in his doctoral dissertation, shines some light on a theory mentioned by for example Burton [4] in his journal article from 1968. The theory is that air induces fouling if it separates as bubbles (undissolved air) on the heating surface. Bennett [8] manages to capture videos and photographic visualizations supporting this theory. In the wake of Bennet's discoveries, a purely theoretical pilot study was performed at Tetra Pak. The results from the calculations for solubility and steam properties performed in the report [9] shows great consistency with the experimental results of Bennett [8]. Both reports support the hypothesis that the mechanism behind what Bennet denominates as "bubble induced fouling" is drying.

1.3 Aim of the study

This thesis is a continuation from the theoretical pilot study aiming for a more practical approach towards bubble induced fouling. The aim of this study is to further examine the relationship between undissolved air bubbles and the fouling rate in milk heat exchangers. This is to be done in a way more resembling the way UHT is performed in Tetra Pak machines and to validate what was found in the pilot study [9]. By performing trial runs with milk on a lab scale THE while varying the dissolved air content and process pressure, the fouling formation rate is measured. From the results, further analysis is applied to explore and understand the mechanism behind bubble induced fouling.

1.4 Scope

The work is limited to experiments performed on a lab scale THE which is to be taken into consideration when reading the report. Results obtained from the experiments can be uncertain when scaling up to a commercial plant. The results are more focused on examining patterns than quantifying absolute correlations.

1.5 Disposition

The report is initiated with a theory part, large parts of this section can be skipped if one has fundamental knowledge in heat transfer and milk processing. Following is the material & methods section where the experimental setup as well as the fouling monitoring devices are described. The results, discussion and conclusion chapters are followed by notations used in the report as well as the bibliography. Lastly the appendices consist of graphs not fitted in the report as well as a start-up protocol for the machine used in the project.

When “the writer” is stated, the author of this thesis is intended as the person

2 Theory

2.1 Literature review

During the initiation phase of this project, in the beginning of 2016 before the writer was involved, a literature search was performed at Tetra Pak. The aim was to find relevant literature and information regarding the influence of air on milk fouling. Keywords in the search were "air", "milk OR dairy", "heating OR uht OR pasteurization" and "fouling OR run time OR pressure drop". Found in the search was the earlier mentioned dissertation by Bennett from 2007, called "Aspects of Fouling in Dairy Processing" [8]. Beyond this, several journal articles by Jeurnink et al. collected in his dissertation was of interest, for example "Mechanisms of fouling in dairy processing" [5] and "Fouling of heat exchangers by fresh and reconstituted milk and the influence of air bubbles" [7].

A similar search was performed prior to this thesis to get up to date and conclude if any information or reports had been done on the topic since. Also, citations of Bennett's dissertation were checked and some search words were added such as "bubble" or "bubble induced fouling". Not much material of interest has reached the public domain since 2007 according to the writer's discoveries and knowledge. One German journal article published 2014 by Sprunk et al. [10] with relevant topics was found but no new relevant information was deemed to have been introduced. The article was analyzed with the writer's very limited German skills, translation tools and the English abstract. It is very possible that internal projects within companies has been conducted yielding results without publishing.

2.2 Milk

2.2.1 Composition

The main contents of milk are a mix of water, proteins, fat, carbohydrates and minerals, but also trace amounts of substances such as vitamins and enzymes [2, p. 18]. The total solids (TS) content for whole milk is usually around 13 wt% [2] [11], the composition can be seen in Table 2.1. Since milk is a product originating from a living animal, variations between breeds, cows within the same breed, milking seasons and feeding can have a dependence on the composition [2, p. 22] [11]. Milk is slightly acidic due to the lactic acid and has a pH around 6.5-6.7 [12].

Table 2.1. Composition of the total solids in cow's milk from two different references, the Dairy Processing Handbook [2] and Ullman's Encyclopedia of Industrial Chemistry [11].

Solid substance (wt%)	[2]	[11]
Protein	3.4	3.3
Fat	3.9	3.8
Carbohydrates	4.8	4.8
Minerals	0.8	0.7
Organic acids	n/a	0.2
Total solids	12.9	12.8

2.2.2 Fat

The fat in milk is present in the form what is called an emulsion or dispersion, meaning small droplets of a fluid in another and therefore not a true solution [2, p. 19]. Butter is also an emulsion with small water droplets which is called a water-in-oil emulsion [11]. In the case of milk it is the other way around, called an oil-in-water emulsion, and the fat is present in fat globules which are surrounded by a membrane with complex structure [2, p. 23] [11].

The milk fat is fairly stable towards heat treatment and is not very altered by this [11]. However, milk fat is sensitive to mechanical treatment which is utilized in the homogenization and mention later in the report.

2.2.3 Proteins

The proteins are divided into two major subgroups: whey proteins and casein proteins. The caseins agglomerate and form big, relative the size of a protein, clusters called micelles [11]. A micelle can consist of hundreds and thousands of single casein proteins [2, p. 28], but at present time it is not yet fully determined the actual appearance of a casein micelle. Caseins make up about 80 % of the proteins in milk and are by the light scattering capabilities of casein micelles the reason behind the white color in skim milk [2, p. 28]. Casein proteins are not easy precipitated by heat but more easily by acid of enzymes, which is used in cheese making [2, pp. 30, 39].

Whey proteins are the type of proteins often acquired protein powders for body building purposes. They are separated from the main product in cheese making and make up the remaining 20 % of the milk proteins. About 50% of the whey proteins are β-Lactoglobulin (β-Lg) which are heat sensitive. At 60 °C [2, p. 32] – 70°C [5] these proteins start to denature and form complexes with the casein micelles [11]. Denaturation means that a protein loses its tertiary structure and sometimes biological function.

2.2.4 Carbohydrates

Lactose is the carbohydrate occurring predominantly in milk and is found only there, it is a disaccharide consisting of glucose and galactose [2, p. 35]. Lactose mainly affects the color and taste of the milk during heat treatment, and partly converts into lactulose, discussed more thoroughly later.

2.2.5 Minerals

The most occurring minerals are potassium followed by calcium, which has a major influence in the building of bone mass in all mammals drinking their mother's milk [11]. Heating a fluid with minerals alters the equilibrium and can cause them to precipitate. In milk for example different forms of calcium phosphate and calcium citrate precipitate upon heat treatment [5].

2.3 Indirect UHT

The following sections (*Indirect UHT* & *UHT processed milk*, including subheadings) are based on the writer's knowledge gained from working with process design of UHT treatment plants for milk processing if not referenced otherwise.

UHT is based on the same process as pasteurization, to heat up a product to a certain temperature for a certain time to kill bacteria, but when referencing to UHT it is denoted as sterilization instead of pasteurization. UHT can be performed as direct or indirect heating, meaning direct contact with the heating media or separated by a wall. Direct heating is performed by injecting

steam into preheated product or spreading product through a nozzle into a space of steam. Direct heating is only considered briefly in this thesis for comparative reasons.

2.3.1 THE

The kind of heat treatment regarded in this thesis is performed in THE, tubular heat exchanger. The different pipes/sections of the THE are often gathered in an insulated package, see Figure 2.1, where the tubes are placed in parallel going back and forth.

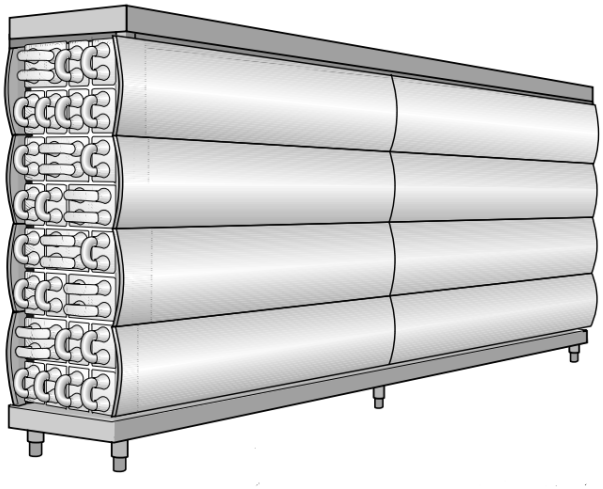

Figure 2.1. A tubular heat exchanger unit with covering insulating sides as a compact device, figure from [2, p. 101]

A closer look at the edge of the unit and the cross sections of two types of tubes is visualized in Figure 2.2. The product that is heated flows in the inner tube(s), called tube side, and the heating medium on the exterior, called shell side. The heating medium can be either steam, water or hot product. The case of heating unprocessed cold product with already processed hot product is called regenerative heating. It increases the energy efficiency of the process but as a tradeoff, some of the controllability and preciseness is lost. It should be noted that an exception exists when heating regeneratively. The processed product (heating medium in this case) then flows on the tube side and the unprocessed product on the shell side. This is since a higher pressure is always maintained on the tube side than the shell side. If a crack in the process would occur, product should leak into the heating medium, alternatively, processed product should leak into unprocessed, as to not loose sterility on the aseptic side.

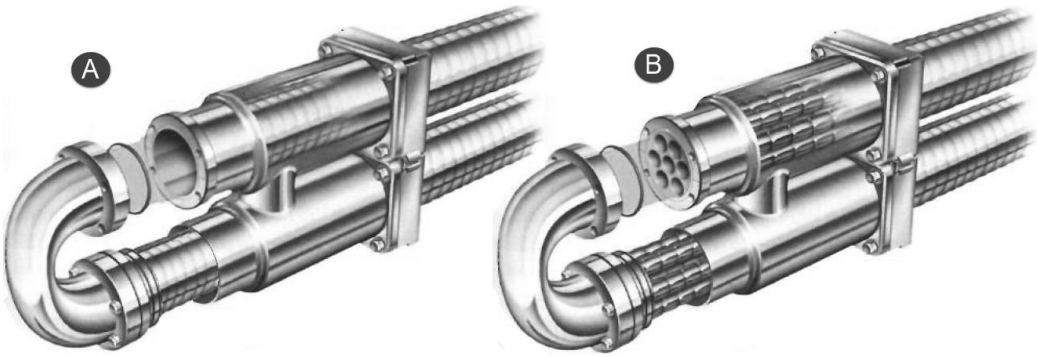

Figure 2.2. Cross section of two types of tubular heat exchangers: (A) Monotube and (B) Multitube. Figure from [2, p. 102]

The two main configurations for THE are monotubes and multitubes, see (A) and (B) respectively in Figure 2.2, however more configurations exist. The multitube is a bundle of smaller tubes placed concentrically in a revolver type configuration where the flow is spread even in the channels. The pipes can either be smooth or corrugated. In the latter, turbulent flow is easier to obtain at lower flow rate but the capital cost is higher and the pressure drop is increased. The manner of heating is almost exclusively in countercurrent flows with several advantages. The product that is heated meats the heating medium in its coldest place and gradually encounters warmer medium when it is heated, see Figure 2.3. This minimizes the temperature difference and enables a higher outlet temperature of the product compared to concurrent flows.

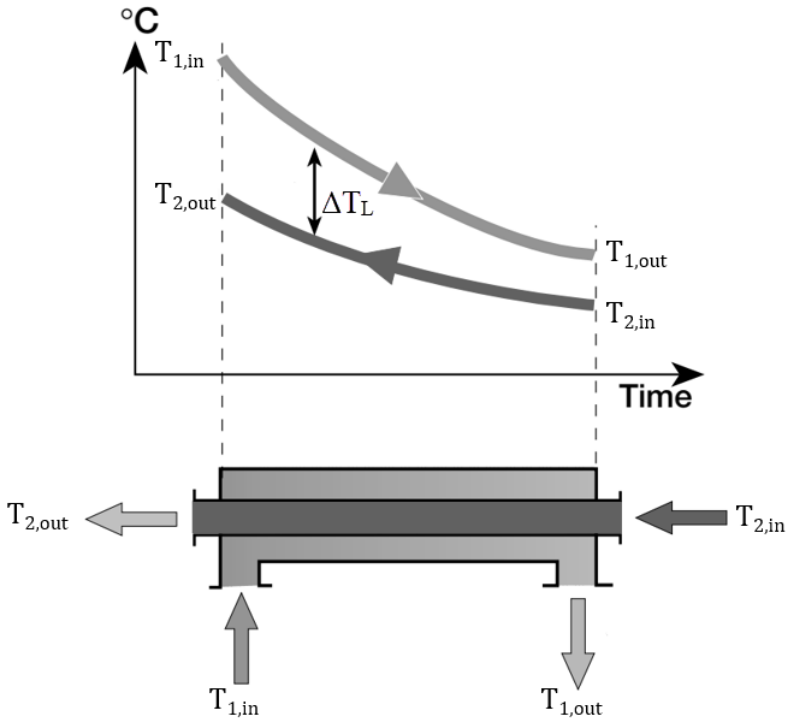

Figure 2.3. Visualization of a countercurrent THE and the notations used in the calculation of the logarithmic mean temperature difference, figure from [2, p. 95].

2.3.2 Heat transfer

Transport of heat is the main process in UHT processing, all heating and cooling processes follow fundamental heat exchanger and thermic calculations. Eq. 1 [13] calculates the heat load to or from a fluid taking mass flow, heat capacity and temperature difference into account. Eq. 2 [13] is a heat exchanger specific calculation utilizing the overall heat transfer coefficient, the area of the heat exchanger and the logarithmic mean temperature difference. The heat load transported from one fluid is always taken up by the other and equal to the heat load over the heat exchanger, applying conservation of energy and neglecting heat losses [14].

$$Q = \dot{m}_1\left(c_{p1,in} \cdot T_{1,in} - c_{p1,ut} \cdot T_{1,ut}\right) = \dot{m}_2(c_{p2,ut} \cdot T_{2,ut} - c_{p2,in} \cdot T_{2,in}) \qquad \textit{Eq. 1}$$

$$Q = k \cdot A_{HE} \cdot \Delta T_L \qquad \textit{Eq. 2}$$

The logarithmic mean temperature is calculated to obtain an overall measure since the temperature difference can differ throughout the heat exchanger, see Eq. 3 [13]. Compare with Figure 2.3 for notations used for the tube and shell side respectively.

$$\Delta T_L = \frac{(T_{1,in} - T_{2,out}) - (T_{1,out} - T_{2,in})}{\ln \frac{(T_{1,in} - T_{2,out})}{(T_{1,out} - T_{2,in})}} \qquad \textit{Eq. 3}$$

The overall heat transfer coefficient is calculated from a combination of the two fluids being heat transferred and the material choice and thickness of the wall, see Eq. 4 [13].

$$\frac{1}{k} = \frac{1}{\alpha_1} + \frac{h_{tube}}{\lambda_{tube}} + \frac{1}{\alpha_2} \qquad \textit{Eq. 4}$$

Often the heat transfer coefficient is empirically obtained by monitoring temperatures and flows in a heat exchanger. But it can also be theoretically calculated as followed from several factors such as heat capacity, flow profile and is highly temperature dependent. The Reynolds and Prandtl number can be calculated, see Eq. 5 and Eq. 6, respectively, as input to the Dittus-Boelter equation [15] where the Nusselt number is approximately determined, see Eq. 7 [15]. The Dittus-Boelter equation is valid for smooth tubes and Reynolds numbers above 10’000. It is not exact science since it is an empirical correlation but can work as a crude estimation for the purpose.

$$Re = \frac{d_h v \rho}{\mu} \qquad \textit{Eq. 5}$$

$$Pr = \frac{C_p \mu}{\lambda} \qquad \textit{Eq. 6}$$

$$Nu = 0{,}023\, Re^{0,8} Pr^{n} \qquad n = \begin{cases} 0{,}4 \text{ for fluid being heated} \\ 0{,}3 \text{ for fluid being cooled} \end{cases} \qquad \textit{Eq. 7}$$

From the value obtained in the Dittus-Boelter equation the heat transfer coefficient for the fluid at a given state can be obtained from the definition of the Nusselt number, see Eq. 8 [13].

$$Nu = \frac{\alpha d_h}{\lambda} \quad \rightarrow \quad \alpha = \frac{Nu\, \lambda}{d_h} \qquad \textit{Eq. 8}$$

The transportation of heat from the bulk medium to the bulk product can also be divided into several sub steps, see Figure 2.4 . Heat convection, i.e. heat traveling from the bulk fluid to the boundary layer can be seen in Eq. 9 [13].

$$|Q| = \alpha_i A\, (T_{i,b} - T_{i,w}) \qquad \textit{Eq. 9}$$

Heat conduction, specifically in circular walls, i.e. the heat conducted through the heat exchanger pipes can be seen in Eq. 10 [13]. All calculations regarding heat load are set equal to match steady state. The heat traveled from bulk medium to the wall is equal to the heat traveled through the wall and equal to the total heat load from bulk medium to bulk product.

$$Q = \lambda_{tube} 2\pi L \frac{(T_{w,o} - T_{w,inn})}{\ln\left(\frac{d_{inn}}{d_o}\right)} \qquad \textit{Eq. 10}$$

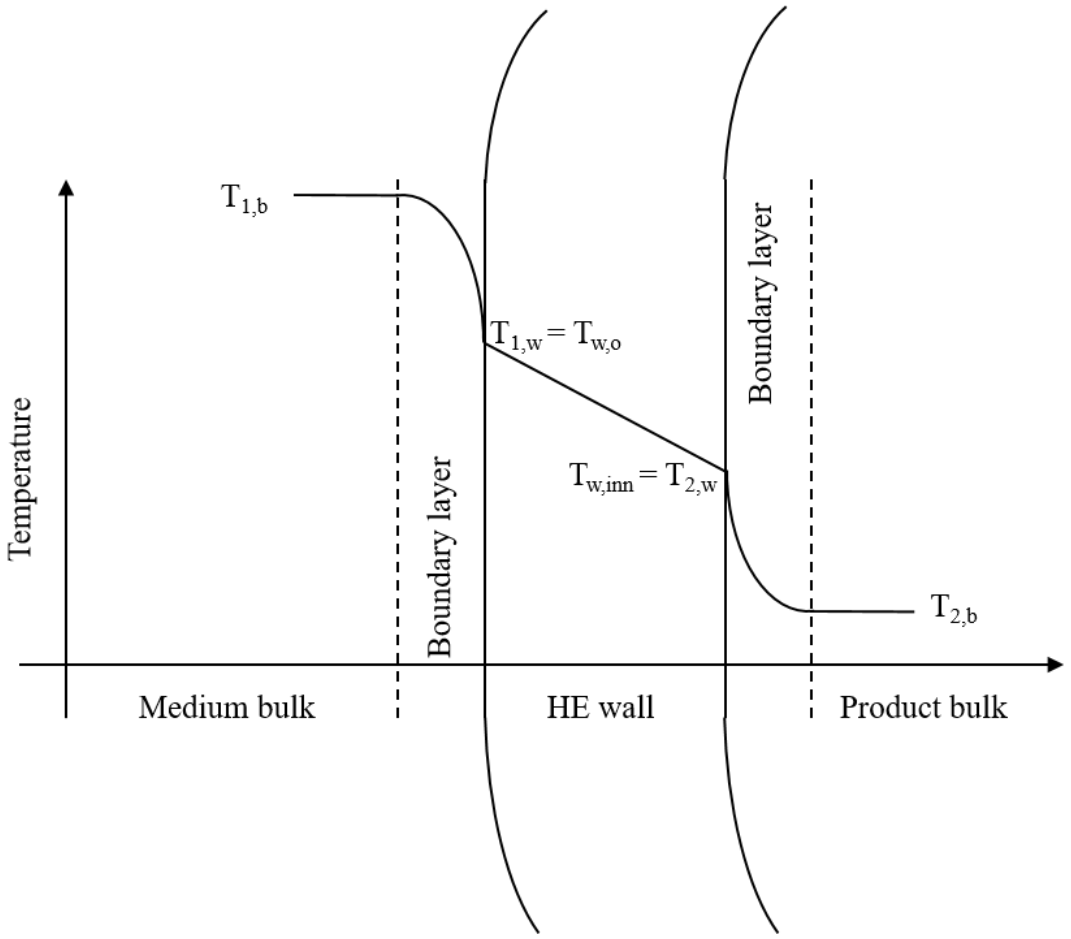

Figure 2.4. Schematic visualization of the fluids divided by the heat exchanger wall, and the heat exchanging processes occurring.

2.3.3 Preheating section

A simplified process flow chart for UHT processing is shown in Figure 2.5, numbers in parentheses in the following section refers to this figure. Storing milk for 12-24 hours chilled or at room temperature after milking and before processing is found to reduce the amount of fouling formed [4] [8]. Storing for longer periods than this has instead an increased effect on the fouling amount, while the risk of developing possibly dangerous micro-organisms is present. After storing, the milk is pre low temperature pasterurized presented into the processing system usually chilled at around 4 °C. The pressure in the system must be maintained albeit pressure drops due to piping, valves and bends to make sure the product is not boiling when heated above the atmospheric pressure boiling point. Initially the product is pumped (2) up to sufficient pressure coming from a balance tank (1) and the preheating stage is initiated (3). The milk is preheated to around 70 °C before it reaches the homogenizer (4). In the homogenizer, the fat globules are smashed into smaller pieces by forcing the flow through a small channel at high velocity resulting in a, as one can conclude from the name of the process, homogeneous product. Homogenization is utilized to avoid separation and clumping in the product.

After the homogenizer, which raises the temperature in itself by a couple degrees due to high pressure energy transforming to heat [2, p. 136], the product is then heated further (5) until it reaches the stabilizing holding tube (6). The idea behind this unit is to denature and stabilize

the proteins in an early stage. Fouling starts to become an issue when the milk is heated above 70 °C [5], since the whey proteins start to denature at 65 °C and is almost totally denatured when heated to 90 °C for 5 minutes [2, p. 39]. Because of this reason the product is held for about 30 seconds around 95 °C. The stabilizing holding cell is usually fabricated in a wider diameter than the rest of the plant to manage the pressure drop from fouling formed in this section.

2.3.4 Final heating section

Following the preheating stage is the final heating section (7) where the product is heated to the maximum processing temperature. At the temperature of 135-140 °C the product travels through a holding cell (8) for the desired holding time, a couple of seconds. The length of the holding cell is calculated from the flow, the holding time, and the tube diameter and taking the flow profile in account as a correction factor, see Eq. 11. For example, in a process which has a laminar flow profile, the velocity of the flow in the center is much higher than that at the periphery which is "sticking" to the wall [16]. The correction factor takes this into account and prolongs the holding tube, resulting in some particles traveling in the correct speed would have a longer holding time compared to the slowest [2, p. 247].

$$L_{HC} = \frac{\dot{V} \cdot HT}{\eta \cdot A_{tube}} = \frac{\dot{V} \cdot HT \cdot 4}{\eta \cdot \pi \cdot d_{tube}^2}$$

Eq. 11 [2, p. 100]

When the heat exchange in the preheating section is performed in a regenerative matter (3), uneven or decreased heat transfer with time can be obtained. This manner of heating is undesired in the final heating section since a steep and predictable temperature curve is wanted. In the final heating section, heat is always added directly with steam or a hot water circuit (9) to maintain control over the heating phenomenon. It is also required to use a small temperature difference in the final heating section. The combination of small temperature differences and fast heating processes calls for a great heating area in the final heating section according to Eq. 2.

2.3.5 Cooling section

After the holding cell the product is cooled down to desired packing temperature. It is either cooled with ice water, cooling water or tower water and most often a combination of them. In the case visualized in Figure 2.5, the product is initially cooled with cooling water (10) and then further with the cold unprocessed product (3). Regenerative heating is a win-win situation since in the meantime, regenerative cooling is utilized. The phenomenon is similar to what is done in pinch analysis. The cooling medium that is heated up in (10) in the cooling section is afterwards sent to (5) to heat the product after the homogenizer. After processing and cooling the product it is sent to either an aseptic tank or directly to a filling machine to be packed aseptically (11).

Note that the sections (3), (5), (6), (7), (8) and (10) are all collected in the unit shown in Figure 2.1 and each section can consist of several tubes and not just one. Figure 2.5 is not showing this in a true manner.

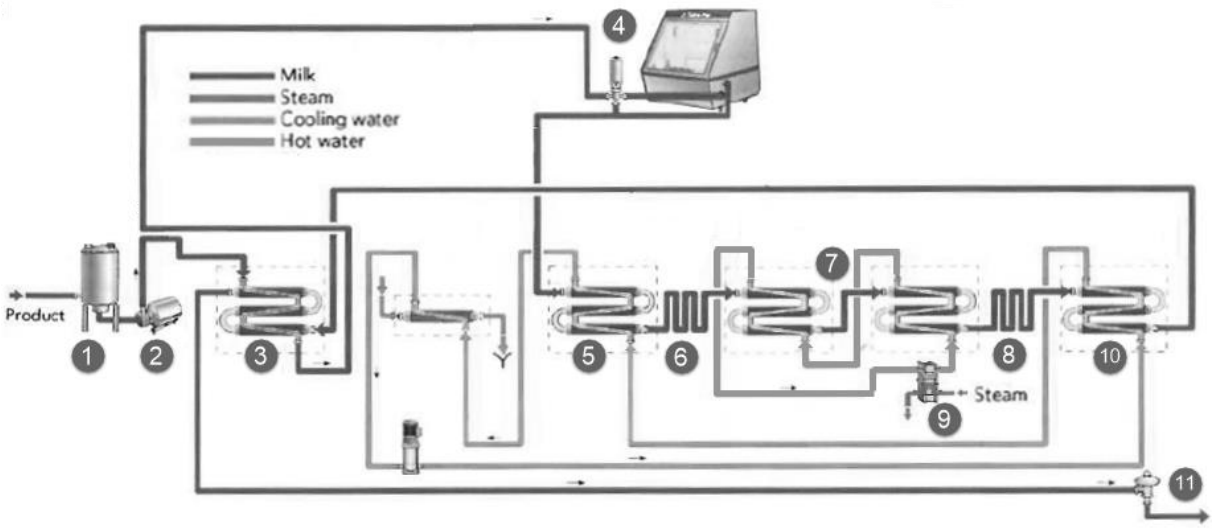

Figure 2.5. A simplified process flow chart for UHT milk processing in THE. Figure from [2, p. 259].

1. *Balance tank*
2. *Pump*
3. *First preheating section*
4. *Homogenizer*
5. *Second preheating section*
6. *Stabilization holding tube*
7. *Final heating section*
8. *Holding tube*
9. *Plate heat exchanger for hot water circuit*
10. *Cooling section*
11. *Product sent to aseptic tank or filling machine*

2.4 UHT processed milk

2.4.1 The product

UHT milk is defined as commercially sterile meaning that the product is free from microbes that can grow in the conditions it is meant to be stored [2, p. 247]. The product is packed aseptically and can be stored in ambient temperature (25-40 °C depending on location) up to a couple of months. Of course, once the product is opened it spoils in a matter of days just as regular milk. Shelf life is however dependent on the definition of when the milk is "spoiled" i.e. factors as sedimentation, separation, increase in viscosity and worsening of smell, taste or color [2, p. 249].

When treating milk at high temperatures the Maillard reaction is taking place between the lactose and amino acids of the proteins in the product [2, p. 40]. This reaction results in a brownish color, a boiled, bitter or caramel like taste alteration as well as a sulphureous smell. All these traits are more or less significant for UHT milk. Once the Maillard reaction has been initiated it can proceed even at ambient temperatures, only at a slower rate, which is one of the detrimental effects reducing shelf life.

2.4.2 Lactulose and F_0 values

As mentioned above it is desired to have an as steep temperature curve as possible in the final heating section. If the temperature is increased rapidly and held at this temperature for the holding cell time followed by a rapid cooling, the least impact on the product is obtained while still having a commercially sterile product. The optimal process to depict this has to be with direct heating where the high-pressure steam instantly increases the temperature of the product when they are mixed. After the holding cell the mixed flow is sent to a vacuum vessel where steam is flashed and the temperature rapidly decreases consequently. By this manner of heating a spike in a "time vs temperature" diagram is obtained, compared to a slower process as in indirect heating, see (1) and (2) respectively in Figure 2.6.

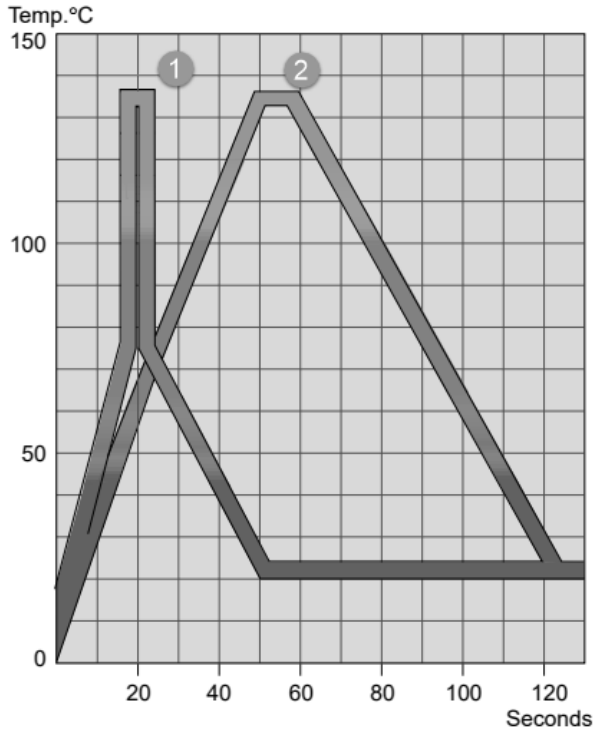

Figure 2.6. Typical temperature curve as a function of time for a direct heating process (1) and an indirect heating process (2). Figure from [2, p. 247]

Lactulose is an epimer, i.e. one of a pair of isomers [17], of lactose and is formed when milk is heat treated [18]. The formation is strongly related to the time/temperature correlation of the heating phenomenon and is used to differentiate how heavily the milk has been heat treated. For example, in Figure 2.6, process (1) would have a lower lactulose value than process (2).

In some way opposing the lactulose value is the F_0 value, which is the effect the time/temperature correlation has on the killing of *Clostridium botulinum* [2, p. 245]. Milk treated for x time at temperature y can have the same F_0 values as milk treated at a higher temperature for a shorter time. Briefly, a high F_0 value (5-6) guarantees a commercially sterile product if the raw milk is up to standard quality [2, p. 245].

2.5 Fouling

Fouling in milk processing UHT plants is one of the major problems concerning process design and run times. It is hard to estimate and requires years of experience with trial and error in the field to grasp the concept and its features in a deeper sense. Tetra Pak experience issues from customers that cannot reach sufficient promised runtimes due to the buildup of fouling, which requires resources and money to resolve. An increased knowledge in the processes and phenomenon behind fouling has a large possible economic gain.

2.5.1 Composition

It is more or less consensus in the dairy business to divide fouling into two categories: type A and type B. The classification was proposed by Burton [4] in 1968 and has been widely used since, see [5] [6] [8] [19] [20] etc. The types are divided partly in which temperature region they occur and partly on the composition of the fouling material.

Type A starts to form at the temperature of 70 °C, reaches a peak at around 100±10 °C, and then starts to decrease [4]. The composition is around 50-60 % protein, 30-35 % minerals and 4-8 % fat [4]. Since denaturation of β-LG starts at 60 °C [2, p. 32], the protein content of type A fouling is mainly β-LG in the lower temperature region, this turns to more casein content reaching increased temperatures [8]. The texture of type A fouling is described as soft, voluminous, spongy and whiteish in color [4]. By a simplified approach, one can say that type A is the fouling that happens in the stabilization holding cell.

Type B dominates the upper part of the heating spectra up to the maximum temperature of the system. The texture is more compact and brittle than type A and has a more greyish color. Composition wise type B includes a lower protein content, about 30-40 %, and larger mineral content, about 70 %, according to Burton [4]. Other references report a slightly different composition of 70-80 % mineral and 10-20 % protein [8]. It should be noted that not a specific boundary exists between the fouling types but more of a sliding scale towards type B with increased temperature. To conclude, at lower temperatures in the fouling span protein content in the fouling matter is predominantly. When the temperature is increased the protein content decreases and mineral fouling constitutes a bigger part in the composition.

Lactose is basically not existent in the fouling and has a high solubility in water. The solubility is just below 19 g/100g water at 25 °C and increases with an increased temperature [21].

2.5.2 Factors affecting fouling

The fouling formation depend on several factors either by alterations in the processing conditions directly or by differences in the product entering the system. Correlations between the factors can also exist which is why it is important to keep the same approach when examining a factor, i.e. try to keep conditions not examined in an experiment constant.

Acidity

Casein micelles are sensitive to a lowered pH in milk, strong internal calcium bonds are created within the micelle [2, p. 30]. This results in growth of the micelles which eventually ends with a dense coagulum if the pH is low enough [2, p. 30]. The effect to this extent is usually achieved only when acid is added to the milk and not within the natural variation of pH in raw milk. A reduction to the lower end within the natural variation has however showed a larger amount of fouling [8].

Milk age
As mentioned above, storing milk for a short time can reduce the fouling amount, as long as the pH is not altered. But aged milk causes more fouling than fresh milk [4]. It has been showed that milk stored at 5 °C for 6 days before processing quadrupled the fouling degree [22].

Seasonal variation
The runtime of UHT, especially sections heated above 120 °C, experiences variations in deposition degree throughout the milking season [22]. Some recognize this effect to changes in feed and thus changes in milk composition [4] [22] and some to natural variation as difference in cows and environmental factors.

Milk preheating
Preheating, also called forewarming, causes denaturation of whey proteins and thus reduces the formation of this fouling later in the process [11]. This is widely accepted and utilized in the stabilization holding tube described earlier [23]. Many variations of time and temperature have been investigated. A sufficiently high temperature at around 95 °C has been shown to be more important than the holding time [24].

Flow velocity
At high enough velocities the product flow becomes turbulent, exceeding a certain Reynolds number. A higher Reynolds number, and thus a more turbulent flow, decrease both fouling rate and amount [25]. The viscous sub-layer at the wall becomes thinner with increased velocity making the particle transfer through diffusion harder [26, p. 18].

Dissolved gases
Out of the several factors affecting fouling formation in UHT, air in milk has long been a known contributor to the phenomenon. Burton [4] states a hypothesis that "It is probable that air only encourages deposit formation if it separates as bubbles on the heating surface, and that its effect will be eliminated if sufficient pressure is maintained in the milk at all times to prevent separation". This was published in 1968 and has since been cited in several journal articles and reports. However, no experimental studies to examine the hypothesis have been stated. A general pattern when reviewing literature is mentions regarding the negative influence of air on fouling, but experimental evidence lacks and in cases with experiments the conditions are stated poorly.

Jeurnink [7] performed experimental studies aimed at exploring the influence of air bubbles on the amount of deposit, both in THE and PHE (plate heat exchanger). He found a significant difference in deposit formation between untreated and deaerated milk. But no measurements regarding air content neither before or after experiments were mentioned. Jeurnink also reports that "visual observations showed that air bubbles were nuclei for the formation of deposit". It is hard to grasp how these observations have been conducted when reading about the experimental rig. The THE utilized in the experiments was a monotube with heating medium flowing in the inner tube and an outer tube of glass. But since milk is not a transparent solution some struggles had to be evident to observe the air bubbles on the inner tube. It should also be noted that a part of Jeurnink's theory regarding the bubble participation in fouling is a bubble bursting. The writer also went into the trap of visualizing the bubbles as soap bubbles which can burst. However, the bubbles are air bubbles surrounded by a fluid media created by an altered solubility equilibrium and can thus only be eliminated by a decreased temperature or increased pressure.

Degassing in a vacuum vessel is a method used to eliminate bad smell and reduce the amount of dissolved gases in the product. The method is commonly used and often included in the design depending on product quality and ability for increased investment/running costs

2.5.3 CIP – Cleaning In Place

CIP is the process of cleaning a UHT plant without having to dismantle the parts and clean them separately. The whole processing unit can be cleaned by running a CIP program where fouling and other dirt is removed and afterwards followed by a sterilization of the plant. Initially water is used to rinse off material that easily comes off. This is done immediately after the closing down of the process as to not dry the fouling which makes it harder to remove [2, p. 462]. Afterwards both acidic and alkali solutions are used to break down the fouling material with water rinses in between [2, p. 462]. The alkali, usually NaOH, breaks down the precipitated proteins and removes fat while the acid, usually HNO_3, dissolves the mineral deposits [27].

Regarding UHT in the dairy industry CIP is performed usually on a daily basis but longer runtimes can be reached, direct UHT usually have slightly longer runtimes. However, comparing with other process plants including heat exchangers in the chemical production industry CIP is very much less frequent. For example, the petroleum or petrochemical business where the process is cleaned more on a yearly than daily basis [6]. If runtimes can be prolonged a longer guaranteed runtime can be assured to customers making Tetra Pak's processing solutions more attractive. With longer runtimes more product is processed per cycle. Cleaning of the machines also becomes less frequent resulting in less use of chemicals, less energy used and less effluent to take care of. According to Georgiadis et al. [28], 65% of the annual cost in a processing dairy is due to interruption of the production, compared to the increase in energy used due to fouling.

Since the dairy business is a very energy demanding business, much is to be gained if the runtimes can be prolonged by controlling fouling phenomenon even slightly.

2.5.4 Formation

Since the process of the deposit formation is not fully understood the fouling phenomenon described in this section is in a general way. In the literature, some in depth analytic approach to the phenomenon are described but merely as hypotheses. The theories consist of chemical reactions, mass and heat transfer and other physical processes for both bulk and surface effects [5] [25].

Initially the product is affected by the heat treatment by equilibrium and denaturation reactions forcing some species to precipitate [23]. The solubility of the minerals is decreased with increasing temperature [5]. Some of the proteins start to denature and aggregate [22]. To conclude, heat treatment forces some parts of the milk to longer be in a true solution [4].

Figure 2.7 shows a visualization which summarizes the assumed possible process steps for fouling in a good manner. The process steps are inspired by a similar figure made by Sprunk et al. [10] and theories of among others Jeurnink et al. [5] and can maintain a decent view of the processes according to today's knowledge. Some processes are visualized in the boundary layer and some in the bulk fluid and a continuous transfer between the layers is occurring [25].

See Figure 2.7 for referenced processes (denoted A-H) in this paragraph. Already at room temperature a monolayer of β-Lg can be formed and adsorb to the heat transfer surface (A). With increased temperature β-Lg denatures and exposes thiol (-SH) groups when the protein loses its

structure. The denatured β-Lg can either attach to the monolayer (B), create small groups of β-Lg (C) or attach to casein micelles (D). The small groups of β-Lg can then become parts of bigger aggregates (E) or travel back to the bulk and exit with the processed product (F). The creation of bigger aggregates can only occur in the presence of precipitated minerals (G), the minerals can also attach to the casein micelles (H) or the heat exchanger surface as mineral fouling (I). [10]

In the bubble, the process of bubble induced fouling described by Bennett [8] is thought to take place, more thoroughly explained below.

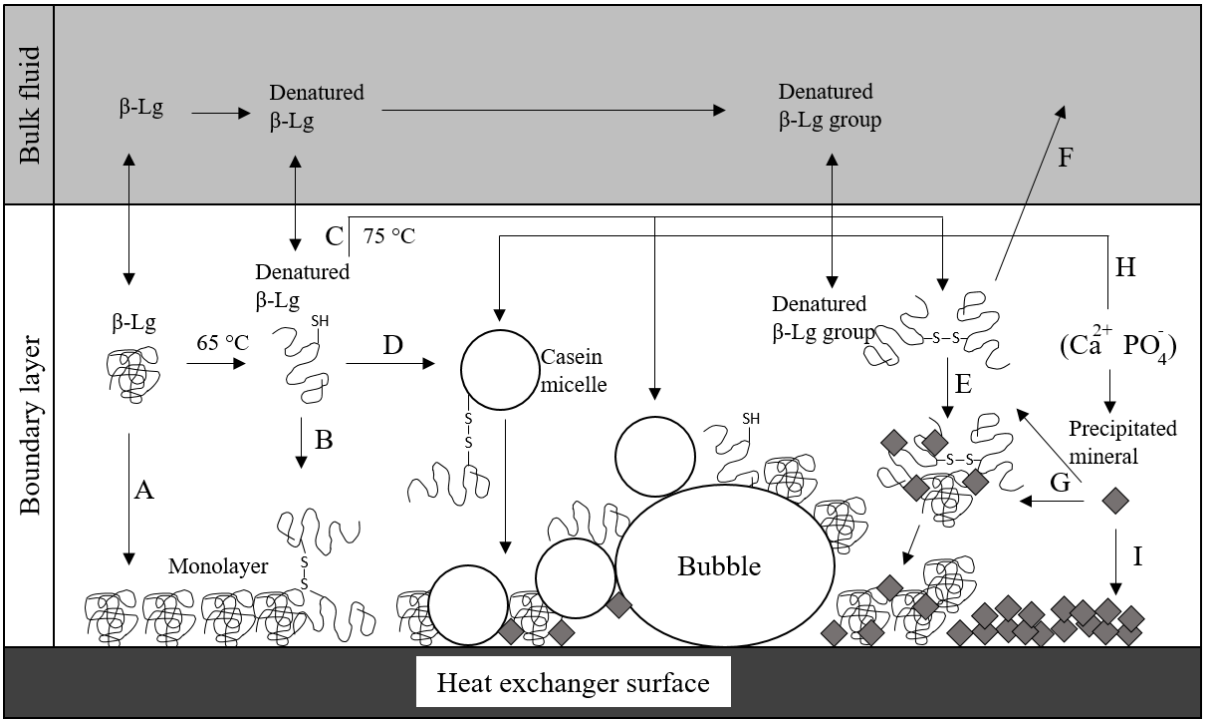

Figure 2.7. Processes for the formation of fouling in milk heat treatment involving whey protein (β-Lg), casein, minerals and gas bubbles. Figure by [10] with inspiration from [5], redrawn by the writer.

Thorough research has been made as to which layer/species that attaches first and the many theories conflict with each other following Bennett's discussion [8]. Some argue that a specific layer is constructed initially and then the other species is attached to this one, one can also envision the course of action to a simultaneous creation. A fact speaking for this process is the absence of lactose in the fouling matter even though it is the biggest contributor to the total solids in raw milk. Since lactose has a high solubility in water (milk is mainly water) it does not precipitate upon heating and does therefore not foul following this argumentation.

The process of fouling over time is often described and divided into different growth periods, much like the phases in bacterial growth, see Figure 2.8. Initially a so-called induction period where not much change is apparent, only a thin layer of fouling is formed which does not affect the heating significantly [6]. The induction phase can last up to an hour and has been shown to actually increase the heat transfer coefficient slightly due to surface roughness creating more turbulent flow [22].

Following the induction period is the fouling period where the growth of fouling is sufficiently substantial to make an impact on the heat transfer or the pressure drop [25]. The behavior of the fouling rate during the fouling period can be constant or nonlinear depending on processing conditions.

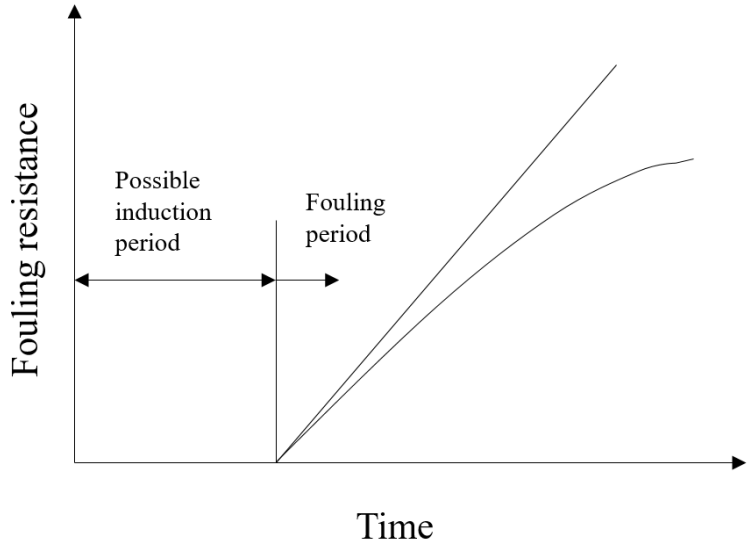

Figure 2.8. The possible fouling periods in the process of fouling growth with increasing fouling resistance over time, figure by the writer with inspiration from [25]

2.6 Fouling dependency of air

This section outlines the supporting theories regarding bubble induced fouling and the main reason behind the initiation of this thesis.

2.6.1 Aspects of Fouling in Dairy Processing – H. A. E. Bennett

MPHE

The classification of type A fouling as foamy and voluminous is with regard to the texture at the end of a run. To identify the process of fouling formation in an early stage one has to either shut down a process early and visually examine heating surfaces or create a strategy to examine the fouling process in real time.

Bennett [8] created a clever experimental rig with a miniature plate heat exchanger (MPHE). The MPHE consisted of several smaller units with a single plate in each unit. The rig can be described as a PHE where all the plates are separated for an enhanced and simplified monitoring. One of the units were modified to include a transparent Perspex (acrylic glass) sight glass. By this constellation Bennett managed to get real time footage and video sequences and could attain strong indications for the bubble induced fouling behavior. The solution used for these experiments were a 0.1% whey solution which was deemed to be transparent enough and still provide a medium for sufficient fouling formation.

Bennett further analyzed one run where bubbles were apparent during the run and a clearly similar pattern was obtained on the MPHE plate after the run, see (e) and (f) respectively in

Figure 2.9. The photograph from the plate after the run was zoomed in and analyzed further, see Figure 2.10.

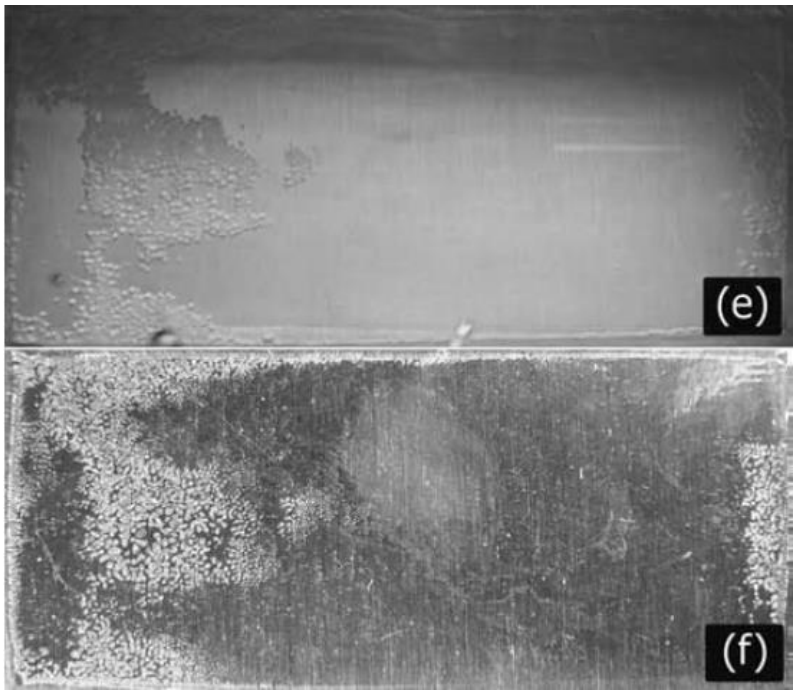

Figure 2.9. Video stills from during a run on the MPHE (e) and a photograph of the plate after the run (f), figure from [8] with republishing permission from Bennett.

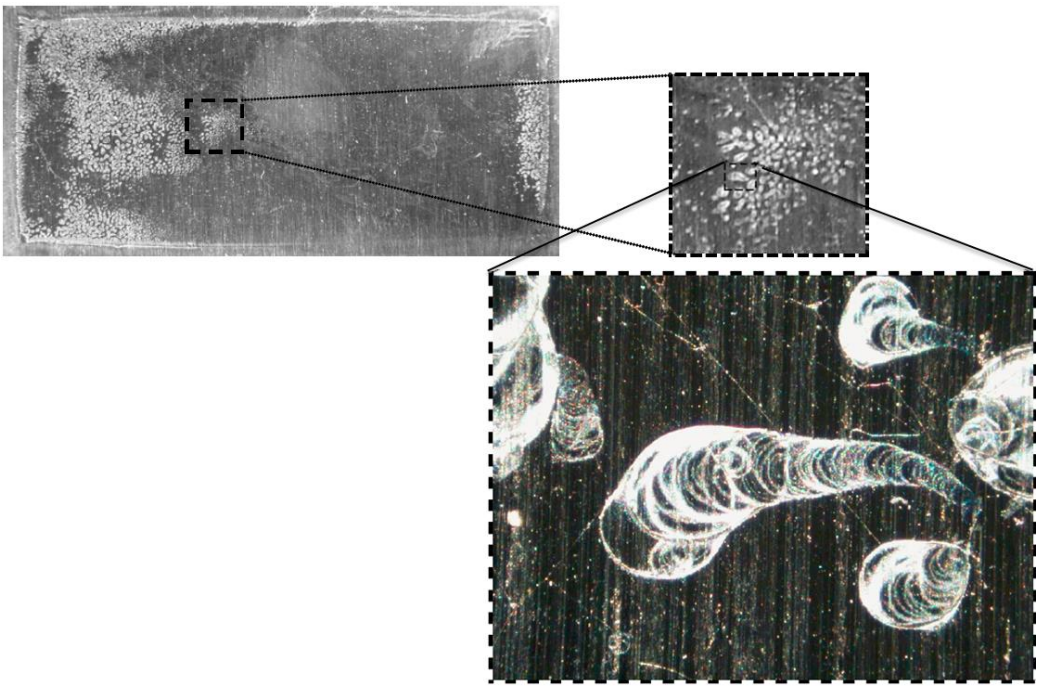

Figure 2.10. Enhancements of the section chosen to further examine from the photograph of the test plate in one of Bennett's runs, figure from [8] with republishing permission from Bennett and slight modifications by the writer.

The fouling footprints obtained in Figure 2.10 correspond to where bubbles were apparent during the run. According to Bennett, bubbles in this area existed for about 3 minutes. In the pattern it can be seen that the bubbles move in the direction of the flow and during the movement they grow bigger. Bennett estimated the number of rings to be 15, resulting in a mean formation time of 12 seconds. He admits this to be a low estimation for the number of footprints, which can clearly be estimated to at least the double resulting in a halved formation time of 5-6 seconds. It was also showed that bubbles created a greater footprint in the surface the longer they stayed, which speaks for some kind of regeneration of solid substance at the bubble surface that can dry out.

THE

Bennett proceeded from the findings obtained in the MPHE to perform runs on THE with whole milk to examine the influence of pressure and flow velocity on the behavior. With pressures ranging from 30-80 kPa (g) and run time of 4 hours the amount of fouling was weighed after each run. A clear relationship between a decrease in fouling amount with an increased pressure was determined.

An interesting feature was also obtained from photographs of the tubes after the runs. In Figure 2.11 (A) and (B), fouling pattern on tubes under same magnification with operating pressures at 30 kPa (g) and 80 kPa (g) respectively are shown. Process specifications regarding flow, run time and temperature profile for product and heating medium were the same between the runs. With an increase in pressure considerably fewer and bigger bubbles seem to have been nucleation sites for fouling. Bennet showed through digital analysis of the photographs also that the area of steel covered in fouling decreased almost linearly with increased pressure.

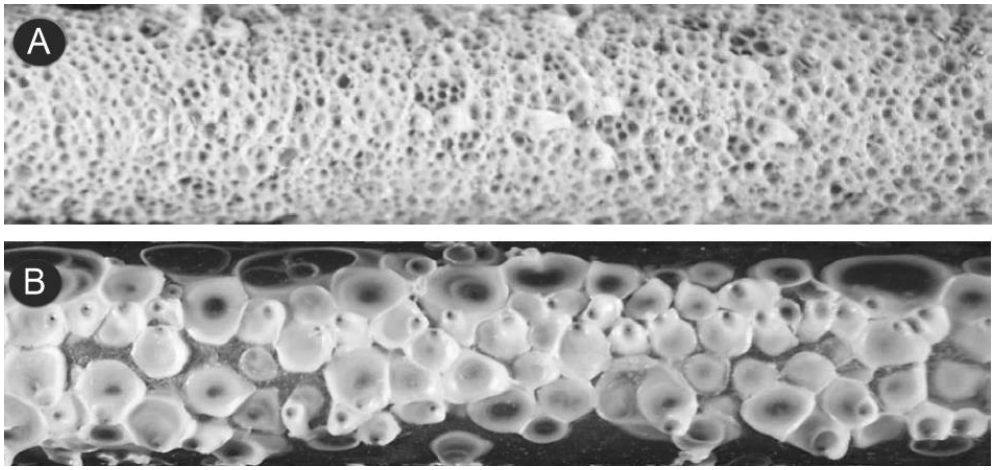

Figure 2.11. Photographs of tubes post run from Bennett's runs with THE: (A) at 30 kPa (g) and (B) 80 kPa (g), figure from [8] with kind republishing permission from Bennett.

Conclusion

Bennett performed several runs with varying pressure and product flow. He found that in his setup, the nucleation of air bubbles could be eliminated by:

- A backpressure of 130 kPa (g) (14)
- A linear velocity of 1 m/s

These numbers are not to be taken as absolute reference values to advance with since they are highly dependent on the setup conditions. The findings from Bennett's MPHE and THE above strongly speaks for bubble induced fouling and the numbers are instead used in this thesis as an incentive to be able to limit air nucleation with high enough pressure in a certain process design.

Bennett proposes in his discussion a 15-statement theory regarding bubble induced fouling, a selection of these is shown below. The numbers in parenthesis refer to Bennett's numbering of the statements

- When bubbles nucleate at the surface a layer of proteins and fat adsorbs to the liquid/gas interface immediately. (1)
- The proteins and other milk solids attach rapidly to the metal surface at the periphery creating a fouling footprint (within 12 seconds in our experiments). (3)
- The creation of a footprint depletes the air/liquid interface of its stabilizing solids and fresh solids immediately enter and spread out on this interface from the adjacent liquid milk. (4)
- The proteins from the milk can attach to the wall or to existing fouling deposits if they are activated either by heat or by enzyme and able to aggregate. […]. This mechanism is independent of and co-exists with the air-bubble fouling mechanism. (10)
- The activation, transport and attachment mechanism of fouling is considerably slower than the air bubble mechanism. (11)
- It is more effective to control air nucleation by increasing the pressure of the system than by using high linear velocities. Unfortunately, the maximum pressure used in industrial plants is dictated partly by cost. There is a relationship between the limiting pressure at which air bubbles cease to nucleate and the temperature of the milk. In this work the value is 130 kPa (g) for a hot side temperature of 90 °C. (14)

From Bennett's statements several theories and thoughts arise. The bubble induced fouling phenomenon is fast (3) and considerably faster than the protein activation mechanism (11). A process system therefore does not require a long time to create an altered heat exchanger surface if bubble nucleation is prone to occur on the surface. Milk proteins can however attach to either the clean heat exchanger or to an already fouled surface (10). Immediately when a bubble is created a layer of precipitated material adsorbs to the interface between liquid and gas stabilizing the bubble (1). Regeneration of solids takes place on the bubble surface meaning new solids appear as soon as the fouling footprint is created and solids are removed from the surface (4).

Findings above is merely the writer's selection from Bennett's work, for further information the reader is advised to read Bennett's dissertation [8].

2.6.2 Tetra Pak Development Report

At Tetra Pak a project was initiated with the purpose of advancing on the topic of "fouling dependency of air" and "bubble induced fouling". A calculation tool was developed to estimate the tendency of bubble nucleation in milk being heat treated. From a state in equilibrium with given temperature and pressure the amount of dissolved oxygen and nitrogen is calculated with

Henry's law and solubility constants. This equilibrium is altered with changed conditions in the THE. With increased temperature the solubility of the gases is decreased, the reverse is valid for increased pressure. At a new state of equilibrium, the amount of dissolved gases is calculated, if the solubility in this state is decreased the difference can thus be used to calculate to amount of undissolved gases. The undissolved oxygen and nitrogen creates "air bubbles" in the product. The bubble simultaneously becomes filled with steam calculated from the steam pressure at the given temperature. From these calculations the volume of bubbles at a new state is calculated. [9]

The steam is evaporated from the product and in total the amount is negligible in comparison to the total flow. But if the evaporation is assumed to be from a boundary layer on the bubble surface drying completely, it would experience a local increase in TS, thus the concept of drying and bubble induced fouling [9]. The drying on the hot surface creates the fouling footprint mentioned by Bennet [8]. The bubble can either grow bigger, move on the surface or be transported in the flow direction and thus be replaced by a new bubble, depending on the flow velocity.

The calculation tool was developed further to include a measure of fouling formation (kg fouling/ m^2 heating surface). The experimental conditions provided by Bennett was entered into the calculation tool and calculated at given pressures. Great correlation was found with fouling formation measurements (kg fouling/ m^2 heating surface) on his runs on the THE when comparing [9]. However, a constant factor of lower values was estimated by the calculation tool, the reason for this is yet unknown by the writer and the author of the Tetra Pak Development Report. Since assumptions had to be made in the construction of the calculation tool some of these could be the origin of the error. Note that the values of fouling potential and formation were compared for the end of each run and not a continuous comparison in time. The proposed process is visualized in Figure 2.12, one can envision the process producing a crater looking fouling footprint similar to found in Figure 2.11.

From two different initial states of dissolved gas, the same amount of undissolved gas volume can be formed at different temperatures and pressures. It is then the temperature which determines the degree of drying on the bubble surface. A higher temperature corresponds to a higher partial steam pressure which forces more steam to evaporate.

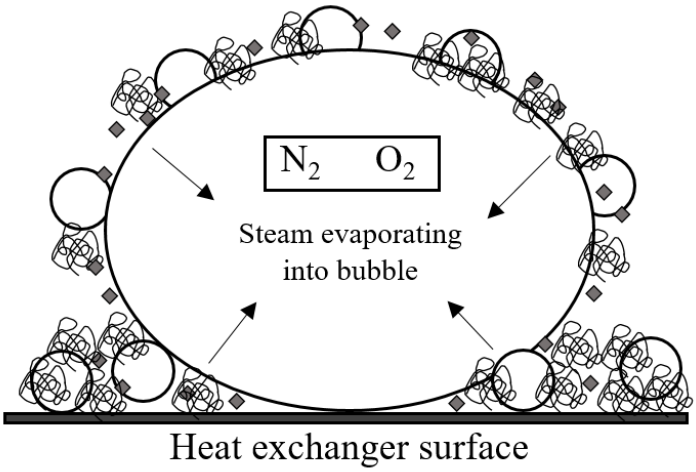

Figure 2.12 The proposed process of bubble induced fouling through drying in the boundary layer of the bubble.

2.7 Monitoring fouling formation

To monitor the buildup of fouling in real time several methods are available. No continuous visual methods were required in this work since Bennett [8] already gained that knowledge. Instead indirect methods, i.e. measuring a variable dependent of the fouling, as compared to direct, weighing or measuring thickness manually, are used in this thesis.

2.7.1 Heat transfer

As the fouling builds up in the tubes of the heat exchanger, it can be visualized as an extra term in Eq. 4 corresponding to the fouling layer, resulting in Eq. 12.

$$\frac{1}{k} = \frac{1}{\alpha_1} + \frac{b_{tube}}{\lambda_{tube}} + \frac{b_f}{\lambda_f} + \frac{1}{\alpha_2} \qquad \textit{Eq. 12}$$

The heat conductivity of the fouling layer is lower than the stainless steel of the tube resulting in a decrease in heat transfer coefficient with a growing fouling layer. According to Eq. 2, if the overall heat transfer coefficient is decreased, less heat will be transferred between the fluids and the milk will not have sufficient outlet temperature. To compensate this effect the medium inlet temperature can be increased, but then the fouling rate will increase and a negative cycle has started. The modification from Eq. 4 to Eq. 12 is very simplified and not as straightforward as adding a term since the remaining factors are not constant. For example, the heat transfer coefficient on the product side changes with an altered heat exchanger surface created by the fouling. Another disadvantage is the difficulty of estimating the heat transfer coefficient of the fouling layer [29].

With this in mind, the build-up of fouling can be modeled from a broader perspective taking only the overall heat transfer coefficient into consideration. In Eq. 13, a ratio between the current and initial heat transfer coefficient can be seen, denoted HTRF (Heat Transfer Reduction Factor). The value of the factor starts at zero, in a clean process, and increases with time as the

coefficient decrease. An uncertainty with this method is whether the fouling resistance is originating from the fouling layer or another way altered heating phenomena.

$$HTRF = \frac{k_0 - k_i}{k_0} \qquad \textit{Eq. 13}$$

2.7.2 Pressure drop

A flow through a pipe experiences pressure drop due to friction along the pipe walls according to the Darcy-Weisbach equation, see Eq. 14 [13]. The hydraulic diameter for a circular pipe is simply the inner diameter of the pipe. For a given pipe length the pressure drop will thus increase when the diameter decreases due to fouling, a relationship used when monitoring the fouling formation in real time. The increase in pressure drop throughout the process with time forces the pumps to deliver an increased output pressure. Eventually the output pressure will be too high for the process to withstand and it must be closed down for cleaning.

$$\Delta p = f\frac{L}{d_h}\frac{\rho\bar{v}^2}{2} = f\frac{L}{d_h^5}\frac{\rho\, 8\,\dot{V}^2}{\pi^2} \qquad \textit{Eq. 14}$$

The approximation of the friction factor is dependent on the flow regime, i.e. laminar or turbulent flow, which is determined from the Reynolds number, see Eq. 15 [13].

$$Re = \frac{d_h v \rho}{\mu} = \frac{4\,\dot{V}\rho}{\pi d_h \mu} \qquad \textit{Eq. 15}$$

For a laminar flow the friction factor is reciprocally proportional to Reynolds, see Eq. 16 [30].

$$f = \frac{64}{Re} \quad [Re < 2300] \qquad \textit{Eq. 16}$$

Blasius correlation [31] can be used for the friction factor in the turbulent region assuming a smooth pipe, see Eq. 17 [30].

$$f = 0.316\, Re^{-0,25} \quad [Re > 2300] \qquad \textit{Eq. 17}$$

Combining Eq. 14, Eq. 15 and Eq. 16 results in a pressure drop equation for laminar flow depending on the length and diameter of the tube as well as the viscosity and flow of product, see Eq. 18.

$$\Delta p = \frac{128}{3.6 \cdot 10^6} \frac{L\dot{V}\mu}{\pi d_h^4} \qquad \textit{Eq. 18}$$

The same reasoning but for turbulent flow with Eq. 17 results in a bit messier expression for pressure drop at turbulent flow depending also on the density in addition to the factors in laminar flow, see Eq. 19.

$$\Delta p = \frac{0.316 \cdot 2 \cdot 4^{0.75}}{(3.6 \cdot 10^6)^{1.75}} \frac{L\rho^{0.75}\,\dot{V}^{1.75}\,\mu^{0.25}}{\pi^{1.75}\,d_h^{4.75}} \qquad \textit{Eq. 19}$$

When the pressure drop at a given time is compared as a ratio to the initial pressure drop on a clean process, many factors cancel out as constants. Assuming constant pipe length, product flow and temperature profile (i.e. constant density and viscosity) the resulting ratio can be seen in Eq. 20 with the exponent denoted as * for a more concise writing.

$$\frac{\Delta p_0}{\Delta p_t} = \left(\frac{d_t}{d_0}\right)^* \qquad *= \begin{cases} 4 & (laminar) \\ 4.75 & (turbulent) \end{cases} \qquad \textit{Eq. 20}$$

The expression for the inner diameter of a pipe at a given time is thus Eq. 21. The height of the fouling layer can be seen in Eq. 22.

$$d_t = d_0 \left(\frac{\Delta \mathrm{p}_0}{\Delta p_t}\right)^{1/*} \qquad \textit{Eq. 21}$$

$$h_f = \frac{d_0}{2}\left(1 - \frac{\Delta P_0}{\Delta P_t}^{1/*}\right) \qquad \textit{Eq. 22}$$

This method of indirect monitoring fouling formation is fairly easy to set up with a differential pressure transmitter. The difference in pressure drop relates to the diameter difference to the power of 4 in the laminar region, where the friction factor also is independent of the pipe roughness, see Eq. 16. But to obtain good heat transfer a flow in the turbulent region is to strive for. Here the expression is precise to a higher power (4,75), but under the assumption that the pipe is smooth. This assumption is valid during start up conditions but will with time fail to be true due to the buildup of fouling, and the fouling being crusty and non-homogenous on the surface. The friction factor of a surface increases with increased roughness, see Moody-chart in for example [13] or [30].

It is unfortunate that a method for monitoring fouling will be invalid when fouling is formed. But if one is understood with the uncertainty the assumptions contribute to, the value of the

fouling height can instead be used as a fouling factor with less absolute reference to the height. Because what is true however, is that the formation of fouling will increase the pressure drop by reducing the diameter and by increasing the “real” friction factor. By using Eq. 17 for non-smooth pipes when a fouling layer is apparent, the calculated fouling height in Eq. 22 will be overestimated since the friction factor is underestimated.

Theoretically a different equation than Eq. 17 could be used for the friction factor, taking surface roughness into account. But since the fouling surface roughness is an unknown factor under dynamic circumstances it would be several other assumptions contributing to more uncertainty. For the purpose of examining and comparing fouling formation between runs Blasius correlation is sufficient as long as the values are not taken as absolute measures of fouling height.

2.8 Monitoring bubble formation

Regarding the creation of bubbles on the heat exchanger surface solely indirect methods are utilized in this work. By equipping the process with oxygen sensors and transmitters, dissolved oxygen in the product can be measured continuously at appropriate positions. The decrease in measurement values between two sensors downstream indicates a reduction in dissolved oxygen due to altered equilibrium.

3 Materials & Methods

3.1 Armfield Modular UHT FT174-26

The experiment runs in this thesis were performed on a laboratory scale UHT delivered from Armfield Limited, seen in Figure 3.2. The unit consists of a small balance tank, a feed product pump, 2 heating sections, a holding cell, a cooling section and a filler. It was rebuilt by Tetra Pak in 2017 to include two hot water circuits for an enhanced monitoring of the heating phenomena as compared to heating with steam, which was the initial heating media. The hot water circuits are still heated with steam. Furthermore, during the time of this thesis work it was equipped with 2 differential pressure transmitters, one covering the preheating section and one covering the final heating section. 2 oxygen transmitters with 4 sensors as well as 2 extra pressure transmitters were added on the product line. Beyond the added instruments the machine has transmitters, sensors and controllers for automatic control. The piping and instrumentation (P&ID) diagram is visualized in a small version in Figure 3.1 and in bigger scale in Appendix A. The Armfield is a dual mode machine able to operate also in a direct heating mode which is not regarded in this work. In Table 3.1 below, relevant data obtained from the actual machine, email correspondence with the company support and the instruction manual supplied from Armfield Ltd [32] can be found.

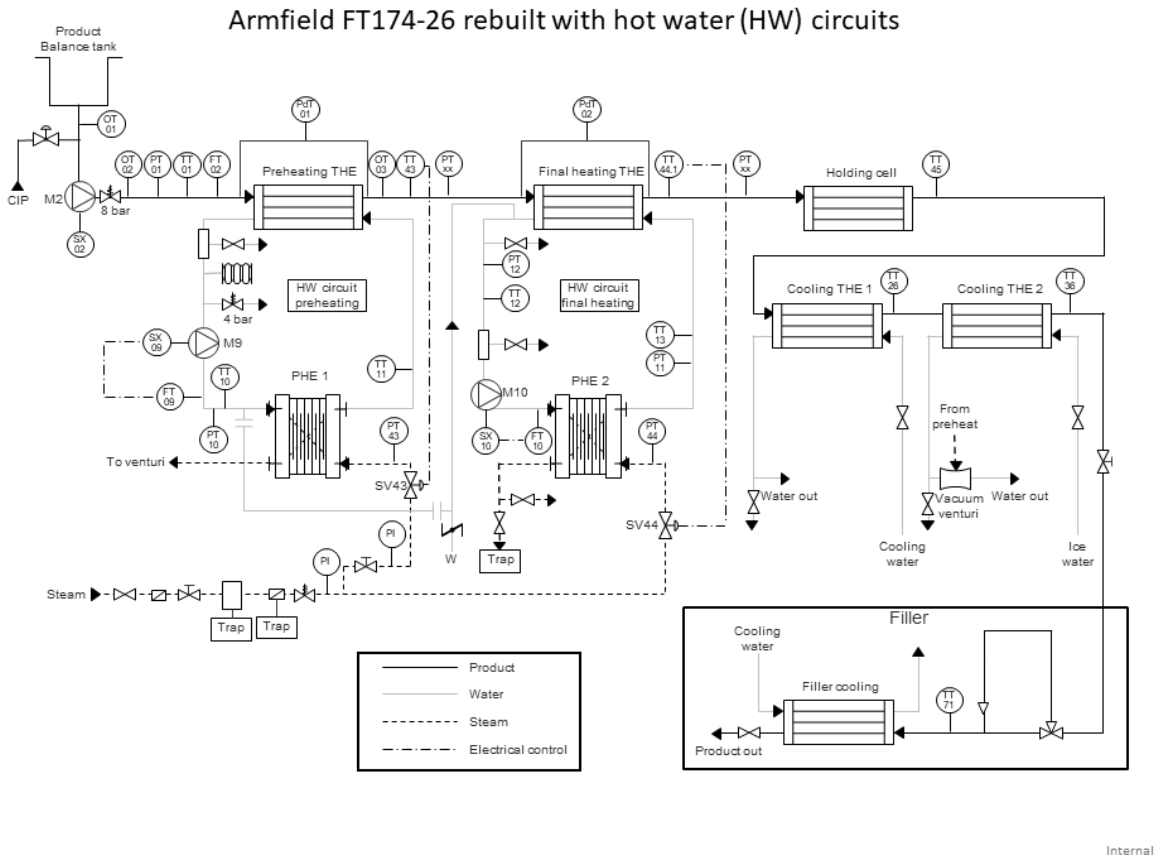

Figure 3.1. Piping and instrumentation process diagram for the Armfield UHT.

Table 3.1. Data regarding the THE used in the experiment runs collected partly from the instruction manual (A), email correspondence (B) and partly from inspecting the machine (C). The letters in parentheses denotes the source of information, values calculated from the data are marked (D).

Armfield Modular UHT FT174-26	**Value**	**Unit**	**Source**
Number of heating sections	2	-	A
Number of tubes per heating section	8	-	A
Number of 180° bends per heating section	7	-	C
Bend diameter	~8.5	cm	C
Tube diameter product side	8.1	mm	A
Product tube wall thickness	0.711	mm	B
Tube diameter medium side	15.8	mm	A
Length heated per tube	0.4	m	A
Material	316 SS	-	A
Heat conductivity 316 SS [33]	13-17	W/ m K	
Assembled test pressure	20	bar	A
Working pressure (maximum)	15	bar	A
Heated length per section	3.2	m	D
Total length per section	4.1	m	D

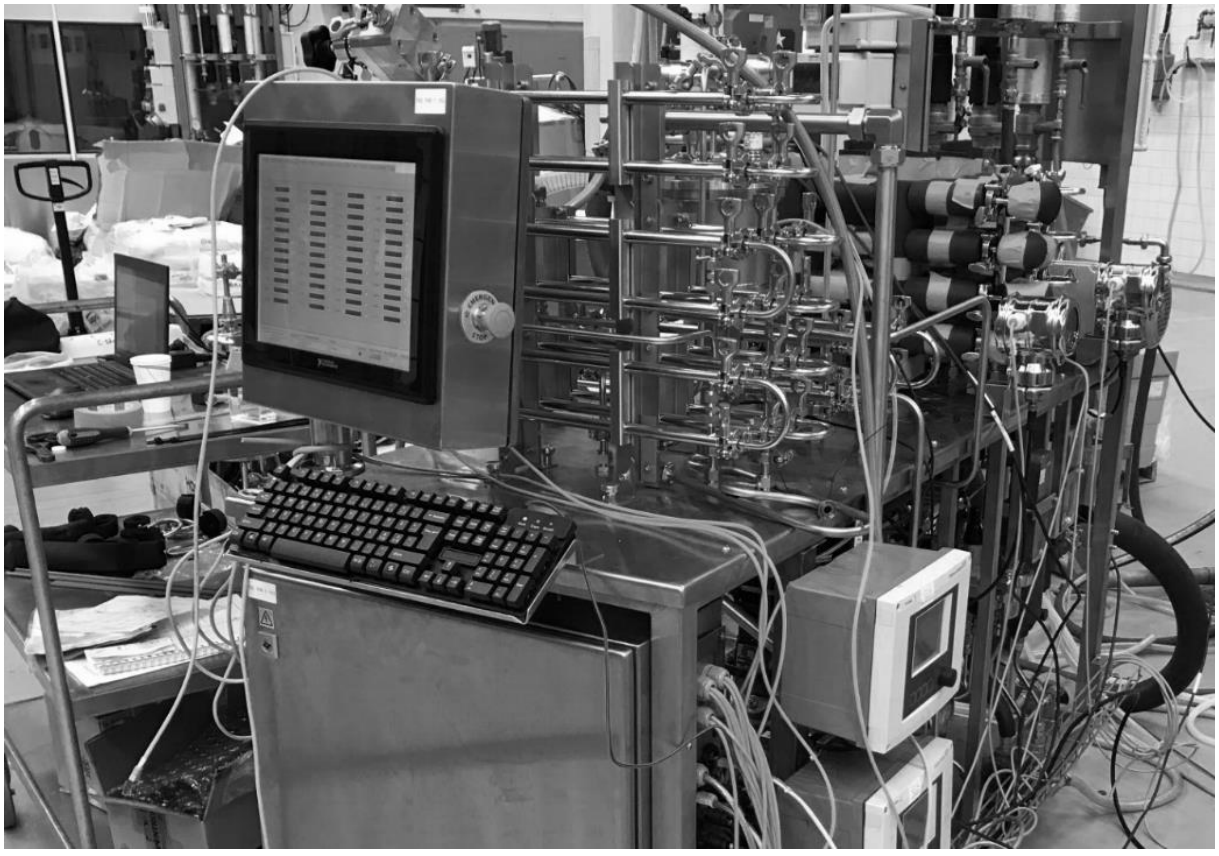

Figure 3.2. The Armfield UHT with touch screen, cooling section behind and PLC in the cabinet below. In the background the insulated heating sections can be seen.

3.2 Operating the Armfield

3.2.1 Hardware and equipment operation

Product configuration
The milk was delivered in “bag in box” packages á 10 L, regular low pasteurized 3% fat Swedish whole milk (“standardmjölk”) was used. Fed to the product pump are two inlets, one connected to water and one dedicated to product coming from the tank upstream. The pump in the unit is a variable speed progressing cavity pump with a frequency converter and has 2 modes of operation. Standard flow mode is used in normal production and ranges from 10-55 l/h approximately. High flow mode is primarily intended for CIP but is available for use in production also and ranges from about 30-140 l/h. During start up the machine is fed with water which is heated to the selected temperature profile throughout the machine. When steady state is reached the inlet is switched to product feed and the experiment run is initiated.

From trial and error, it was discovered that the pump had issues if the product flow not fully had reached the inlet and thus experienced cavity problems. This was not a problem with the water inlet since the pressure from the water supply was very high, but the liquid column in the product tank just barely exceeded the altitude of the pump. The problem was solved with a simple manual throttle valve mounted on the end of the product tube. The valve was open until the product flow reached the outlet and then closed to keep the liquid. Then the tube was connected to the pump and the valve was opened again. The product travels through the THE with heating or cooling water flowing counter current. The processed product was collected in buffer tanks to be sent to destruction and biogas production.

Monitoring conditions on the product line valid for this project were initially very limited. With time several components were, with slight delays, delivered and mounted on the UHT with input from colleagues and help from welders. All components were however dimensioned for a full-size plant which meant weight and size issues when mounting them. Custom made stands and tube spacers had to be manufactured for support and fitting purposes.

Both pressure (PT) and differential pressure transmitters (dPT) where connected to the preheating and final heating sections. The differential pressure sensors had to be located in a horizontal position which meant spacers had to be added due to the bulky and voluminous size of the sensors, see Figure 3.3. Two sensors per dPT where fitted on the UHT, located on the high and low-pressure sides respectively. The signals from the sensors are collected and compared in the transmitter. Compared to a regular PT, which most often refers to gauge pressure, a dPT displays a much more exact measurement of the pressure drop since the comparison is only internal.

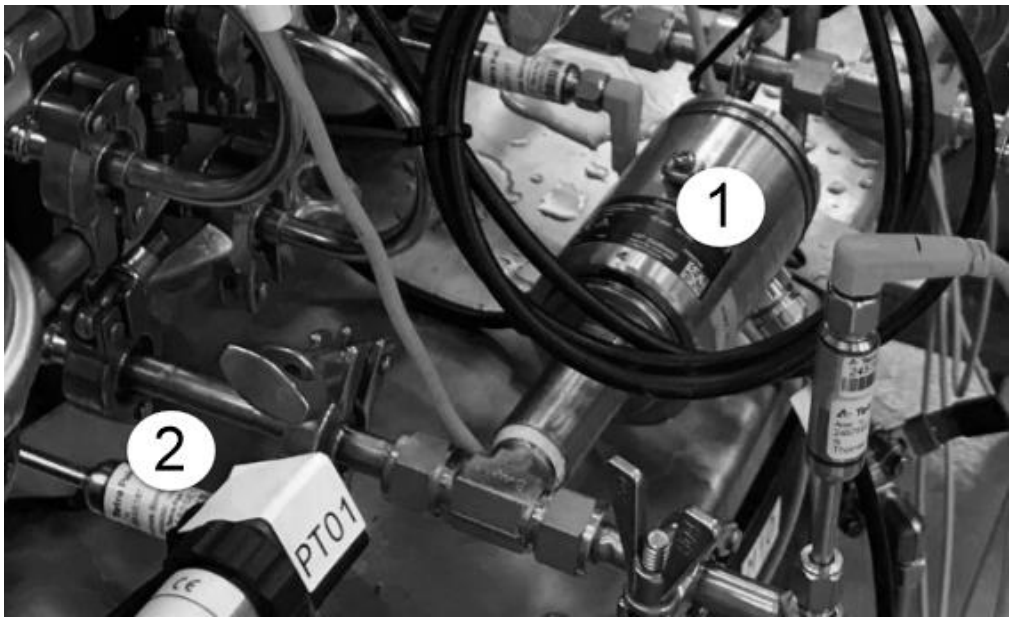

Figure 3.3. Differential pressure sensor (1) and spacer (2) to fit the unit on the preheating section.

The oxygen sensors were quite a hassle to get a grip on. Initially they were mounted on the correct positions throughout the process and tested with circulating water without heating. A temperature limitation of 80 °C for valid measurements [34] resulted in sensors placed after the product tank (OT01), after the pump (OT02) and after the preheating section (OT03). OT04 was sometimes placed after the final heating section (when lower temperature programs were run) and sometimes after the cooling sections. The sensors displayed similar values but with a magnitude of about 3 times the theoretical. After more investigation in the product datasheet [34], the installation orientation was of great importance. The sensors use optics to measure dissolved oxygen levels and is thus very sensitive to partly buildup of deposits and mostly air cushions on the spot cap. An ascending flow was required to assure that the housing was completely filled with liquid. The problem is shown in Figure 3.4 where a housing was unscrewed and opened for a visual examination and troubleshooting before the issue was solved. The sensors were also limited from a horizontal orientation up to 45° with the cap pointing downwards as not to create air pockets. The final positioning of a sensor is visualized in Figure 3.5.

Figure 3.4. Oxygen sensor housing opened up for examination with ascending product flow coming from (1) and sensor cap (2).

Figure 3.5. The positioning of oxygen sensor denoted "OT02" in the flow diagram with the flow direction marked with the arrow.

After each run the machine was opened up for inspection and photographic documentation of the pipes and the fouling. The breaking down of the fouling during cleaning was monitored with the differential pressure as well as opening the machine afterwards.

Process media configuration

The hot water circuits are heated with steam in two separate PHE. They deliver a flow rate of ~370 l/h at maximum capacity and water at ~25 °C. The steam delivered from the steam-boiler

on site has a pressure of well over 7 bar. With steam reducing valves the pressure was reduced to around 2 and 5 bar in preheating and final heating respectively.

Calculations from observed values at steady state on the primary water test showed that the overall heat losses were around 15%, comparing heat transferred from the HW circuits and the heat taken up by the product. These results indicated that the THE had to be thoroughly insulated, partly to reduce the heat losses partly for the sake of the temperature transmitters. The metal in the temperature transmitters radiates heat without proper insulation and thus displays a lower temperature than the real. The temperature transmitters on the HW circuit were initially placed below the THE far away from the inlet and outlet to the product tube. These were moved to better positions as to measure values with less heat loss to the environment and obtaining a better energy balance calculation. With these changes the overall heat loss was decreased to 5% overall losses. In Figure 3.6, before and after photos showing the insulation added by the writer along with the above listed features. The insulation was *Armaflex* from *Armacell* which can withstand a temperature of 175 °C.

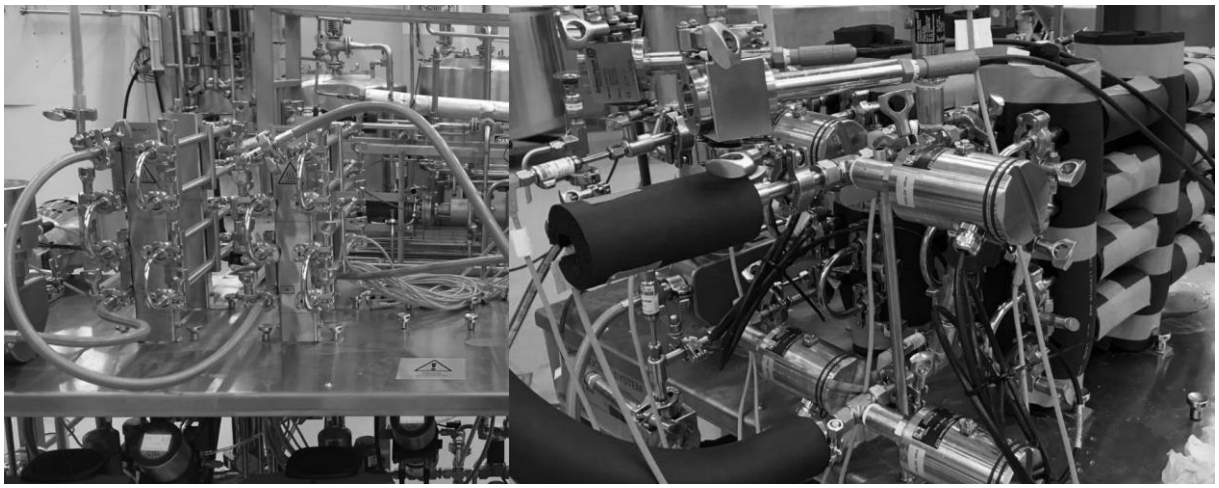

Figure 3.6. The preheat and final heat section in the UHT, stripped machine delivered from Armfield to the left and insulated machine with differential pressure sensors, oxygen sensors etc. to the right.

3.2.2 Software operation & touch screen control

The UHT is controlled and monitored from a PLC (programmable logic controller) connected to a touch screen with the user interface adjusted and enhanced to Tetra Pak standard. Initially the software is switched on and setting for the mode of operation is chosen, see section “Start up protocol” in Appendix B for further specified information. The product flow and temperature profile is set as well as the flows in the hot water circuits. With PID control loops the outlet temperatures from the heating sections are adjusted to the setpoints, see (TT43-SV43) and (TT44.1-SV44) connections in P&ID in Appendix A. Since the flow in each hot water circuits are set values the loop controls the temperatures with regulating steam valves (SV). If the outlet product temperature transmitter (TT) is showing values to low, the steam valve opens more resulting in a greater temperature in the hot water circuit and thus an increased product temperature until reaching the set point. In a similar matter the control loops of the hot water circuits adjust the flows to the setpoints with the flow transmitters (FT) and the pump frequency converters (SX), see (FT09-SX09) and (FT10-SX10) connections in P&ID in Appendix A. The

preset control values of the proportional, integral and derivative terms were used throughout all runs. They resulted in a decent control of the process with a fast reaction without too much overshoot and oscillations.

The HMI on the touch screen consists of several tabs for an enhanced monitoring of the process and ability for manual input if needed, see Figure 3.7. The tab *Process* is an overview, showing product and HW temperatures, flow rates and pressures as well as the steam valve opening percentage in a pedagogic and instinctive way. From this view problems as falling temperatures or flow rates which need direct manual action are visualized. The tab *I/O* contains all values of process data in real time that can be logged. Beyond contents of the *Process* tab all pressures, differential pressure, dissolved oxygen content and the values of the pump frequency converters can be found. Tabs for all PID loops are present as for example *TIC43* showing both the present values of the setpoint, process value and control signal as well as charts showing the trend over time. In *Dev* the deviation of process values from setpoints are displayed as an allowed limit and an absolute difference over a chosen time span. This is utilized to determine if the machine has reached steady state and is ready for a run or if values during a run fluctuates too much to be reliable. In the *Force* tab all valves and pumps can be forced into an active position which is useful when troubleshooting after encountering various issues or problems.

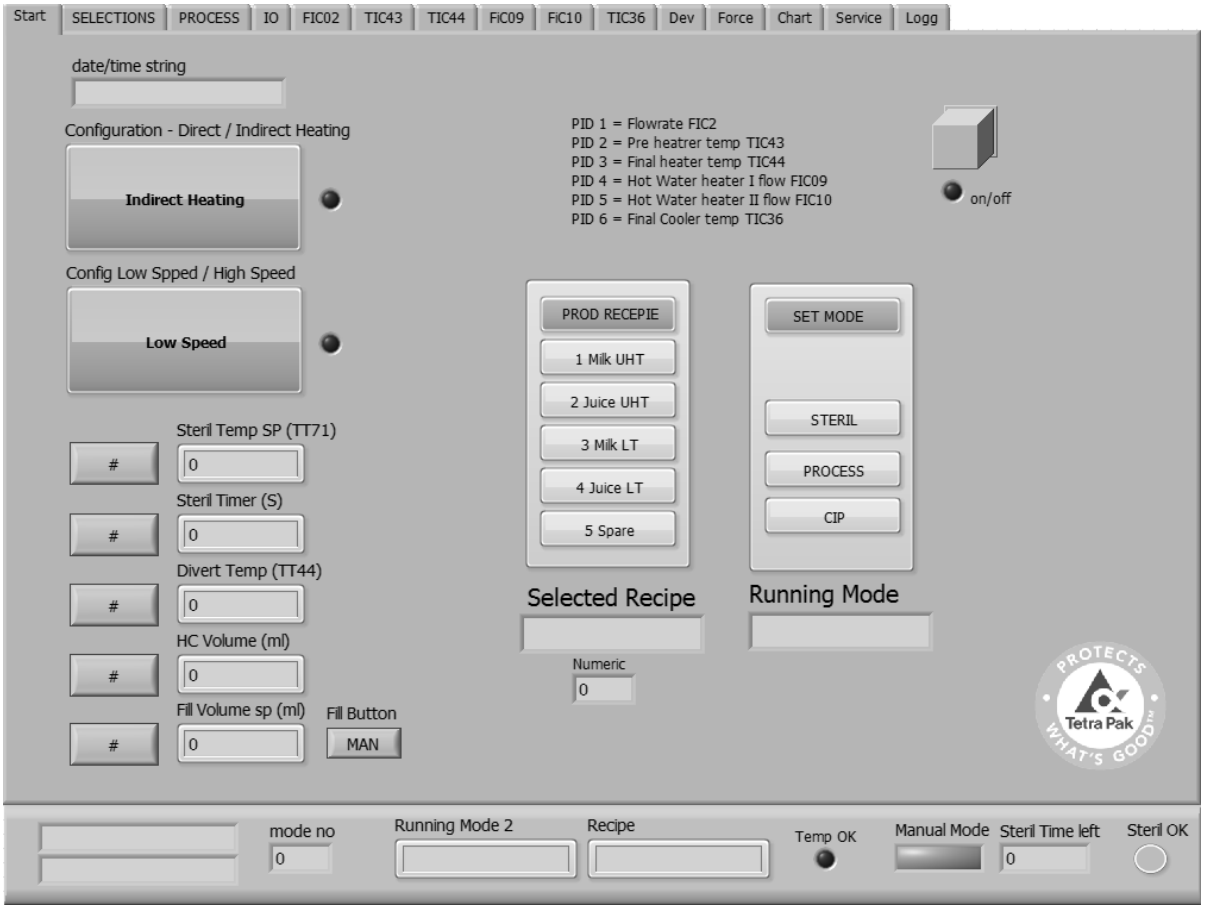

Figure 3.7. The Armfield touch screen with HMI tab "Start" showing.

The writer was included in some steps in the process of constructing and testing the automation and adapting the HMI to the project needs prior the time of the runs. But with the limited knowledge in programming and automation the changes were constructed and implemented by colleagues at the department of R&T.

3.2.3 Logging of process data

The tab *Logg* contains the settings for the logging of process data. For this project another kind of data logging than the predefined was desirable. It was constructed by entering a number of samples to take and the frequency of sample collection in combination with a wait time. By this constellation the logger collected one sample every second for 60 seconds and then waited for 240 seconds (4 minutes) and the was repeated. These logging parameters resulted in a good balance between not receiving a massive amount of data and the uncertainty of not logging temporary peaks or valleys. Variables to log are chosen by checking boxes in the *I/O* view. Since basically only the heating phenomena was of interest to measure in the runs a lot of process values were intentionally disregarded.

3.3 Experimental plan

The design of experiments was created to monitor the fouling rate with varying process pressure and dissolved oxygen level in the product inlet. The array of conditions can be seen in Table 3.2. The goal is to obtain a benchmark in the middle ground of the array and monitor the consequences of a factor by varying it solely or obtain interactions in the corners of the array.

Table 3.2. Array of experimental conditions varying the process pressure and oxygen level

←Increased pressure \ Decreased O_2 level →			
	Low pressure High O_2 level	Low pressure Medium O_2 level	Low pressure Low O_2 level
	Medium pressure High O_2 level	Medium pressure Medium O_2 level	Medium pressure Low O_2 level
	High pressure High O_2 level	High pressure Medium O_2 level	High pressure Low O_2 level

3.3.1 Altering oxygen level

To alter the dissolved oxygen level of the product it was decided to vary the product temperature. The other option was to change the pressure but this solution was harder to implement with the material at hand. An insulated and jacketed 250 L yoghurt tank with an impeller was found unused at the site and thus became dedicated for the purpose, see Figure 3.8. For the jacket either cooling water at ~4 °C, depending on outside temperature, or hot water at ~55 °C was used. The temperature was monitored by switching TT71 to the tank thermometer, see TT71 (Alt. 2) in Figure 3.1.

Figure 3.8. The tank used to store and heat/cool the product during a run.

3.3.2 Altering process pressure

The process pressure in the system is set with a manual back pressure valve. The pressure measurements tended to be a bit noisy and drift from the setpoint if the screw nut was not really tightened. The upper limitation is due to a safety valve releasing at 8 bar and the lower limit is a high enough pressure to avoid boiling in the pipes. When examining the consequences of changing a variable it is important to keep variables not examined constant. If not, the risk of reading something into what was actually a consequence of another process than thought is present.

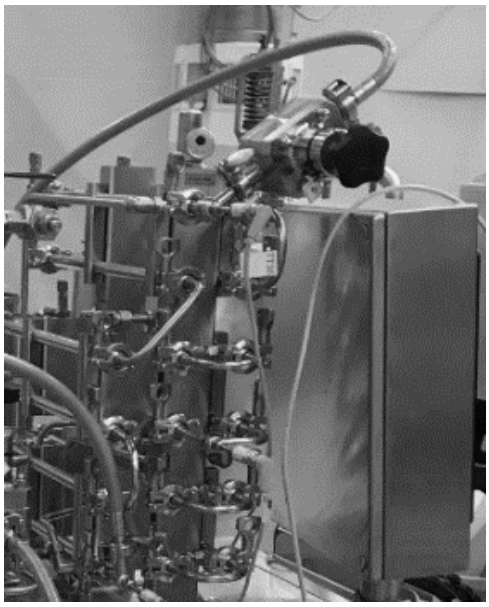

Figure 3.9. The manual back pressure valve visualized in the upper right corner of the picture.

3.4 Determining an operating point

When a suitable flow to operate the unit at was determined, several upper and lower factors constraining the flow were concluded. Either by physical limits (feed pump, THE area) or theoretical (enough flow to utilize certain equations). This was done in an early stage before runs on the THE had begun.

3.4.1 Feed pump

The pump limits the upper bound of the flow capacity and thus limits the Reynolds number that can be achieved in the process. The variable factors Reynolds depend on are the flow, dynamic viscosity and density, see Eq. 15, the two latter are temperature dependent. Consequently, the Reynolds number was calculated at varying flows delivered by the pump and varying temperatures in the UHT range. Polynomials for the viscosity and density with milk temperature as input variables were utilized. The resulting matrix can be seen in Figure 3.10. A turbulent flow regime was aimed towards to be able to utilize Blasius correlation seen in Eq. 17, meaning the lower limit of the flow is constrained by obtaining a high enough Reynolds number.

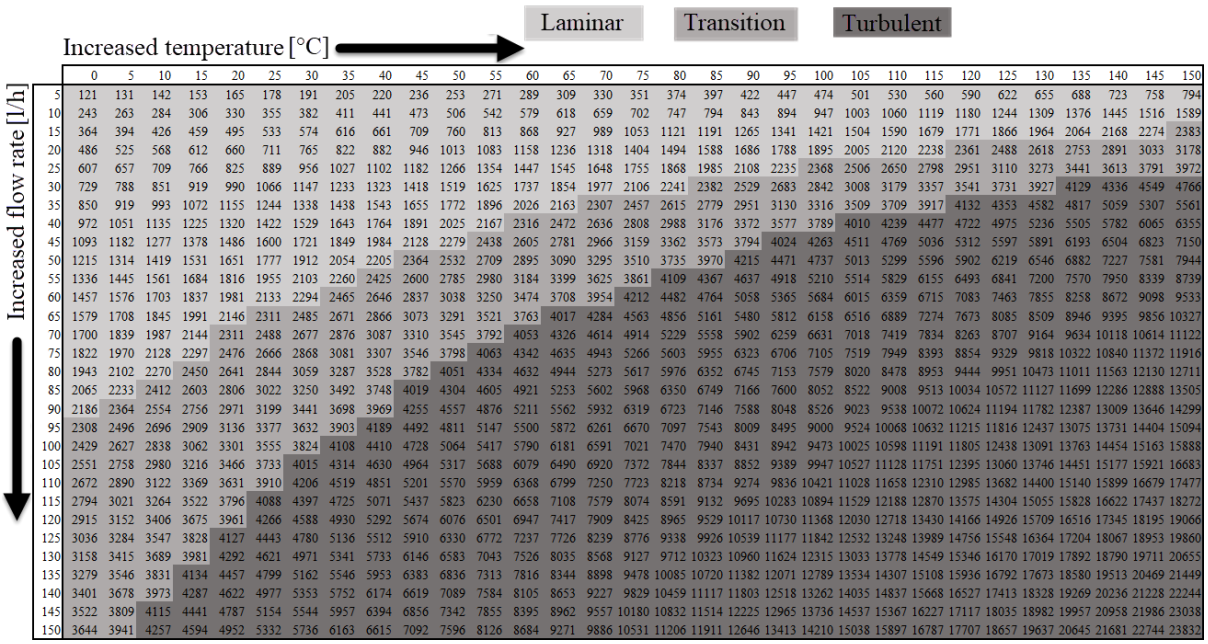

	0	5	10	15	20	25	30	35	40	45	50	55	60	65	70	75	80	85	90	95	100	105	110	115	120	125	130	135	140	145	150
5	121	131	142	153	165	178	191	205	220	236	253	271	289	309	330	351	374	397	422	447	474	501	530	560	590	622	655	688	723	758	794
10	243	263	284	306	330	355	382	411	441	473	506	542	579	618	659	702	747	794	843	894	947	1003	1060	1119	1180	1244	1309	1376	1445	1516	1589
15	364	394	426	459	495	533	574	616	661	709	760	813	868	927	989	1053	1121	1191	1265	1341	1421	1504	1590	1679	1771	1866	1964	2064	2168	2274	2383
20	486	525	568	612	660	711	765	822	882	946	1013	1083	1158	1236	1318	1404	1494	1588	1686	1788	1895	2005	2120	2238	2361	2488	2618	2753	2891	3033	3178
25	607	657	709	766	825	889	956	1027	1102	1182	1266	1354	1447	1545	1648	1755	1868	1985	2108	2235	2368	2506	2650	2798	2951	3110	3273	3441	3613	3791	3972
30	729	788	851	919	990	1066	1147	1233	1323	1418	1519	1625	1737	1854	1977	2106	2241	2382	2529	2683	2842	3008	3179	3357	3541	3731	3927	4129	4336	4549	4766
35	850	919	993	1072	1155	1244	1338	1438	1543	1655	1772	1896	2026	2163	2307	2457	2615	2779	2951	3130	3316	3509	3709	3917	4132	4353	4582	4817	5059	5307	5561
40	972	1051	1135	1225	1320	1422	1529	1643	1764	1891	2025	2167	2316	2472	2636	2808	2988	3176	3372	3577	3789	4010	4239	4477	4722	4975	5236	5505	5782	6065	6355
45	1093	1182	1277	1378	1486	1600	1721	1849	1984	2128	2279	2438	2605	2781	2966	3159	3362	3573	3794	4024	4263	4511	4769	5036	5312	5597	5891	6193	6504	6823	7150
50	1215	1314	1419	1531	1651	1777	1912	2054	2205	2364	2532	2709	2895	3090	3295	3510	3735	3970	4215	4471	4737	5013	5299	5596	5902	6219	6546	6882	7227	7581	7944
55	1336	1445	1561	1684	1816	1955	2103	2260	2425	2600	2785	2980	3184	3399	3625	3861	4109	4367	4637	4918	5210	5514	5829	6155	6493	6841	7200	7570	7950	8339	8739
60	1457	1576	1703	1837	1981	2133	2294	2465	2646	2837	3038	3250	3474	3708	3954	4212	4482	4764	5058	5365	5684	6015	6359	6715	7083	7463	7855	8258	8672	9098	9533
65	1579	1708	1845	1991	2146	2311	2485	2671	2866	3073	3291	3521	3763	4017	4284	4563	4856	5161	5480	5812	6158	6516	6889	7274	7673	8085	8509	8946	9395	9856	10327
70	1700	1839	1987	2144	2311	2488	2677	2876	3087	3310	3545	3792	4053	4326	4614	4914	5229	5558	5902	6259	6631	7018	7419	7834	8263	8707	9164	9634	10118	10614	11122
75	1822	1970	2128	2297	2476	2666	2868	3081	3307	3546	3798	4063	4342	4635	4943	5266	5603	5955	6323	6706	7105	7519	7949	8393	8854	9329	9818	10322	10840	11372	11916
80	1943	2102	2270	2450	2641	2844	3059	3287	3528	3782	4051	4334	4632	4944	5273	5617	5976	6352	6745	7153	7579	8020	8478	8953	9444	9951	10473	11011	11563	12130	12711
85	2065	2233	2412	2603	2806	3022	3250	3492	3748	4019	4304	4605	4921	5253	5602	5968	6350	6749	7166	7600	8052	8522	9008	9513	10034	10572	11127	11699	12286	12888	13505
90	2186	2364	2554	2756	2971	3199	3441	3698	3969	4255	4557	4876	5211	5562	5932	6319	6723	7146	7588	8048	8526	9023	9538	10072	10624	11194	11782	12387	13009	13646	14299
95	2308	2496	2696	2909	3136	3377	3632	3903	4189	4492	4811	5147	5500	5872	6261	6670	7097	7543	8009	8495	9000	9524	10068	10632	11215	11816	12437	13075	13731	14404	15094
100	2429	2627	2838	3062	3301	3555	3824	4108	4410	4728	5064	5417	5790	6181	6591	7021	7470	7940	8431	8942	9473	10025	10598	11191	11805	12438	13091	13763	14454	15163	15888
105	2551	2758	2980	3216	3466	3733	4015	4314	4630	4964	5317	5688	6079	6490	6920	7372	7844	8337	8852	9389	9947	10527	11128	11751	12395	13060	13746	14451	15177	15921	16683
110	2672	2890	3122	3369	3631	3910	4206	4519	4851	5201	5570	5959	6368	6799	7250	7723	8218	8734	9274	9836	10421	11028	11658	12310	12985	13682	14400	15140	15899	16679	17477
115	2794	3021	3264	3522	3796	4088	4397	4725	5071	5437	5823	6230	6658	7108	7579	8074	8591	9132	9695	10283	10894	11529	12188	12870	13575	14304	15055	15828	16622	17437	18272
120	2915	3152	3406	3675	3961	4266	4588	4930	5292	5674	6076	6501	6947	7417	7909	8425	8965	9529	10117	10730	11368	12030	12718	13430	14166	14926	15709	16516	17345	18195	19066
125	3036	3284	3547	3828	4127	4443	4780	5136	5512	5910	6330	6772	7237	7726	8239	8776	9338	9926	10539	11177	11842	12532	13248	13989	14756	15548	16364	17204	18067	18953	19860
130	3158	3415	3689	3981	4292	4621	4971	5341	5733	6146	6583	7043	7526	8035	8568	9127	9712	10323	10960	11624	12315	13033	13778	14549	15346	16170	17019	17892	18790	19711	20655
135	3279	3546	3831	4134	4457	4799	5162	5546	5953	6383	6836	7313	7816	8344	8898	9478	10085	10720	11382	12071	12789	13534	14307	15108	15936	16792	17673	18580	19513	20469	21449
140	3401	3678	3973	4287	4622	4977	5353	5752	6174	6619	7089	7584	8105	8653	9227	9829	10459	11117	11803	12518	13262	14035	14837	15668	16527	17413	18328	19269	20236	21228	22244
145	3522	3809	4115	4441	4787	5154	5544	5957	6394	6856	7342	7855	8395	8962	9557	10180	10832	11514	12225	12965	13736	14537	15367	16227	17117	18035	18982	19957	20958	21986	23038
150	3644	3941	4257	4594	4952	5332	5736	6163	6615	7092	7596	8126	8684	9271	9886	10531	11206	11911	12646	13413	14210	15038	15897	16787	17707	18657	19637	20645	21681	22744	23832

Figure 3.10. Reynolds number calculated at varying flow and temperature (and thus varying viscosity and density). The different flow regimes are color coded and defined above the chart.

3.4.2 Hot water circuits

The next issue was regarding if the hot water circuits could manage to heat a sufficiently high product flow to the desired temperature profile. The given capacity of the pumps in the circuits is more than double compared to the product pump maximum capacity. By this fact and since milk and water are similar heat property wise the capacity of the hot water circuits was deemed to probably not be a problem. The steam supplied to heat the hot water circuits is designed for a much larger plant and in abundance delivered in a Tetra Pak pipeline and therefore neither a cause of an issue.

3.4.3 THE

Even though the hot water circuit has enough capacity to heat up the product flow, another limiting factor was the area of the heat exchangers. According to Eq. 2, the smaller heat exchanger area the bigger temperature difference is needed for a given heat load. To examine the limit of product flow where the heating area is sufficient to exchange the required amount of heat with a reasonable logarithmic mean temperature difference, an excel sheet with calculations was constructed. The built-in excel solver was utilized to solve the iterative calculation steps. Initially the product heat load required was calculated from Eq. 1 with flow, temperatures and temperature dependent heat capacity polynomials as input. The medium heat load was matched to this value by the same method and a constraint and varying the temperatures and flow of the heating medium. The objective of the solver was to minimize the difference in heat load calculated separately from Eq. 1 and Eq. 2. The complexity of the problem was that when the medium heat load was matched to the product heat load changing the medium temperature and flow, both the logarithmic mean temperature difference and overall heat transfer coefficient was altered rendering a new scenario. The solver managed to converge nicely with some initial help of defining reasonable start values.

According to the solver results, the THE could theoretically manage to heat a product flow of 140 l/h at the desired temperature profile. At this point the medium inlet flow is at maximum and has a temperature of above 160 °C, the logarithmic mean temperature difference is about 35 °C, which is to high. The results from the solver are not to be taken as absolute truth due to the many uncertainties and approximations (calculations of Nusselt number in Eq. 7 and neglecting heat losses), but were useful as a tool in encircling the limits for an operating point.

Processing at maximum capacity is never a good idea since a margin is needed to take care of temporary peaks and the steam valve has to open more with time due to fouling build up. The process has a safety valve releasing at 8 bar. To be able to analyze a greater pressure span the maximum temperature was decreased compared to the initial thought, since the fluid in the tubes must not boil.

With the limitations mentioned above the operating point chosen was a flow of 100 l/h heated up to 120 °C maximum temperature. This was a trade-off between taking the air bubble fouling phenomenon into a more UHT perspective than Bennett did and the limitations originating from the Armfield's performance.

3.4.4 Comparison with Tetra Pak Indirect UHT

An aim of this study was to examine the air bubble induced fouling phenomenon found by Bennet in a way more resembling how Tetra Pak machines work. With the use of the Armfield UHT this could partly be obtained, but some limitations on the machine made this goal hard to implement.

Reynolds number

The operating point was chosen with an as high Reynolds number as possible in mind. Fully developed turbulence (>4000) is reached at around 40 °C and evolves to values above 10 000 at the higher temperature span. Tetra Pak's indirect UHT usually starts at 10 000 reaches values in the 100 000 area. This can be seen both as a similarity and difference but compared to what could have been the case, the experimental configuration is fairly well setup.

Heating process

Compared to Bennett's process configuration [8] the heating process in the Armfield is much more similar to Tetra Paks configuration. For example, the tube configuration of a monotube heated with medium on the outside, Bennett used concentric tubes heated both from the middle tube and outer tube. However, differences are still present, for example the lack of stabilization holding tube and deaerator.

Run time

The trade-off from increasing the product flow rate resulted in an increased temperature difference between product and heating medium, thus also an increased wall temperature. This combined with a significantly lower flow velocity (~0.5 m/s) than in a Tetra Pak UHT (>1.5 m/s) led to decreased run times. Although this is negative in general it can be seen as positive for this project. It can sometimes be hard to create fouling even when wanted and the high fouling rate in these runs led to being able to perform many runs within the time limitations.

3.5 Processing experimental run data

3.5.1 Analyzing raw data

Each run resulted in a log file with all process data in a text file format obtained from the PLC with an ethernet cable. From here on the process from raw data to analyzable results, for each run, will be demonstrated with an example run, X11. The file was imported into Excel by a few steps in the *Text Import Wizard* and switching all dots to commas due to format differences. In Excel, the data from the runs were collected in separate sheets in the file *Armfiled experiment runs 2018.xlsx*, see Figure 3.11. For each collection of samples (60 samples every 5 minutes) the average value, standard deviation and relative standard deviation was calculated and checked throughout the run to observe any possible strange behavior or irregularities, see Figure 3.12. Each average calculated from 60 samples is from here on, slightly incorrectly, called a sample for simplified reasons.

		Date	Time [s]	Flow after M2 [kg/h]	Temp prod after M2 [°C]	Temp prod after preheat [°C]	Temp prod after final heat [°C]	Temporary BT temp	Pressure after M2 [bar]	Pressure after preheat [bar]	Pressure after final heat [bar]	Pressure steam preheater [bar]	Pressure steam final heater [bar]	Diff. Pressure preheat [bar]	Diff. Pressure final heat [bar]	Dissolved oxygen 1 [mg/L]
			Time [s]	FT02	TT01	TT43	TT44.1	TT51/71	PT01	PT03	PT04	PT43	PT44	dP01	dP02	OT01
Start at row	100		21:59,2	100,02818	7,80067	68,262053	119,30945	4,496338	6,125274	5,974072	5,930355	2,126271	3,491052	0,064145	0,057703	10,474806
Sample interval [/s]	1		22:00,3	100,0328	7,793405	68,265069	119,39649	4,498541	6,121093	5,974836	5,931032	2,131532	3,495265	0,064161	0,057924	10,47638
Sample time [s]	60		22:01,4	99,996448	7,729116	68,354709	120,25351	4,493532	6,10228	5,974035	5,930867	2,146604	3,50017	0,064089	0,057505	10,491764
Wait time [s]	240		22:02,5	99,92249	7,726381	68,350565	120,34918	4,493427	6,101986	5,97439	5,930381	2,156485	3,504477	0,063812	0,057618	10,488026
Cells for average	60		22:03,5	99,903575	7,719794	68,473434	120,35694	4,497387	6,106317	5,974513	5,931842	2,162492	3,507824	0,063938	0,057025	10,488558
Amount of rows	840,00		22:04,5	100,04018	7,644854	68,766739	120,51844	4,492981	6,106842	5,975552	5,931547	2,169038	3,512213	0,063768	0,057016	10,485882
Samples in run	14		22:05,6	100,05437	7,645792	68,833439	120,62046	4,494817	6,09381	5,975118	5,931845	2,166047	3,519292	0,063779	0,056972	10,50162
			22:06,7	100,04054	7,639431	68,833649	120,68117	4,493853	6,084558	5,975402	5,932184	2,176906	3,525548	0,063912	0,057044	10,49322
			22:07,7	99,988875	7,638996	68,839524	120,7625	4,494267	6,064753	5,975705	5,932637	2,18365	3,5325	0,063896	0,057565	10,493653
			22:08,8	99,953306	7,632877	69,251404	120,85448	4,495211	6,013964	5,975915	5,933209	2,196418	3,541214	0,064004	0,057152	10,51065
			22:09,9	100,01058	7,625378	69,349306	120,93633	4,495866	5,986939	5,976579	5,933166	2,198542	3,547046	0,064117	0,057123	10,517555
			22:11,0	99,956027	7,559213	69,463336	121,00514	4,496443	5,965523	5,976887	5,933888	2,206702	3,551846	0,063845	0,057342	10,504158
			22:12,1	99,96773	7,555594	69,465775	121,09164	4,493952	5,953657	5,976646	5,933383	2,202928	3,561891	0,064089	0,057316	10,512204
			22:13,1	99,91577	7,553745	69,531367	121,16478	4,494529	5,963988	5,976054	5,933794	2,215411	3,567745	0,064217	0,057141	10,509804
			22:14,1	99,895412	7,550021	69,537163	121,2465	4,495788	5,987486	5,977228	5,934217	2,215766	3,573195	0,064194	0,057046	10,510571
			22:15,1	99,902329	7,55161	69,641123	121,25272	4,496417	6,015269	5,976616	5,933889	2,208302	3,576825	0,063881	0,05638	10,51008
			22:16,2	99,929538	7,54872	69,716287	121,41487	4,49959	6,068328	5,976584	5,934273	2,222404	3,588253	0,064101	0,05697	10,509863
			22:17,3	99,9735	7,544996	69,712379	121,42143	4,499958	6,091675	5,977356	5,934446	2,227985	3,591402	0,064155	0,056785	10,511988
			22:18,4	99,922982	7,540049	69,826803	121,50541	4,495397	6,107255	5,976785	5,934699	2,227305	3,594571	0,063925	0,05749	10,527982
			22:19,5	100,00966	7,472765	69,841306	121,6132	4,496732	6,12646	5,976761	5,934055	2,234128	3,604789	0,063961	0,057547	10,525523
			22:20,5	100,03451	7,469432	70,003016	121,61094	4,496706	6,12629	5,976864	5,93455	2,238475	3,610145	0,063876	0,057838	10,535969
			22:21,6	100,02556	7,470265	70,168161	121,75256	4,49369	6,12258	5,977057	5,935171	2,250472	3,616223	0,063961	0,057639	10,538664
			22:22,6	100,10135	7,470031	70,17005	121,75623	4,495761	6,118573	5,977128	5,934851	2,241215	3,609952	0,063732	0,057333	10,536185
			22:23,7	100,04949	7,462531	70,168109	121,92463	4,494791	6,112813	5,977401	5,934896	2,252649	3,606892	0,063874	0,057046	10,550035
			22:24,7	100,0803	7,46451	70,169499	121,92518	4,497178	6,109119	5,976649	5,934822	2,260048	3,605268	0,064001	0,056784	10,544114

Figure 3.11. The raw data from run X11 imported into Excel.

		Time [s]	Flow after M2 [kg/h]	Temp prod after M2 [°C]	Temp prod after preheat [°C]	Temp prod after final heat [°C]	Temporary BT temp	Pressure after M2 [bar]	Pressure after preheat [bar]	Pressure after final heat [bar]	Pressure steam preheater [bar]	Pressure steam final heater [bar]	Diff. Pressure preheat [bar]	Diff. Pressure final heat [bar]	Dissolved oxygen 1 [mg/L]
1	Average	00:00:31	100,0	7,4	70,3	121,6	4,5	6,1	6,0	5,9	2,3	3,5	0,064	0,057	10,5
	Std. dev		0,1	0,2	1,0	0,7	0,0	0,1	0,0	0,0	0,1	0,1	0,0	0,0	0,0
	Rel. dev		0%	2%	1%	1%	0%	1%	0%	0%	2%	3%	0%	1%	0%
2	Average	00:05:35	100,0	6,9	69,9	119,6	4,5	6,1	6,0	5,9	2,1	3,2	0,064	0,057	11,0
	Std. dev		0,1	0,0	0,2	0,1	0,0	0,1	0,0	0,0	0,0	0,0	0,0	0,0	0,0
	Rel. dev		0%	0%	0%	0%	0%	1%	0%	0%	1%	1%	0%	1%	0%
3	Average	00:10:37	100,0	6,9	70,0	120,2	4,5	6,1	6,0	5,9	2,1	3,2	0,065	0,057	11,5
	Std. dev		0,1	0,0	0,1	0,4	0,0	0,1	0,0	0,0	0,0	0,0	0,0	0,0	0,0
	Rel. dev		0%	0%	0%	0%	0%	1%	0%	0%	0%	1%	0%	1%	0%
4	Average	00:15:41	100,0	7,0	70,1	119,7	4,6	6,1	6,0	5,9	2,1	3,2	0,065	0,057	11,7
	Std. dev		0,1	0,0	0,1	0,3	0,0	0,1	0,0	0,0	0,0	0,1	0,0	0,0	0,0
	Rel. dev		0%	0%	0%	0%	0%	1%	0%	0%	0%	2%	0%	1%	0%

Figure 3.12. The calculated average and deviations for each collection of samples at the given process times for run X11.

3.5.2 Calculating fouling height & HTRF

Each run was transferred into a compiled sheet in Excel where all calculations were performed. The fouling height was calculated at every sample time according to Eq. 22. The measured value from the differential pressure transmitters includes both friction, which we want to measure, as well as pressure difference originating from height difference and one-time losses

(valves, bends etc.). These had to be subtracted from the measured value before entering Eq. 22. The calculated fouling height was plotted over time for each run, see Figure 3.13.

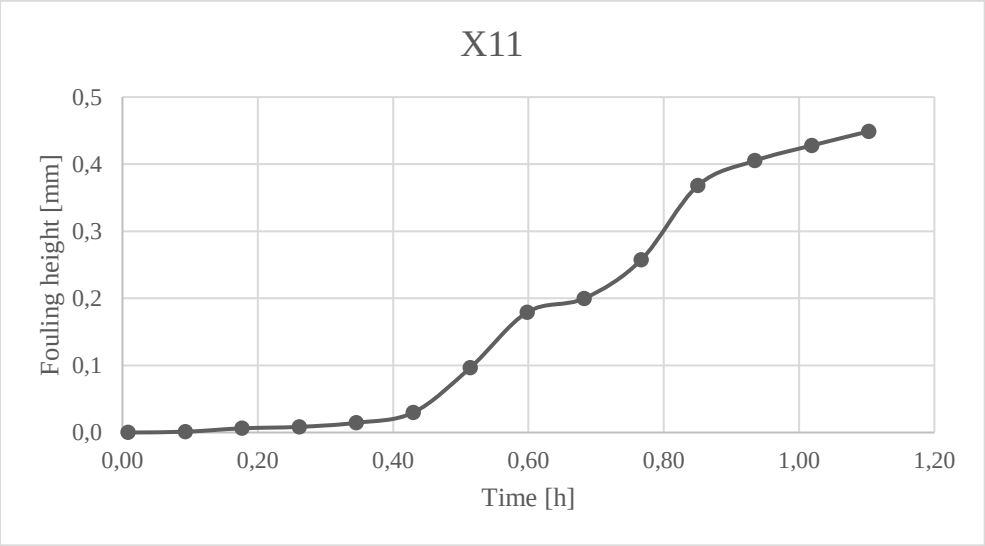

Figure 3.13. The calculated fouling height over time for run X11.

The heat load and heat loss were calculated to analyze the results from the insulation. The heat load was then used to calculate the overall heat transfer coefficient at each time sample together with the logarithmic mean temperature difference and the heat exchanger area, according to Eq. 2 and Eq. 3. The heat transfer reduction factor (HTRF) was then calculated with Eq. 13, comparing the heat transfer coefficient at each sample time with the initial. In Figure 3.14 the HTRF over time can be seen.

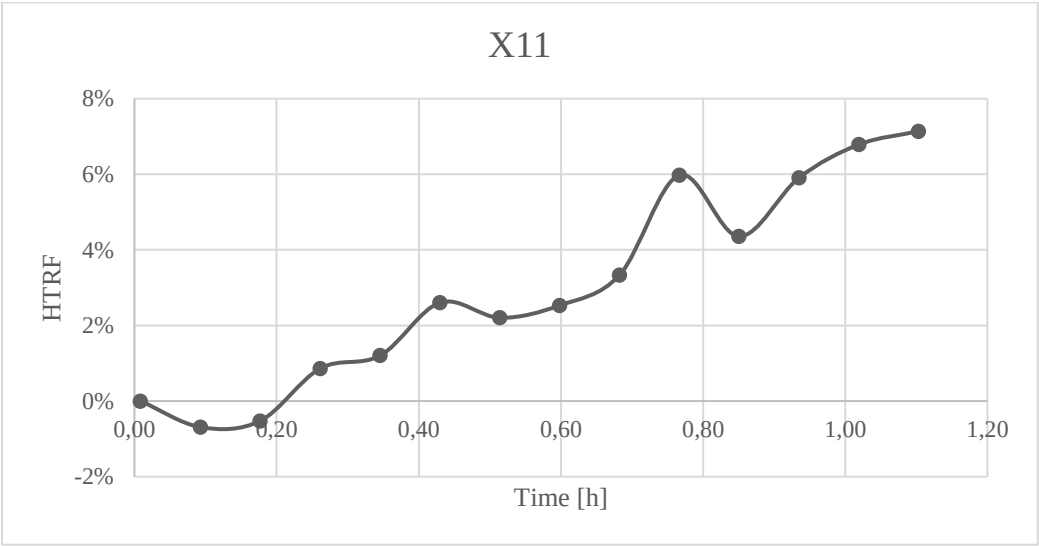

Figure 3.14. The calculated heat transfer reduction factor over time for run X11.

The graphs of fouling height and HTRF were analyzed further, see Figure 3.15. To maintain an as objective view as possible the writer only had the graphs at hand when analyzing and no process data as pressure or oxygen level etc. This was done as not to create the results expected or wanted and read in behavior not really observed, but to obtain the actual behavior of the fouling phenomenon. In each graph the induction period, i.e. the period before something starts to happen, was identified, see (1) in Figure 3.15. From this point two lines were drawn, one corresponding to the initial inclination of the curves (2) and one corresponding to the overall inclination from induction period to the end of run (3). The units of the inclination for these curves are either [mm h^{-1}] when referencing to fouling height rate or [% h^{-1}] when referencing to HTRF rate.

The main reason two lines were drawn originates from reasoning regarding smooth pipes brought up earlier (section Theory, Monitoring fouling formation, Pressure drop). With time, the fouling layer will be overestimated and the calculations are thus less reliable in the latter time span. The initial fouling rate was drawn as a tangent to the curve following the induction period and the total fouling rate as a straight line matching the overall inclination ignoring temporary peaks or valleys.

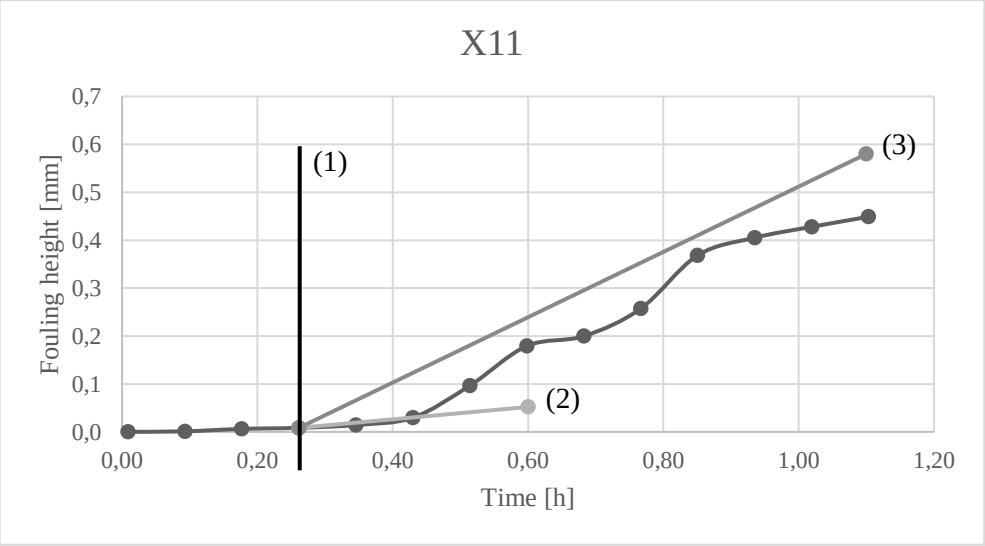

Figure 3.15. The calculated fouling height over time for run X11 with identified induction period (1), initial fouling rate (2) and overall fouling rate (3).

It is uncertain how the HTRF rate differs between initial and overall measurements. As mentioned earlier the product heat transfer coefficient is altered by a fouled heat exchanger surface but the altered direction is not further analyzed. One can envision a more turbulent flow caused by an increased roughness on the surface, but it is unsure to what degree.

3.5.3 Surface temperature & theoretical fouling rate

The calculations regarding tendency for bubble nucleation requires the product temperature on the heat exchanger surface, simply called the surface temperature. By utilizing the calculations regarding heat transfer and fluid properties, Eq. 1 - Eq. 10, the surface temperature was calculated from both the medium and product bulk temperatures. The mean value from these calculations was used since they both seemed to overestimate the heat transfer properties.

The tool based on drying calculations developed in the pilot project at Tetra Pak [9] was during the time of this project developed further. With the structure of the main calculations intact a calculation for fouling rate [mm/h] was introduced. Beyond entering process data as flow rate, pipe diameter and product density, the state in the balance tank (initial state) was entered as product temperature and measured oxygen level. The new state was entered as a measured pressure and the calculated surface temperature. See Figure 3.16 for an overview of the input and output to the calculations.

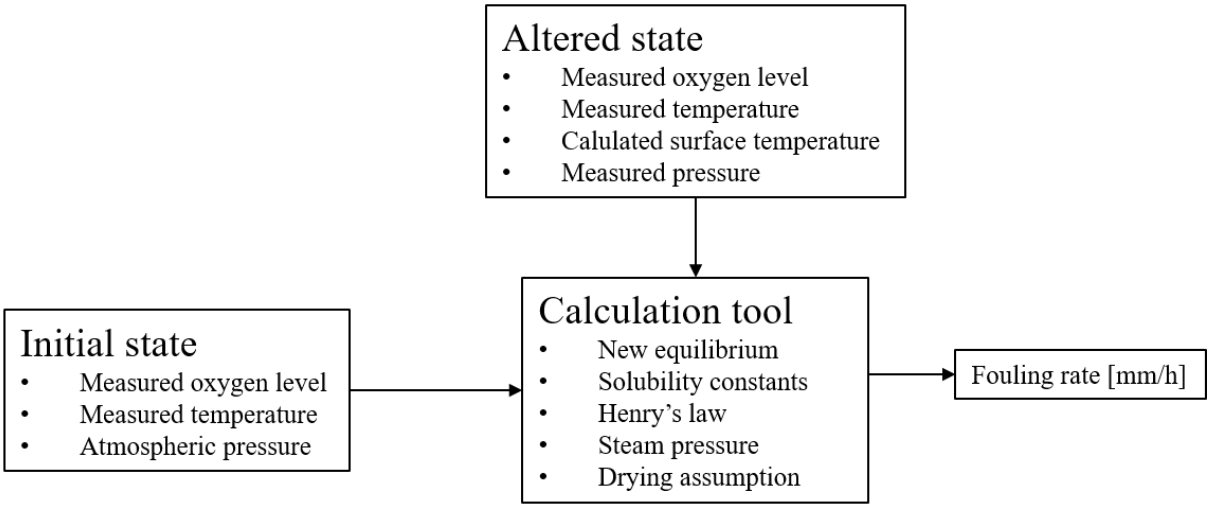

Figure 3.16. A layout overview showing the input and output from the calculation tool.

Several macros in excel were developed by the writer with the purpose of saving time of copying and pasting run data and clicking around in the solver options. By entering which run and sample to analyze in scroll boxes and utilize click buttons with macros, the data analysis was automated to work with just initial input.

The use of the calculation tool was a mean to merge process data into only one variable. The process data between runs were sometimes similar but differed decimals in pressure and oxygen level. Instead of comparing similar pressures and oxygen levels the values were used as input to the calculations resulting in just a comparable fouling rate between runs. This calculated fouling rate was used as comparison to the experimental fouling rate or HTRF rate.

4 Results

4.1 Following the experimental plan

During the course of the project several experimental and trial runs as well as water tests were conducted. Due to the time limitations a master thesis project prevails and due to delays of equipment, the experimental plan could not be followed satisfactory. 17 experimental runs (denoted X01-X17) with at least 100 L milk each run were performed. Before beginning a run, a time of preparing the machine and finding dissolved oxygen equilibrium was present. All milk packages were opened by hand with carpet knife and scissors and poured into the balance tank. Following a run was the CIP process which took about an hour. With this in mind a process cycle lasted for at least half a working day. Some days double runs were performed but this caused stress and the risk of making mistakes increased. The master thesis turned towards more instrumentation of the Armfield and added devices than initially planned.

The runs X01-X06 eventually became dedicated to a lot of trial and error and getting to know the machine since the process data had to be disregarded. During this time the issue with the oxygen sensors became present and resolved and the writer gained a lot of insight in how runs could be performed more efficiently. X07-X11 were conducted in the range of high dissolved oxygen level (around 12 mg/L by cooling the milk to ~4 °C) with varying pressure. During run X09 the pressure was set really high, exceeding 7 bar, which resulted in milk dripping from the safety valve which had released. The pressure had probably temporarily exceeded 8 bar and when examining the results the run was determined to have failed. The experiment runs X12-X16 were performed in the low oxygen level region (around 6 mg/L by heating the milk to ~50 °C).

A final date for experimental runs was set early in the experimental plan to have sufficient time for data processing and analyzing as well as presentation preparations. During the last days a crossroads of either obtaining the middle ground of the experimental array (keeping the milk at room temperature) or taking the runs into a more UHT perspective (increasing the maximum process temperature to ~140 °C) was reached. It was decided to go for the latter option since reaching the UHT perspective was from the beginning an aim in the project. This would somehow result in an extra dimension in the experimental array with altered temperature profile. This decision resulted in a negative outcome for the reliability of the project results since the middle ground of the array was not reached and comparability between oxygen levels was quite low.

During run X17, where the maximum temperature was set to 137 °C, the machine was very much pushed to the boundary of its performance ability. The steam reducing valves was opened fully to have an as high pressure as possible in the entering steam. Eventually the water in the final heating hot water circuit started to boil and the pump was close to cavitation. The process had to be shut down and restarted with adjusted settings, setting a higher temperature between the heating sections letting the preheating section heat more. A second attempt at the run was performed but again troubles with the heating circuits were encountered. Too much steam was flowing to the preheating section, which resulted in steam not condensing in the PHE and steam going out in the drain pipe. A plastic gasket placed on the drain pipe melted and suddenly steam started leaking and the run had to be shut down again. After these events the ordered milk had run out and the time experimental phase had come to an end. The finished experimental plan showing the experiments and failed runs can be seen in Table 4.1.

Table 4.1. The resulting experimental plan with runs corresponding to experimental condition variables and failed runs.

↓ Increased pressure / Decreased O_2 level →					
Low pressure High O_2 level	X10	Low pressure Medium O_2 level		Low pressure Low O_2 level	X14
Medium pressure High O_2 level	X07	Medium pressure Medium O_2 level		Medium pressure Low O_2 level	X12
High pressure High O_2 level	X08 X11	High pressure Medium O_2 level		High pressure Low O_2 level	X13 X15 X16
Not filled into experimental plan: X01-X06, X09, X17					

4.2 Compiled results

In Figure 4.1 and Figure 4.2 the fouling layer and HTRF over time can be seen for all successful runs in the experimental plan, referred to as *all runs* forward. The figures are very crowded and difficult to analyze from this view, the runs with high dissolved oxygen level has a darker tone than the ones with low dissolved oxygen level. In between each series the differentiation is done with different markers. What can be seen, in Figure 4.1, is a pattern of the high oxygen level runs shifting upwards and left. This pattern speaks for a generally thicker fouling layer at a given time if the product has more dissolved oxygen in the inlet, resulting from either an increased fouling rate or a shorter induction period. This pattern is not as obvious in Figure 4.2 but is present to some degree. When analyzing fouling layer runs the inclination of the curve directly corresponds to the fouling rate. The case is not the same when analyzing HTRF runs, but the graphs are more used like patterns for fouling rate instead of absolute correlations with numbers.

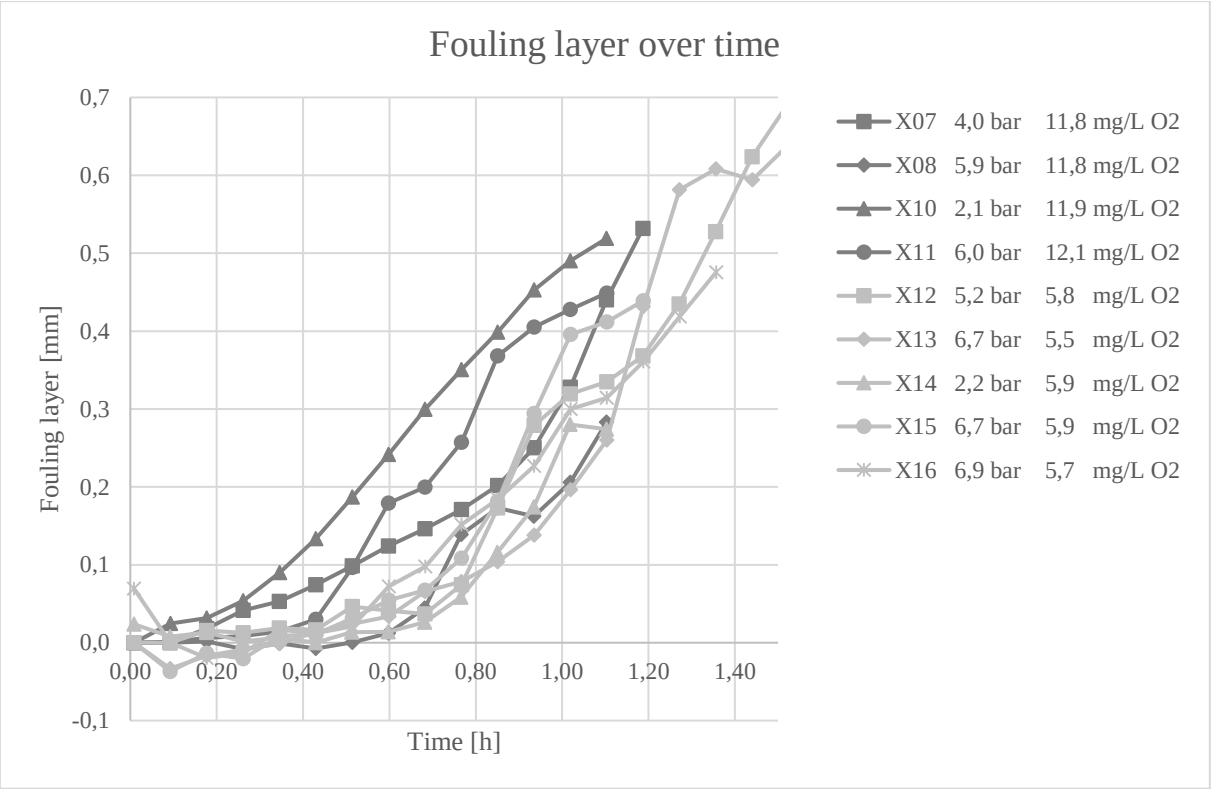

Figure 4.1. An overview of the fouling layer development over time for all runs.

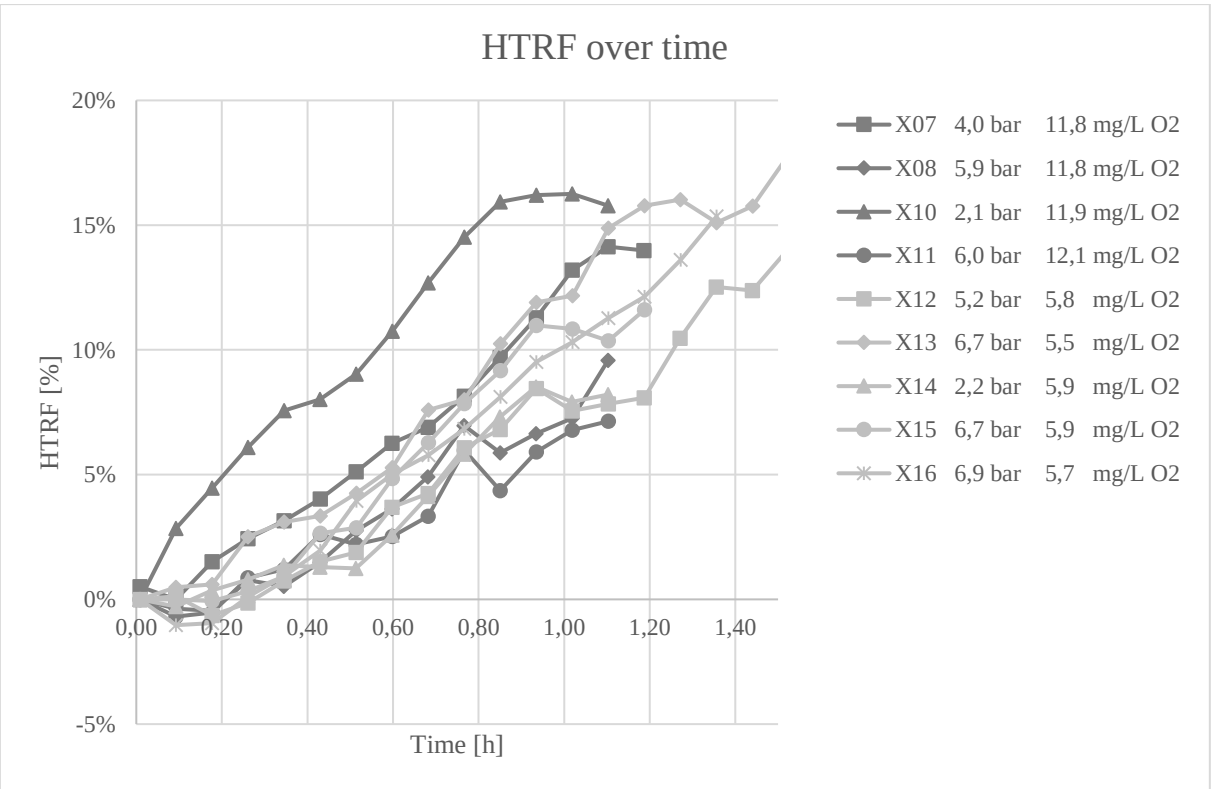

Figure 4.2. An overview the of the HTRF development over time for all runs.

For further analyzes, each set of experimental conditions were divided into sub groups, high and low oxygen level runs. The fouling layer and HTRF for the high level oxygen runs can be seen in Figure 4.3 and Figure 4.4 with the varying pressure between runs. From Figure 4.4 one can see a pattern of graphs shifting downwards and right with increasing pressure, i.e. a lower fouling layer or heat transfer reduction. The same pattern is obtained in Figure 4.3 if analyzing up to 0,5 hours. After this time, run X11 (~6 bar) seem to surpass run X07 (~4 bar). Overall one can see a generally longer induction period in both figures with an increased pressure.

A similar comparison as above for the low level oxygen runs can be seen in Figure 4.5 and Figure 4.6. All runs seem to follow the same pattern of similar induction period and both HTRF and fouling rate. Some runs with low level oxygen were performed for a longer time span but for comparative reasons all graphs have the same time axis bounds. The pattern of longer induction period and lower values with increased pressure, seen in Figure 4.3 and Figure 4.4, is not apparent in Figure 4.5 and Figure 4.6.

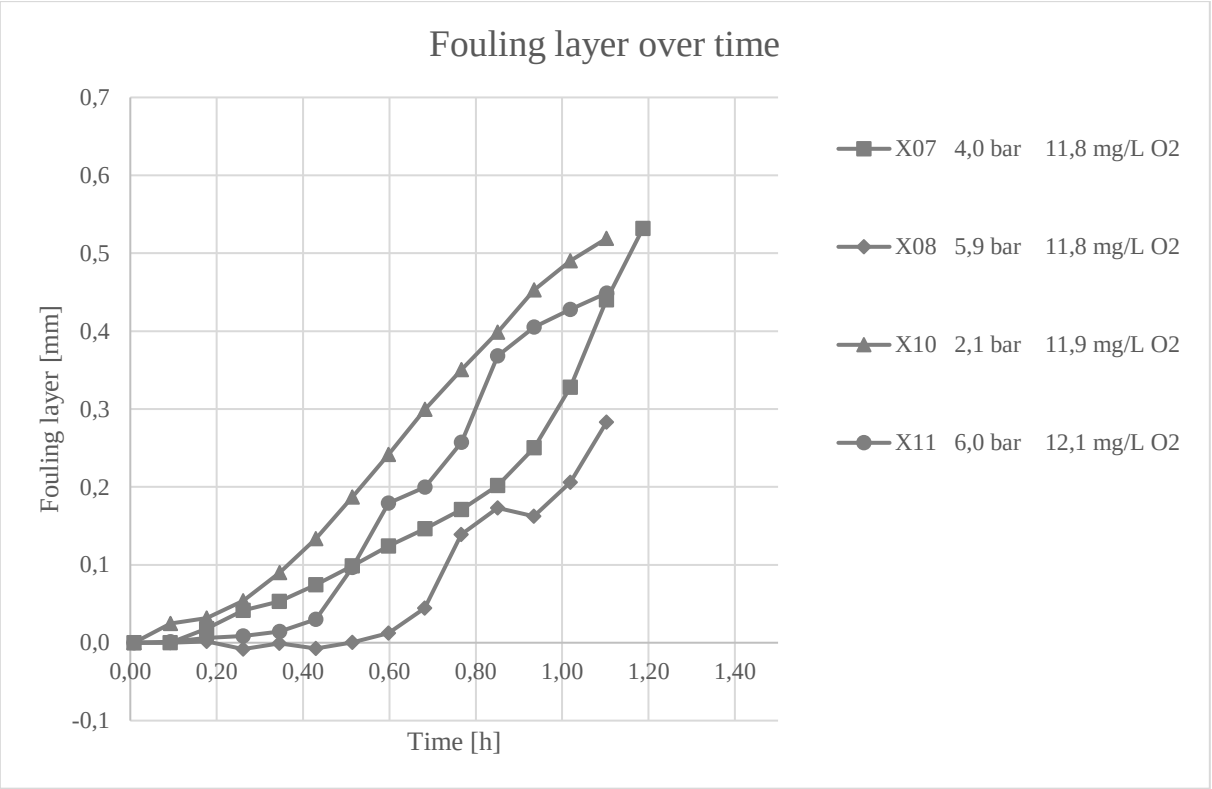

Figure 4.3. The fouling layer development over time for the high dissolved oxygen level runs.

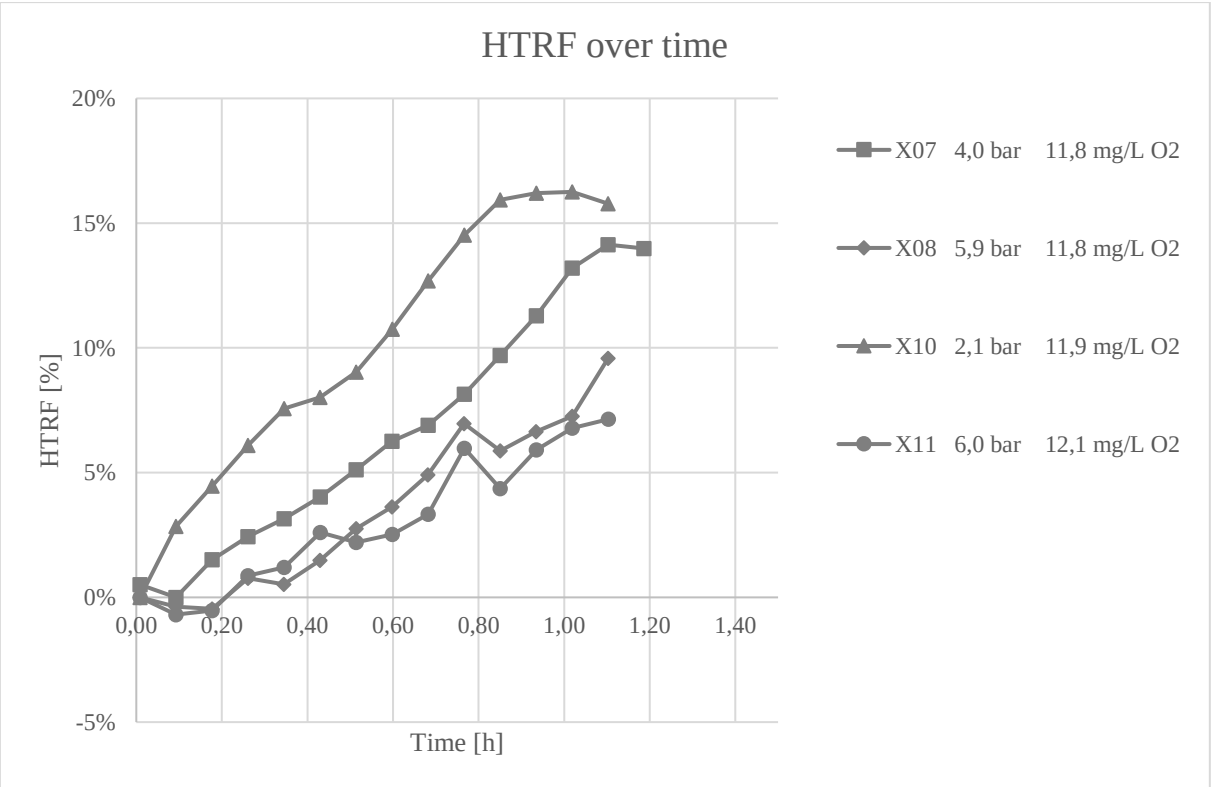

Figure 4.4. The HTRF development over time for the high dissolved oxygen level runs.

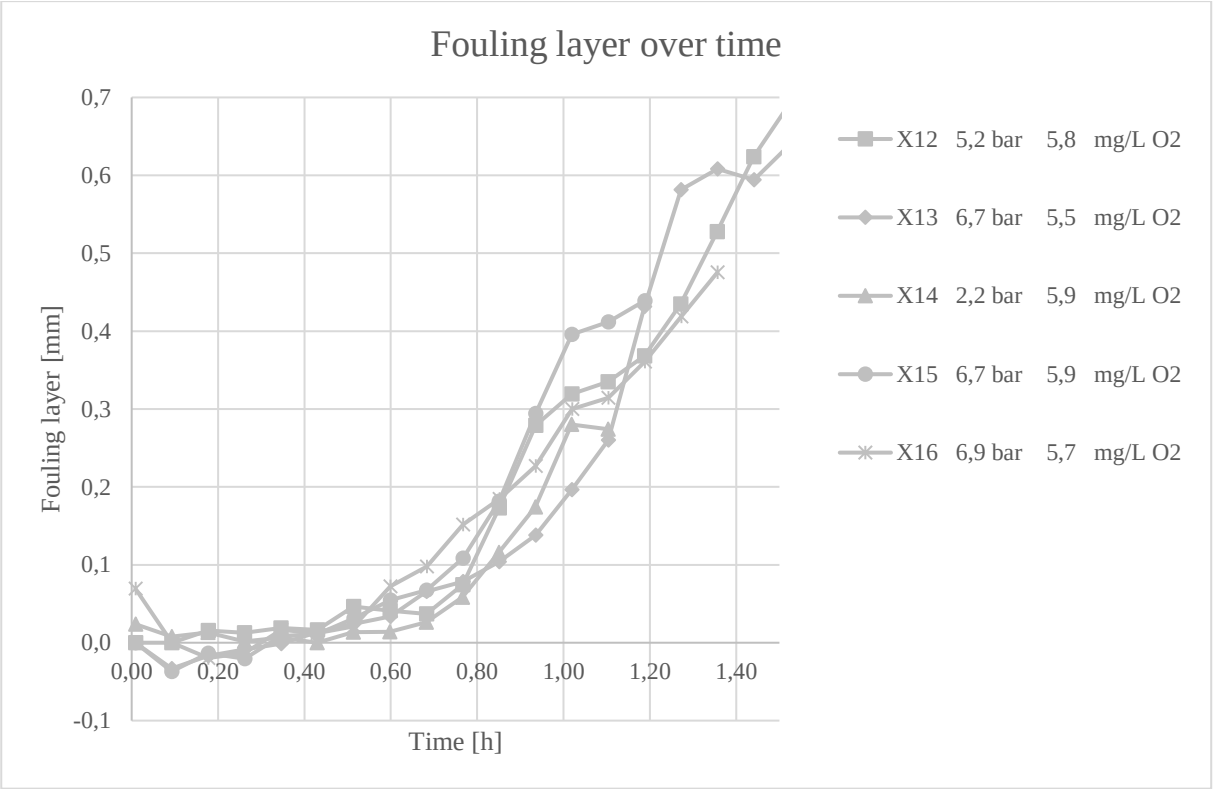

Figure 4.5. The fouling layer development over time for the low dissolved oxygen level runs.

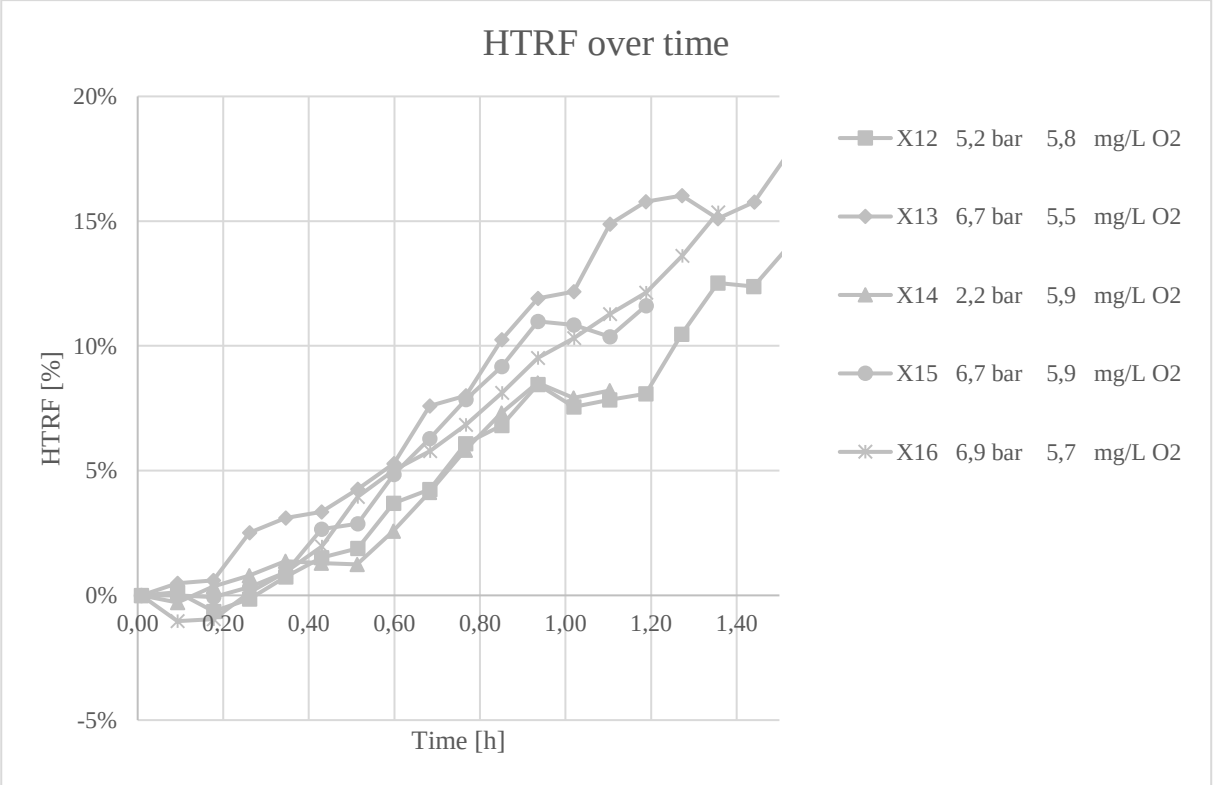

Figure 4.6. The HTRF development over time for the low dissolved oxygen level runs.

4.3 Calculated & experimental fouling rate

Even though the runs were divided into separate sets of experiments, high and low level dissolved oxygen, some differences between them are present. The oxygen levels range from 11,8-12,1 and 5,5-5,9 for high and low runs respectively since it was determined by the fluctuating temperature in the product balance tank. Also, the pressures of runs aimed to fill in the same box in the experimental plan differ slightly, due to the manual setting of the back pressure valve. See for example runs X08 and X11 (5,9 and 6,0 bar respectively) or X13, X15 and X16 (6,7, 6,7 and 6,9 bar respectively). This is where the drying calculations come in very handy. Since they reduce and merge the number of varying factors to analyze in runs from 3 (oxygen level, process pressure and surface temperature) to 1 (calculated fouling rate in mm/h). The calculated fouling rate is used below for many comparisons, sometimes comparing with experimental fouling rate and sometimes comparing with HTRF rate or induction period, obtained as in Figure 3.15. The latter comparisons are not as straightforward when comparing numbers but more used to validate and find patterns.

Figure 4.7 shows the relationship between experimental initial fouling rate and calculated fouling rate for each run. Not much can be gained from analyzing the figure from this view unfortunately. If the runs with low oxygen level are excluded, a power law trendline with a good match can be fitted, see Figure 4.8. What can be seen here is a clearly increased initial fouling rate with decreasing process pressure, but not a linear relationship between the experimental method and theoretical calculation. A similar result is obtained from the HTRF method of monitoring fouling rate, see Figure 9.1 in Appendix C.

The results from analyzing the low level oxygen runs in the same manner are however inconclusive, see Figure 9.2 and Figure 9.3 in Appendix C. This is mainly because the low oxygen level in combination with a high pressure resulted in nil fouling rate calculated from the drying phenomena. The experimental fouling rate was also very inconsistent and followed no reliable pattern with varying pressure.

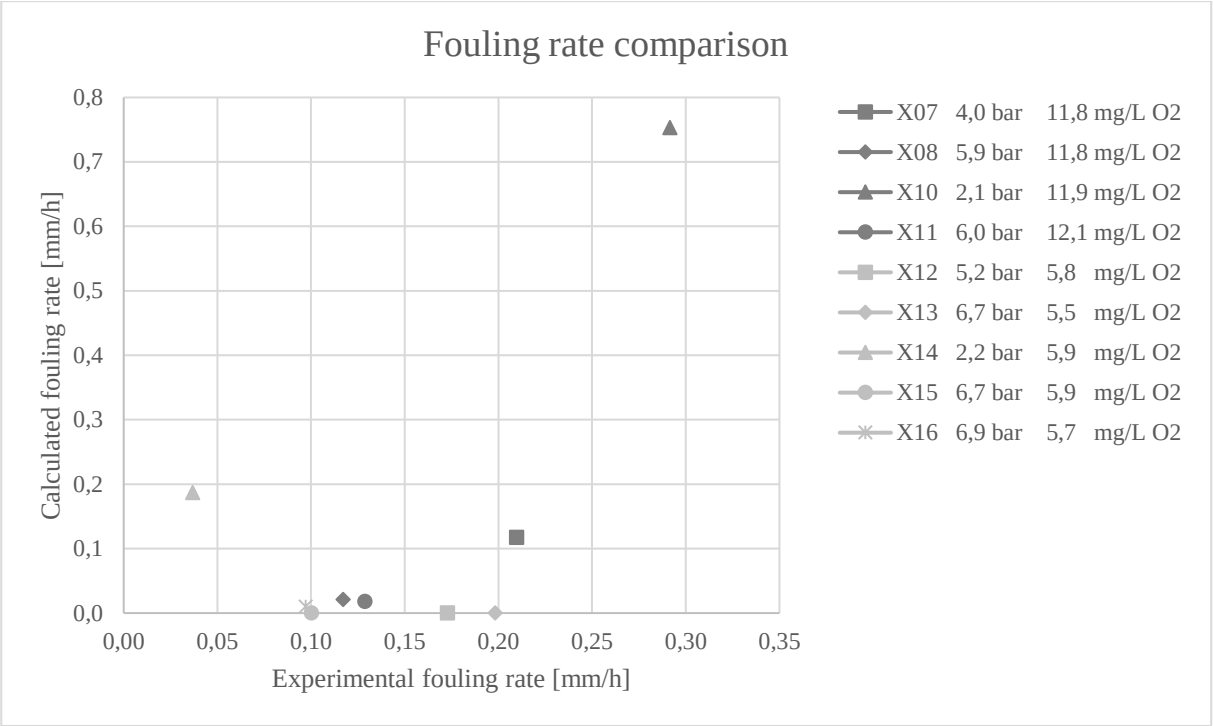

Figure 4.7. Experimental fouling rate (initial) versus calculated fouling rate for all runs.

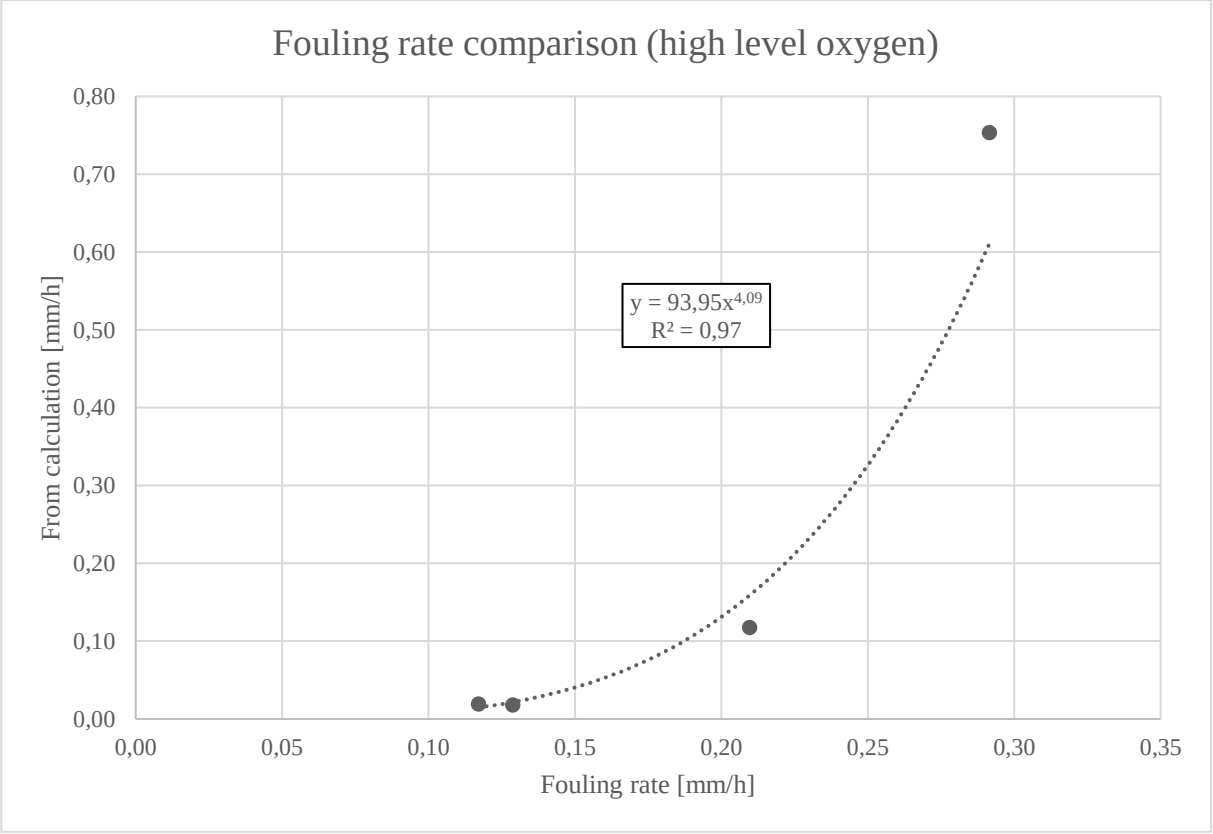

Figure 4.8. Experimental fouling rate (initial) versus calculated fouling rate for the runs with high oxygen level. With runs starting from left: X08, X11, X07 & X10

4.4 Induction period

Analyzing the defined induction period from each run and comparing with the calculated fouling rate should result in an opposite pattern than above. An increased pressure should increase the induction period if the hypothesis is right. In Figure 4.9 the relation between calculated fouling rate and induction period for each run is shown. Comparing between experimental sets, the induction period is generally longer for the low level oxygen runs.

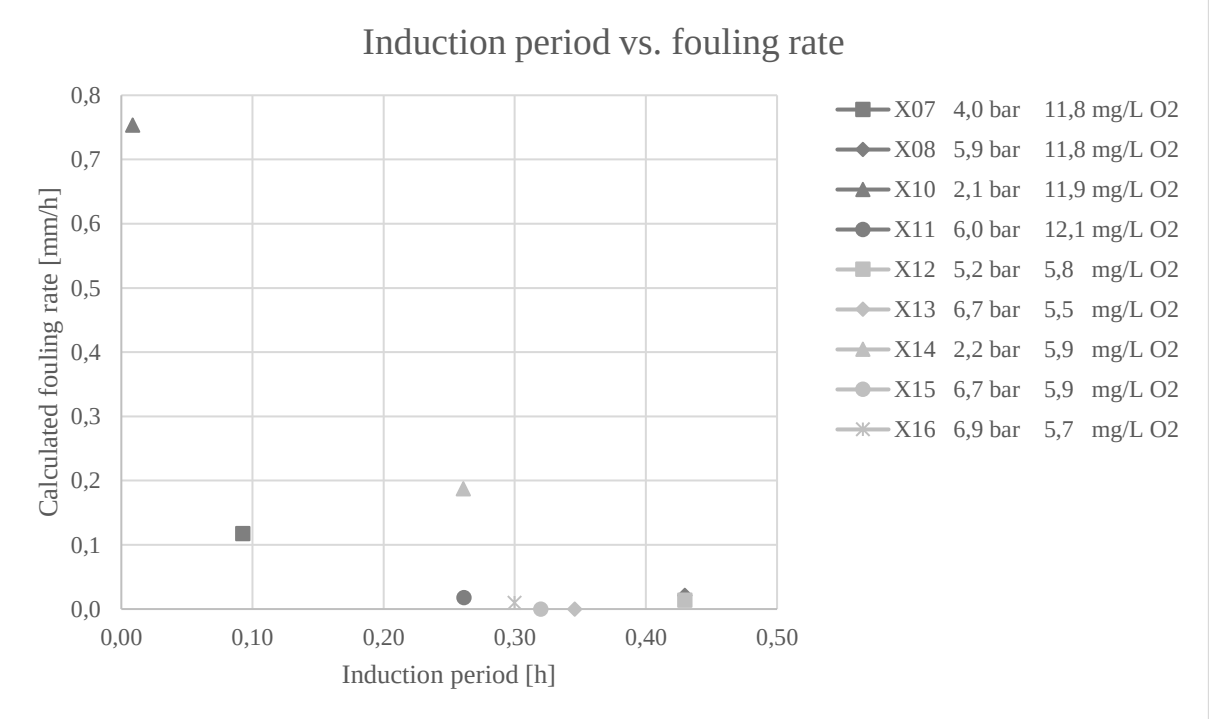

Figure 4.9. Induction period defined from the differential pressure method versus the calculated fouling rate for all runs.

If again, the experimental sets are divided, it is easier to analyze within the same oxygen level. In Figure 4.10 the runs with high oxygen level are shown in the same view as Figure 4.9 with a trendline fitted, the correlation is good. With increased pressure the induction period is longer. The behavior of following a power expression well is reasonable. When decreasing the pressure very much the fouling starts to form immediately, thus a non-existing induction period. When increasing the pressure, the induction period is prolonged but only until a limit where it cannot be longer or another fouling phenomenon starts. Figure 4.11 is identical to Figure 4.10 but with a logarithmic scale on the axes. The same graphs but with the induction period defined from the HTRF method can be seen in Figure 9.4 and Figure 9.5 in Appendix C. The behavior obtained for the high oxygen level runs could not be found for the low level oxygen runs, the induction period was very similar in time and followed no pattern pressure wise, see Figure 9.6 and Figure 9.7 in Appendix C.

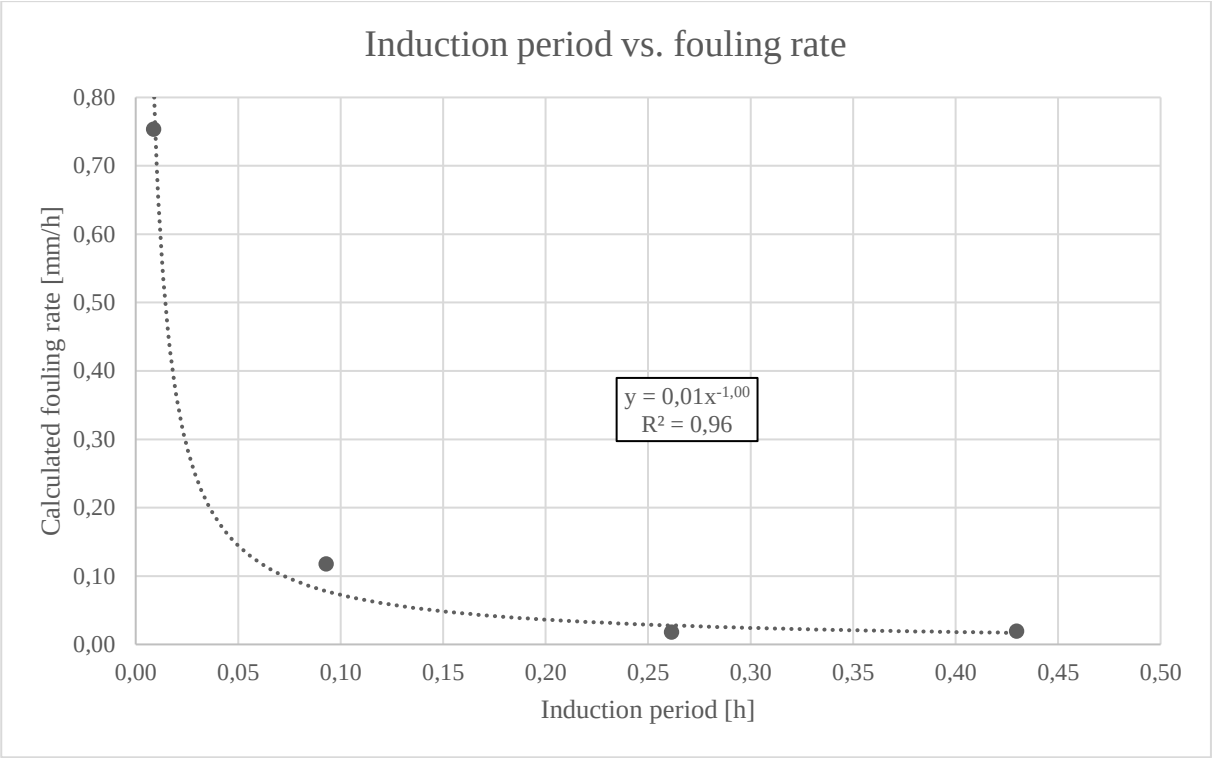

Figure 4.10. Induction period defined from the differential pressure method versus the calculated fouling rate for the high level oxygen runs. With runs starting from left: X10, X07, X11 & X08.

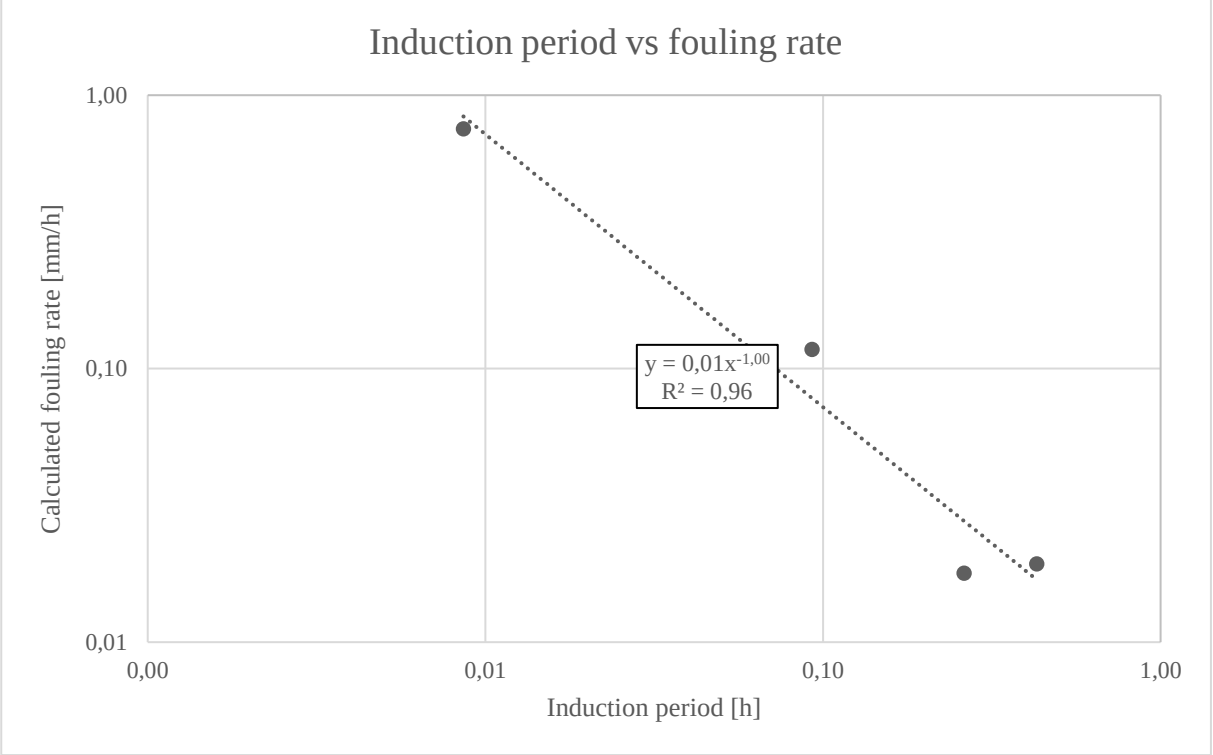

Figure 4.11. Induction period defined from the differential pressure method versus the calculated fouling rate for the high level oxygen runs with logarithmic scale axes. With runs starting from left: X10, X07, X11 & X08.

4.5 Comparison between fouling monitoring methods

The analyzed results consist of graphs originating from both the differential pressure measurements and heat transfer measurements. The method chosen to visualize is not a matter of choosing the best result matching the hypothesis at all time but more consequence of saving space in the report. All graphs are present in Appendix C for analysis. A comparison of the initial fouling rate and initial HTRF rate is shown in Figure 4.12. A good linear correlation can be seen. For the overall fouling rate the correlation is not as good, which is expected from discussions above, the correlation can be seen in Figure 9.8 in Appendix C. The correlation between the induction period obtained from the two methods is also a good linear regression. Generally, the HTRF method seem to indicate a slightly shorter induction period, see Figure 4.13.

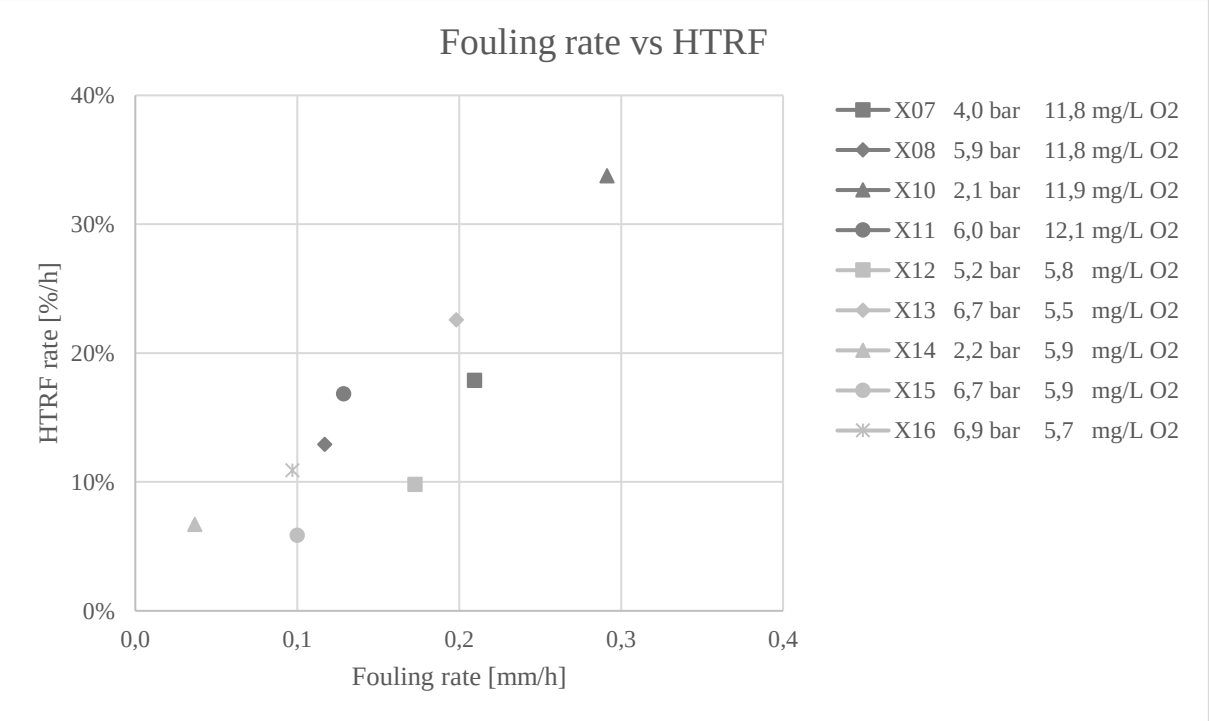

Figure 4.12. Comparison between the initial fouling rate and initial HTRF rate. The correlation is good.

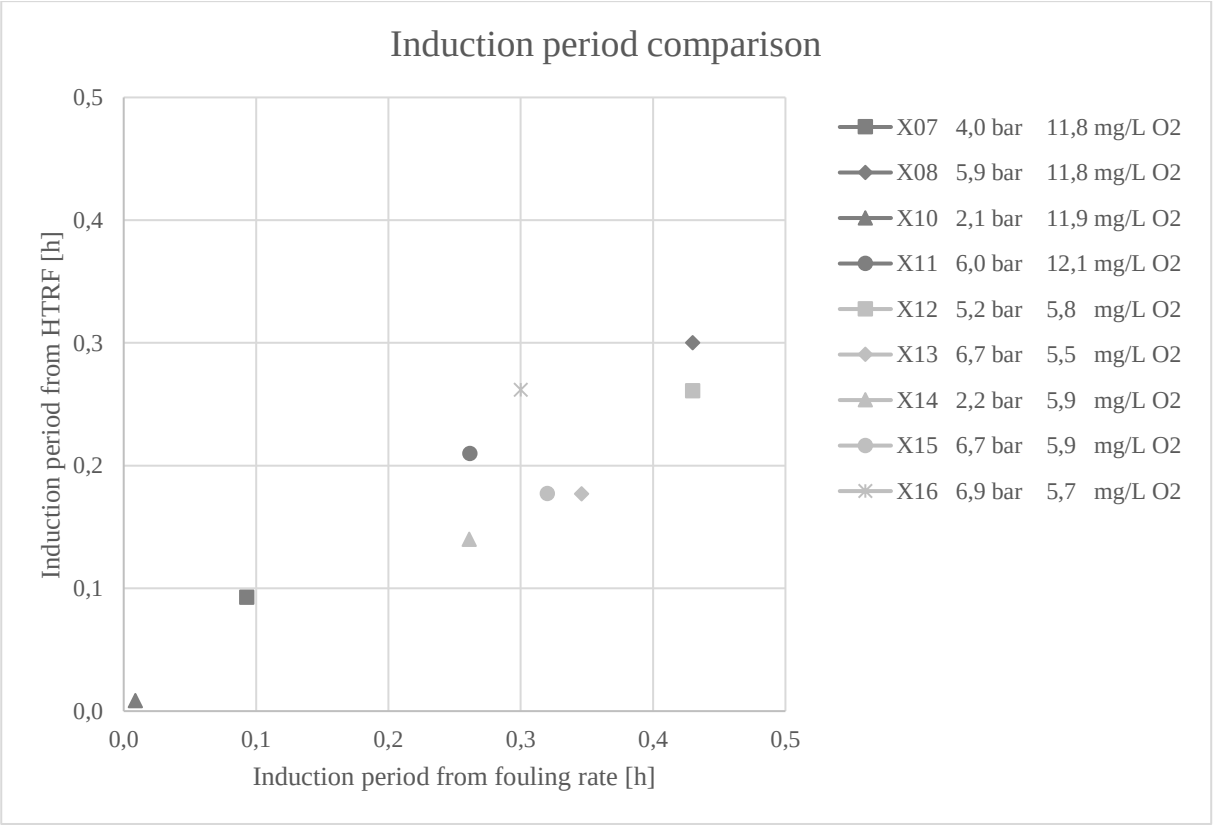

Figure 4.13. Comparison between the induction period for both fouling monitoring methods

5 Discussion

5.1 Results from runs

The initial thoughts which arose from the early analysis of Figure 4.1-Figure 4.6 seem to be correct with the deeper analysis in mind performed in Figure 4.7-Figure 4.11. The use of the drying calculation tool had its pros and cons. The correlation obtained in Figure 4.8 matches the data good but optimally it would be a linear 1:1 correlation. There is probably a nonlinear phenomenon in reality which is lost in an assumption and not taken into consideration in the model. Another nonlinear behavior was obtained regarding induction period in Figure 4.10 which however, is not very strange. The comparison was between a calculated fouling rate (mm/h) and an induction period (h).

In the experimental plan section, the topic of keeping variables not examined constant was brought up which turns the light towards the variable of changing the dissolved oxygen level. This was done by changing the product temperature which is known to alter conditions in milk. The high oxygen level runs were cooled which probably is not a problem as long as the milk is not contaminated. For the low level runs the milk was stored at around 50 °C for sometimes over an hour. The time perspective was a necessity for the milk to reach equilibrium and oxygen level tests were taken continually. Thinking that the milk was affected by this treatment is not impossible. Tracing this treatment to the inconclusive results for the low level runs is not at obvious, but still possible.

It is also a possibility to think that the limit for bubble nucleation was reached. The drying calculations regarding the low oxygen level experiments indicated that the oxygen level was so low and the pressure so high that no bubble nucleation was present. If this is true in reality is uncertain, but the runs fouled eventually anyway. Maybe the drying fouling phenomenon was limited and another fouling phenomena entered in its place. In general, the results originating from the runs with high oxygen level were more reliable and conclusive.

5.2 Monitoring methods

It was shown that dividing the fouling rate into the initial and total was a good decision. It was known from the beginning that the fouling layer would be overestimated from calculations with time as the surface turns from smooth to fouled. The results from the initial fouling rate showed consistency for some runs (mainly high oxygen) while the total fouling rate showed no consistency. A reason for this could be a local analysis on a longer phenomenon. If the inclination of the total fouling rate is determined by a local peak or valley in the graph, the analysis could be based on false premises. Another source of error is the fluctuating fouling and HTRF curves.

The use of two methods for studying the build-up of fouling was positive. Some aspects of the phenomenon were caught by one method and some by the other. Some differences occurred but generally they showed the same results. An interesting part of the differences is the temporary peaks and valleys of the fouling and HTRF curves. In Figure 5.1 the fouling layer development is shown for X11 with small peaks at around 0,6 and 0,85 hours. In Figure 5.2 the HTRF development is shown for the same run with peaks at around 0,45 and 0,75 and a valley at around 0,85. The temporary peaks in the fouling layer curve could be explained by fouling coming off. If a tube is temporarily blocked the differential pressure would rise until maybe the blockade

falls of and the differential pressure falls again. This example would affect the HTRF less since only a small section of the pipe is blocked which does not affect the overall heat transfer which takes place all over the pipe.

If the fouling is evenly distributed the differential pressure and heat transfer would be affected more to the same degree. If the air bubble phenomenon is present, one can also envision bubbles on the surface. Air bubbles probably limit the heat transfer, due to the insulating properties of air, and maybe the differential pressure less.

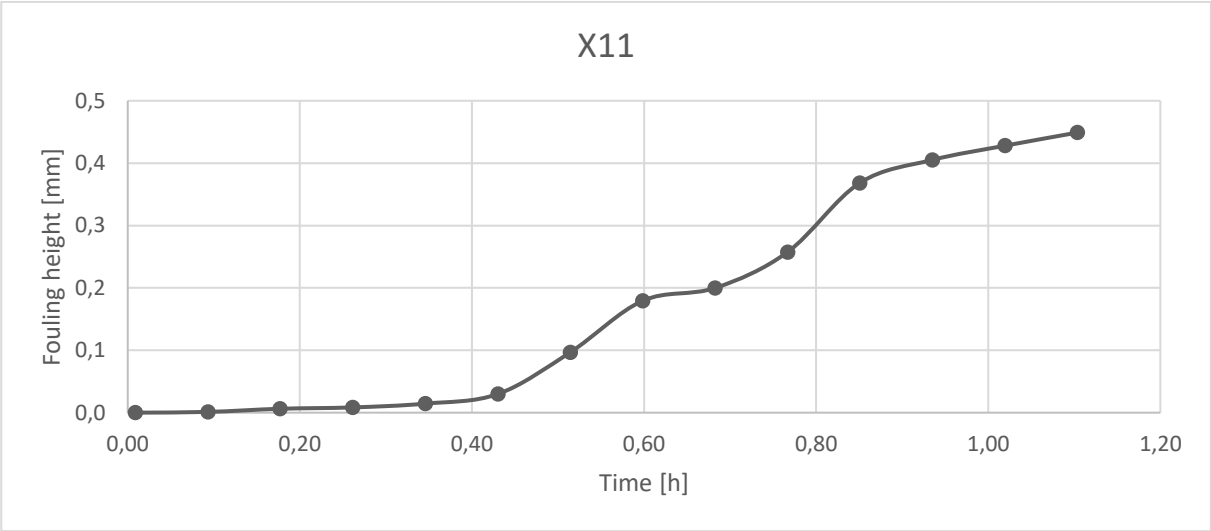

Figure 5.1. The fouling layer development over time for run X11

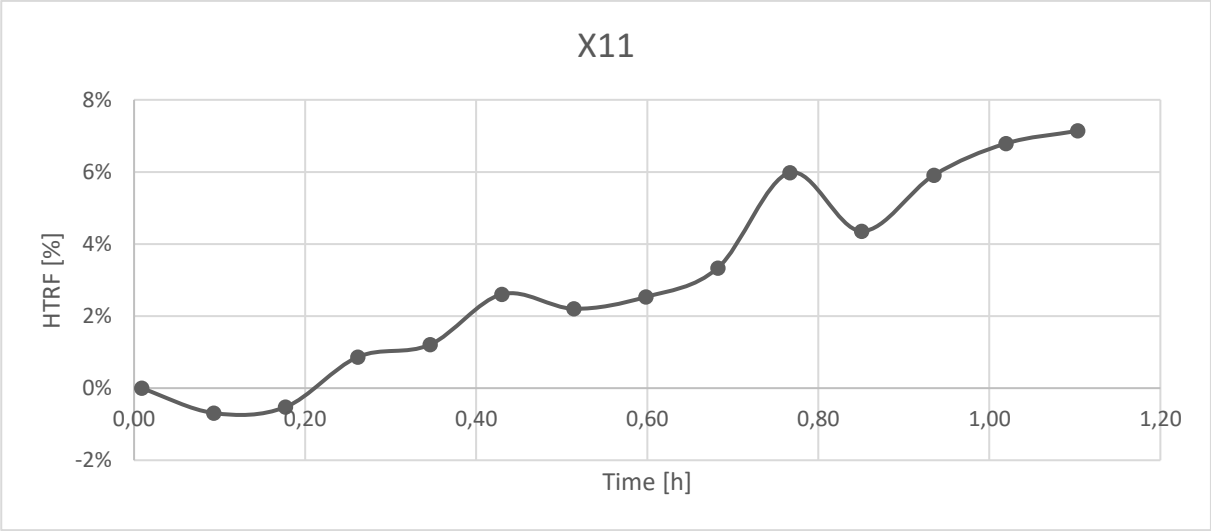

Figure 5.2. The HTRF development over time for run X11

Generally the temporary increase in heat transfer performance (mentioned in Theory, Fouling, Formation) can be seen as a pattern throughout all runs. The behavior can be seen up to 0,2 hours in Figure 5.2.

5.3 Direct fouling measurements

In an early stage of the project it was planned to measure the fouling manually. One option was to measure the fouling height with a sliding caliper or to analyze photographs taken post run. Photographs were taken on the end of the tube, see Figure 5.3, but after a few runs it was determined as a solution hard to implement. The reason can be seen in Figure 5.4, the hot water entered a few centimeters into the tube at (A) and the surface measure shown in Figure 5.3 is located at (B). The fouling layer displayed in the photograph would thus not correspond to the fouling layer inside the tube. Another risk was also the creation of a thicker layer due to the gasket acting as a slight obstruction in the flow path in the tube coupling.

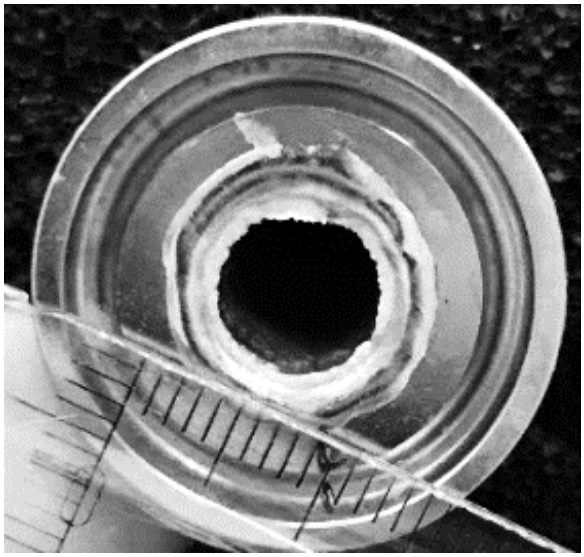

Figure 5.3. The end of a heat exchanger tube in the final heating section with the fouling on the inner surface of the tube.

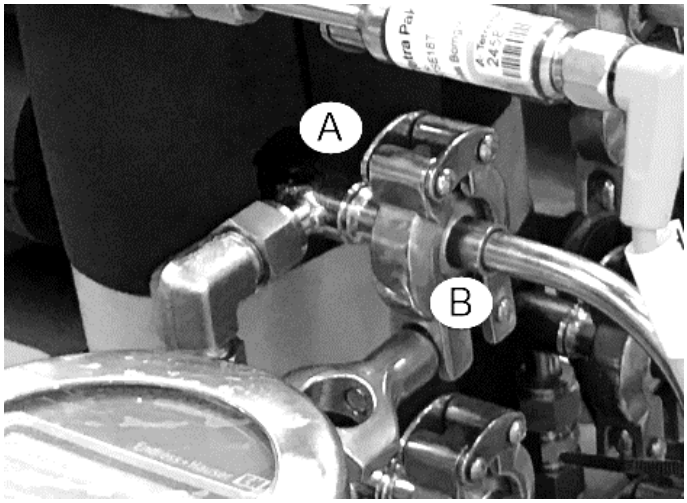

Figure 5.4. The configuration of hot water inlet to the outer tube at (A) and the opening for the product tube with clamp at (B).

6 Conclusions

To summarize, the aim of the project was to mainly analyze the phenomenon of bubble induced fouling in a UHT perspective and partly to validate the drying calculations developed in the calculation tool. Right from the start a trade-off to reduce the temperature program to 120 °C limited the UHT perspective. Some limitations both timewise and from the machine pushed the project in a direction of not obtaining complete fulfillment of the project goals.

The results from the project points in two directions, one indicating that air has a big impact on the fouling evolution and in the opposite direction. The runs with high dissolved oxygen content had both a longer induction period and decreased initial fouling rate with an increased pressure. These two factors result in a decreased fouling height at a given time with increased pressure.

The runs with low dissolved oxygen level had inconclusive results. The induction period was very similar in time and the fouling rate showed no particular pattern at varying pressure. Either the milk was processed somehow by the pretreatment or a limit was reached where the air bubble phenomenon no longer was the main fouling process. Regarding the influence of varying oxygen level in the inlet, an increased level resulted in generally earlier induction periods, comparing at similar pressures, and thus an increased fouling height at a given time.

Neither the wall temperature or flow velocity was varied in this project but the parameters are thought to affect the fouling tendency. The fouling tendency is shown to be increased with:

- Decreased process pressure
- Increased oxygen level

The drying calculations came in handy for several analyses but seemed to miss a nonlinear behavior shown from the experimental data.

6.1 Future work

If more time had been dedicated to the project more runs would have been conducted. Partly to fill in the middle ground gap in the experimental plan, which leaves a lot of questions, and partly for the replicability of the results. Having, as in some places, only one run to represent a box in the experimental plan is not optimal. One should probably work with pressure instead of temperature to adjust the dissolved oxygen content in the milk since some issues with the results originated from this method.

If the results from further work is more conclusive and reliable, the trials should be brought into UHT perspective to gain more knowledge about high temperature air bubble fouling. If this is to be done on the Armfield, some other variable has to be changed to the worse as a trade-off. It would also be interesting to analyze the fouling matter to see what type of fouling it is and the contents of it.

The calculations must be revisited and adjusted to match empirical data. Gases like carbon dioxide and argon could be included in the model. They are present in the atmosphere in a lower level but has different solubilities than oxygen and nitrogen.

7 Notations

Table 7.1. Latin letter symbols

A	m^2	Area
c_p	$J\ kg^{-1}\ K$	Heat capacity
d	m	Diameter
d_h	m	Hydraulic diameter
f	$-$	Friction factor
g	$m\ s^{-2}$	Gravitational acceleration
(g)	$-$	Gauge pressure
HT	s	Holding time
h	m	Height
k	$W\ m^{-2}K^{-1}$	Overall heat transfer coefficient
L	m	Length of tube
$\dot{m}$	$kg\ s^{-1}$	Mass flow rate
PHE	$-$	Plate heat exchanger
p	Pa	Pressure
R	$m^2K\ W^{-1}$	Heat transfer resistance
Re	$-$	Reynolds number
T	$°C\ /\ K$	Temperature
THE	$-$	Tubular heat exchanger
TS	$-$	Total solids
$\dot{V}$	h^{-1}	Volumetric flow rate
v	$m\ s^{-1}$	Local velocity
$\bar{v}$	$m\ s^{-1}$	Mean velocity
$wt\%$	$g\ (100g)^{-1}$	Weight percentage
Q	W	Heat load

Table 7.2. Greek letter symbols

α	$W\ m^{-2}\ K^{-1}$	Heat transfer coefficient fluid
Δ	$-$	Difference
δ	m	Thickness of HE wall
η	$-$	Correction factor
λ	$W\ m^{-1}\ K^{-1}$	Heat conductivity
μ	$Pa\ s$	Dynamic viscosity
ρ	$kg\ m^{-3}$	Density

Table 7.3. Subscript symbols

0	–	At time=0, initial state
b	–	Bulk
f	–	Fouling layer
HC	–	Holding cell
HE	–	Heat exchanger
i	–	Fluid index
in	–	Inlet
inn	–	Inner
L	–	Logarithmic mean
o	–	Outer
out	–	Outlet
t	–	At time t
tr	–	Transition
$tube$	–	Heat exchanger tube
w	–	Wall

8 Bibliography

[1] "Food Safety - Raw Milk Dangers," Centers for Disease Control and Prevention, 15 June 2017. [Online]. Available: https://www.cdc.gov/foodsafety/rawmilk/raw-milk-questions-and-answers.html. [Accessed 29 November 2017].

[2] G. Bylund, Dairy Processing Handbook, 3rd ed., Lund: Tetra Pak Processing Systems AB, 2015.

[3] "Wikipedia - Fouling," Wikimedia Foundation Inc, 4 October 2017. [Online]. Available: https://en.wikipedia.org/wiki/Fouling. [Accessed 30 November 2017].

[4] H. Burton, "Reviews of the progress of Dairy Science - Section G. Deposits from whole milk in heat treatment plant - a review and discussion," *Journal of Dairy Research,* vol. 35, no. 2, pp. 317-330, 1968.

[5] T. J. M. Jeurnink, P. Walstra and C. G. de Kruif, "Mechanisms of fouling in dairy processing," *Netherlands Milk & Dairy Journal,* vol. 50, pp. 407-426, 1996.

[6] B. Bansal and X. D. Chen, "A Critical Review of Milk Fouling in Heat Exchangers," *CRFSFS: Comprehensive Reviews in Food Science and Food Safety,* vol. 5, pp. 27-33, 2006.

[7] T. J. M. Jeurnink, "Fouling of heat exchangers by fresh and reconstituted milk and the influence of air bubbles," *Milchwissenschaft,* vol. 50, no. 4, pp. 189-193, 1995.

[8] H. A. E. Bennett, "Aspects of Fouling in Dairy Processing," Massey University, Palmerston North, 2007.

[9] T. Skoglund, "Fouling dependancy of air - DR0030228," Tetra Pak Processing Systems AB, Lund, 2016.

[10] M. Sprunk, S. Nöbel and J. Hinrichs, "Versuchsaufbau zur beschleunigten Bildung von Fouling aus Magermilchkonzentrat/ Experimental Setup for Increased Formation of Fouling from Skim Milk Concentrate," *Chemie Ingenieur Technik,* vol. 86, no. 8, pp. 1223-1229, 2014.

[11] R. Jost, "Ullman's Encyclopedia of Industrial Chemistry - Milk and Dairy Products," Wiley-VCH Verlag GmbH & Co. KGaA, 15 July 2007. [Online]. Available: http://onlinelibrary.wiley.com/doi/10.1002/14356007.a16_589.pub3/abstract. [Accessed 14 December 2017].

[12] A. M. Helmenstine, "What is the Acidity or pH of Milk?," ThoughtCo, 11 June 2017. [Online]. Available: https://www.thoughtco.com/what-is-the-ph-of-milk-603652. [Accessed 15 December 2017].

[13] M. Alveteg, Handbook - physical properties, correlations and equations in chemical engineering, Lund: Department of Chemical Engineering, Faculty of Engineering, Lund Univeristy, 2013.

[14] The Editors of Cncyclopedia Britannica, "Physics - Conservation of energy," Encyclopedia Britannica, Inc, 21 August 2017. [Online]. Available: https://www.britannica.com/science/conservation-of-energy. [Accessed 8 December 2017].

[15] J. Daeseong, S. A.-Y. Omar, M. A. Raga'i, P. Jongchark och C. Heetaek, ”Experimental inverstigation of convective heat transfer in a narrow rectangular channel for upward and downward flows,” *Nuclear Engineering and Technology*, vol. 46, nr 2, pp. 195-206, 2014.

[16] The Editors of Encyclopedia Britannica, "Physics - Laminar flow," Encyclopedia Britannica, Inc, 9 April 2014. [Online]. Available: https://www.britannica.com/science/laminar-flow. [Accessed 6 December 2017].

[17] "Wikipedia - Epimer," Wikimedia Foundation, Inc, 18 September 2017. [Online]. Available: https://en.wikipedia.org/wiki/Epimer. [Accessed 12 December 2017].

[18] S. Adachi, "Formation of Lactulose and Tagatose from Lactose in strongly heated milk," *Nature - International journal of science*, vol. 181, pp. 840-841, 1958.

[19] E. Wallhäußer, M. Hussein and T. Becker, "Detection methods of fouling in heat exchangers in the food industry," *Food Control*, vol. 27, pp. 1-10, 2012.

[20] S. Prakash, O. Kravchuk and H. Deeth, "Influence of pre-heat temperature, pre-heat holding time and high-heat temperature on fouling of reconstituted skim milk during UHT processing," *Journal of Food Engineering*, vol. 153, pp. 45-52, 2015.

[21] J. J. Machado, J. A. Coutinho and E. A. Macedo, "Solid-liquid equilibrium of alpha-lactose in ethanol/water," *Fluid Phase Equilibria*, vol. 173, pp. 121-134, 2000.

[22] P. de Jong, "Impact and Control of fouling in milk processing," *Trends in Food Science & Technology*, vol. 8, pp. 401-405, 1997.

[23] H. Burton, "Chapter 10 - Fouling of Heat Exchangers," in *Ultra-high-temperature processing of milk and milk products*, Shinfield, Reading, Springer US, 1988, pp. 292-309.

[24] R. W. Bell and C. F. Sanders, "Prevention of milkstone formation in a high-temperature-short-time heater by preheating milk, skim milk and whey," *Journal of Dairy Science,* vol. 27, no. 6, pp. 499-504, 1944.

[25] S. D. Changani, M. T. Belmar-Beiny and P. J. Fryer, "Engineering and Chemical Factors Associated with Fouling and Cleaning in Milk Processing," *Experimental, Thermal and Fluid Science,* vol. 14, pp. 392-406, 1997.

[26] T. R. Bott, Fouling handbook, Rugby: Inst of Chemical Engineers, 1990.

[27] N. Memisi, S. Veskovic Moracanin, M. Milijasevic, J. Babic and D. Djukic, "CIP cleaning processes in the dairy industry," *Procedia Food Science,* vol. 5, pp. 184-186, 2015.

[28] M. C. Georgiadis, G. E. Rotstein and S. Macchietto, "Optimal Design and Operation of Heat Exchangers under Milk Fouling," *American Institute of Chemical Engineers (AIChE) - Bioengineering, Food and Natural Products,* vol. 44, no. 9, pp. 2099-2111, 1998.

[29] A. Andrys, L. Hamberg och A. U. Grundelius, ”In-line measurement of fouling build-up - theory and calculations. DR0024630,” Tetra Pak Processing Systems, Lund, 2009.

[30] S.-E. Mörtstedt och G. Hellsten, Data och diagram, Värme- och kyltekniska tabeller i SI-enheter, Stockholm: Norstedts Tryckeri, 2nd edition, 1975.

[31] ”Wikipedia - Darcy friction factor formulae,” Wikimedia Foundation, Inc, 22 January 2018. [Online]. Available: https://en.wikipedia.org/wiki/Darcy_friction_factor_formulae. [Använd 24 January 2018].

[32] Armfield Limited, *Modular UHT/HTST Heat Exchanger Processing System FT174X - Instruction Manual Issue 15,* 2016.

[33] "Stainless Steel - Grade 316," AZO Materials, [Online]. Available: https://www.azom.com/properties.aspx?ArticleID=863. [Accessed 31 January 2018].

[34] Endress+Hauser People for Process Automation, ”Technical Information Memosens COS81D,” [Online]. Available: https://portal.endress.com/wa001/dla/5001068/9333/000/01/TI01201CEN_0217.pdf. [Använd 12 April 2018].

9 Appendices

9.1 Appendix A – P&ID

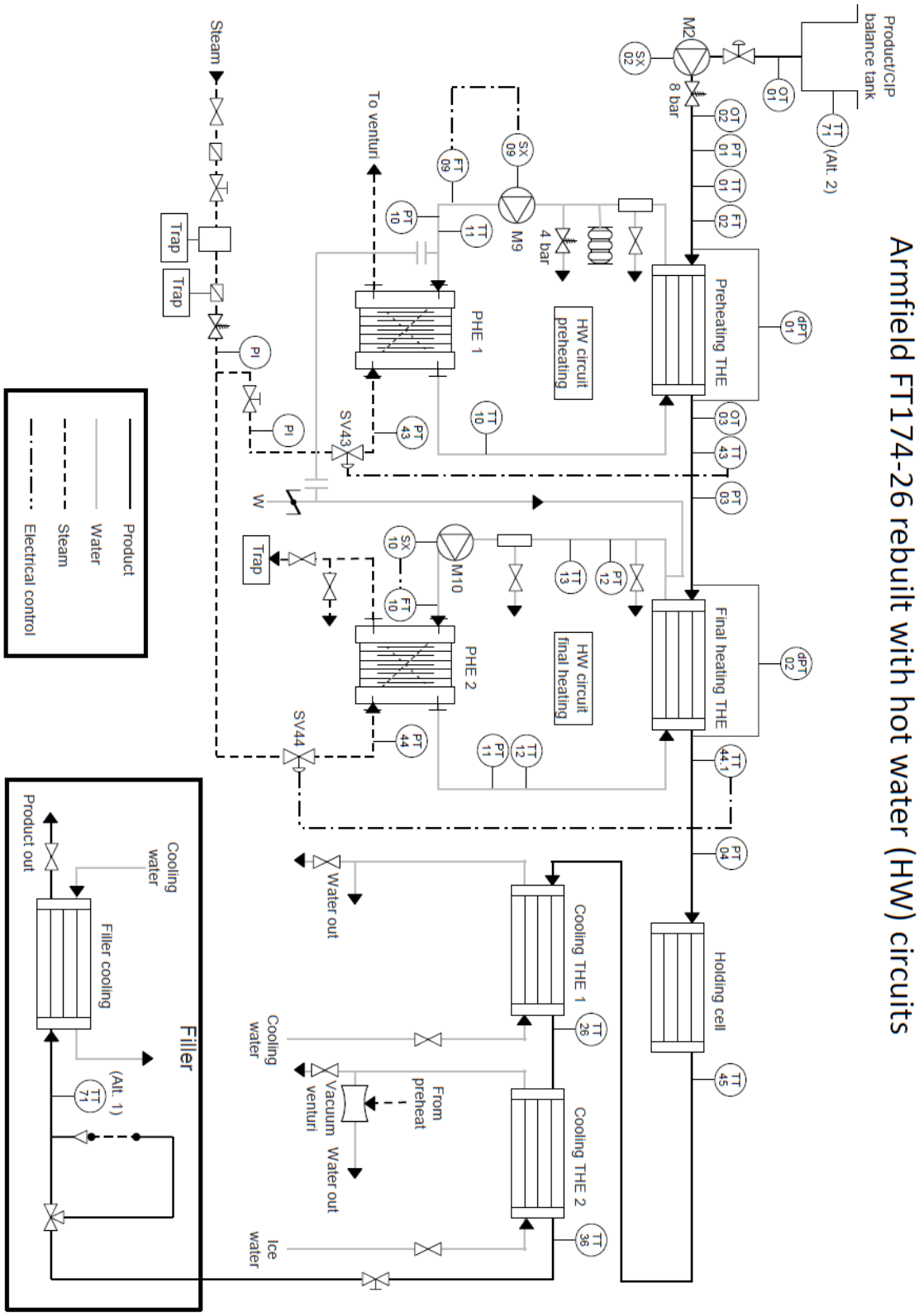

9.2 Appendix B – Start up protocol

9.2.1 Processing

1. Turn on the power to the machine which starts the software.
2. Press “On” on the start screen of the software to initiate the program.
3. Check that the heat exchanger and all flow paths are configured correctly according to the mode of operation (indirect heating). Follow the product from inlet to outlet.
4. Check that the steam on the media side is configured correctly according to the mode of operation (indirect heating).
5. Check that all media connections to the machine are open (deionized water, pressurized air for pneumatic valves, steam, cooling water, ice water)
6. Enter mode of operation in HMI (Sterilization, Process, CIP). If CIP see instructions below. Sterilization not used in project, thus no instructions at hand.
7. Enter a low product flow (~30 l/h) through HMI and start the process with water.
8. Let it run for a while and check so that the water exits in outlet, no leaks are present and all air collected in the system has escaped.
9. Enter desired product flow and increase the process pressure with the back pressure valve. Make sure nut is screwed tight
10. Enter desired temperature program and flow in hot water circuits and start heating.
11. Check steam pressure from pipeline and set desired steam pressure with the steam reducing valves
12. Let machine reach steady state, check deviation from set points in “Dev” tab with desired settings.
13. Check that steam valves not are fully open (~50% open is good for handling unexpected events).
14. Chose logging settings and chose variables to log.
15. Open valve on product inlet to let product reach the outlet
16. Close the valve and mount the product pipe to the product pump.
17. Switch to product processing in HMI, start logging when machine is filled with product.
18. Process product for desired time
19. When finished, switch to water inlet
20. Turn off heat and let machine cool down

9.2.2 CIP

1. Follow “Processing” until step 6
2. Machine has predefined flow and temperature profile regarding CIP.
3. No back pressure needed since below 100 °C
4. Rinse machine with fresh water going to drain for ~10 minutes.
5. Move outlet to balance tank and start water circulation by switching to “product” inlet.
6. Add NaOH and circulate for ~20 minutes
7. Switch to fresh water inlet and empty machine of NaOH and dirt for ~10 minutes, move outlet to drain.
8. Move outlet to balance tank and start water circulation by switching to “product” inlet
9. Add HNO_3 and circulate for ~20 minutes
10. Switch to fresh water inlet and empty machine of HNO_3 and dirt for ~10 minutes, move outlet to drain.
11. Turn off heat and let machine cool down

For further information see Armfield instruction manual [32]

9.3 Appendix C - Figures

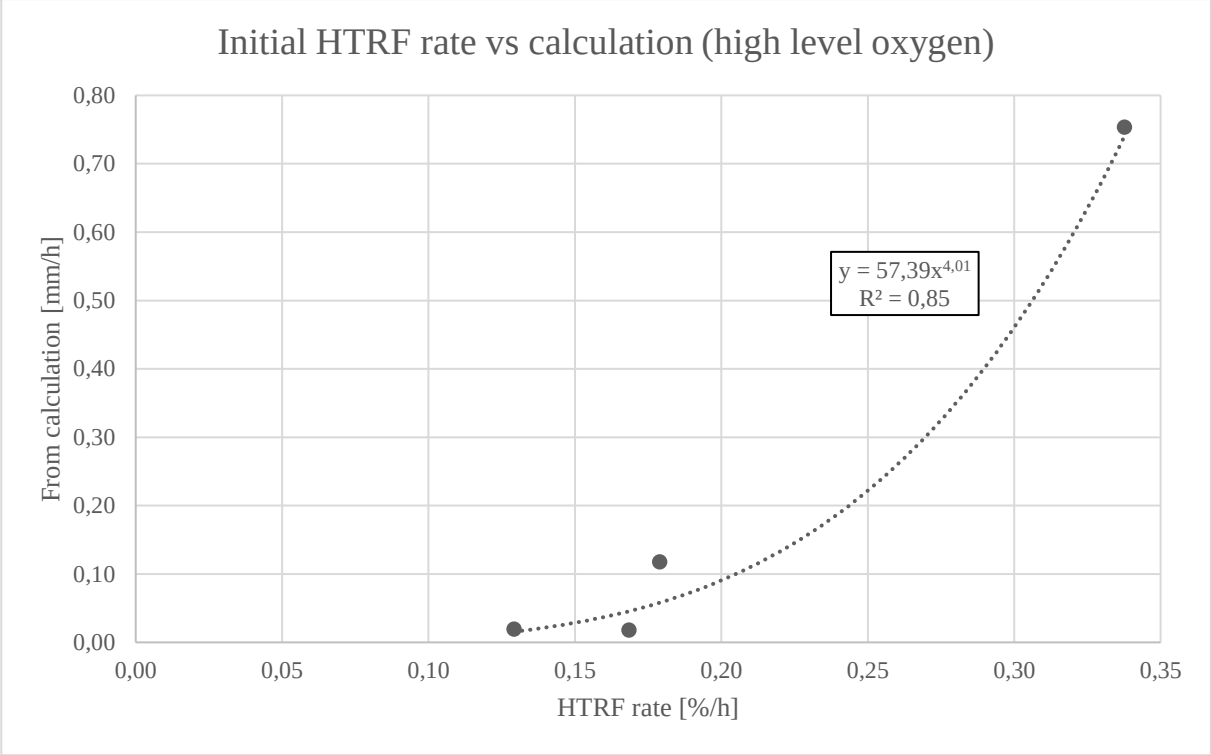

Figure 9.1. The initial HTRF rate versus the calculated fouling rate for the high level oxygen runs. Runs starting from left: X08, X11, X07 & X10.

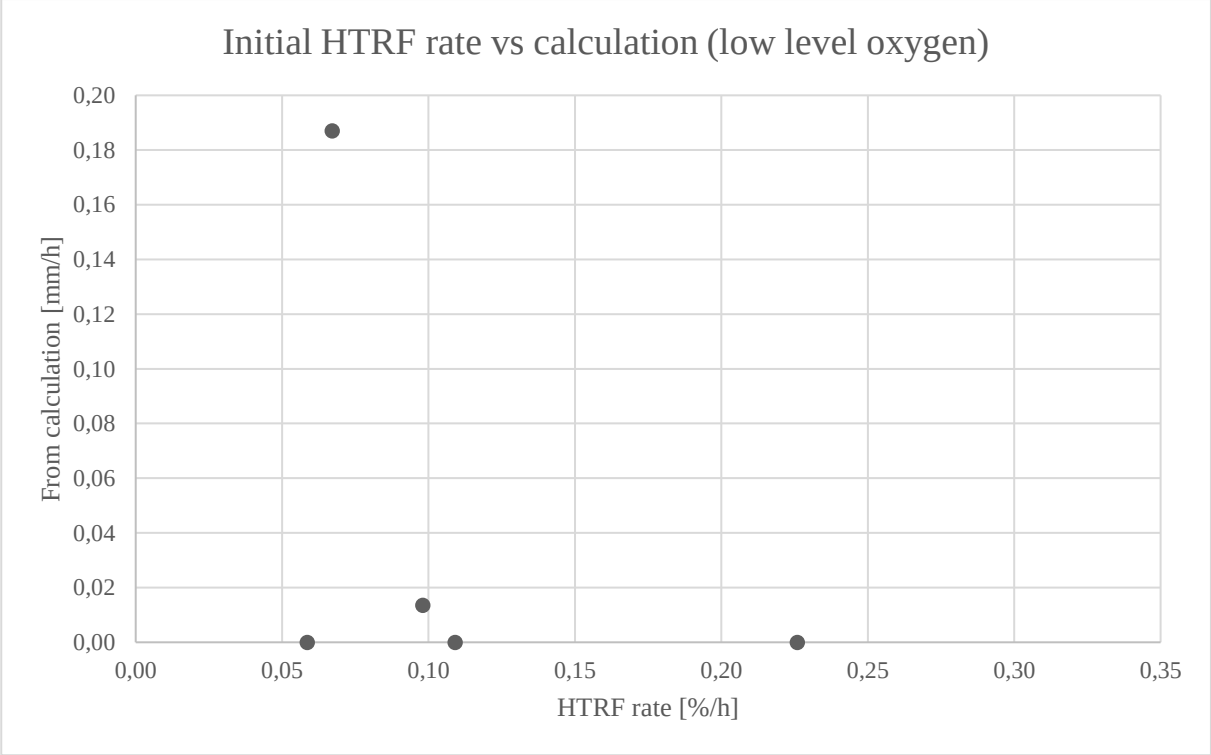

Figure 9.2. The initial HTRF rate versus the calculated fouling rate for the low level oxygen runs. Runs starting from left: X15, X14, X12, X16 & X13.

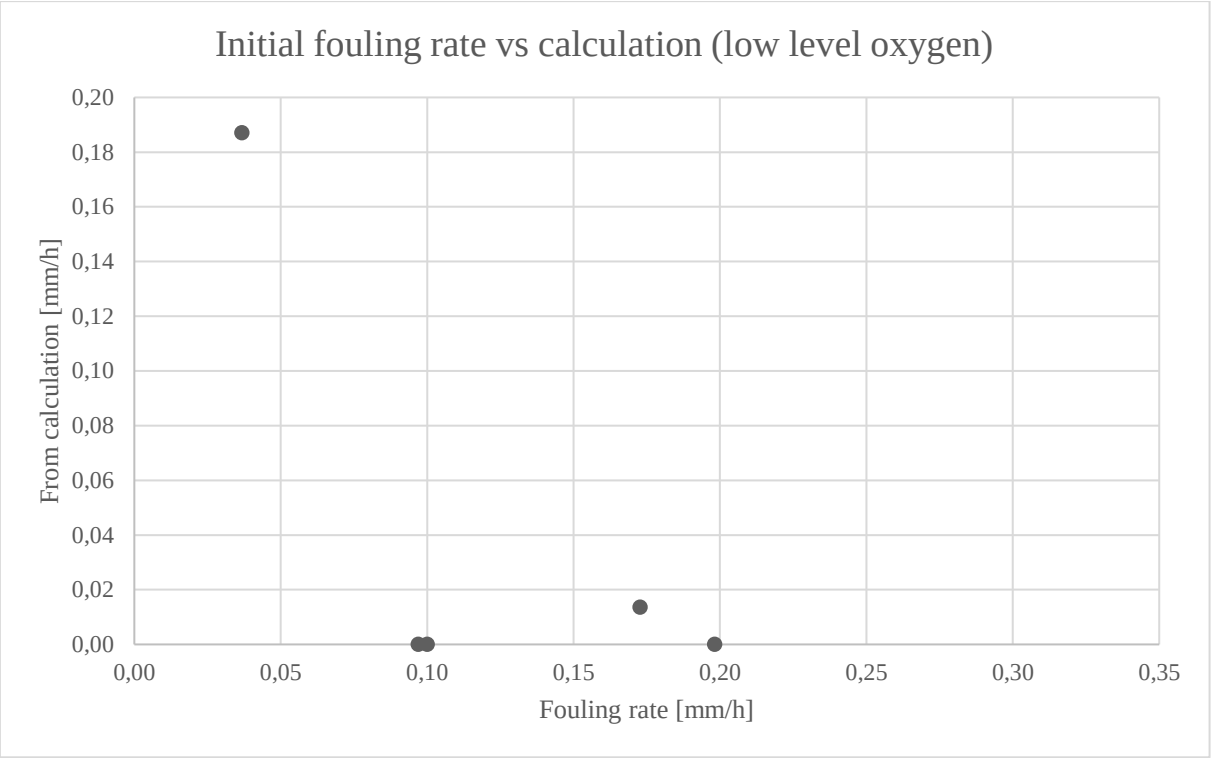

Figure 9.3. The initial fouling rate versus the calculated fouling rate for the low level oxygen runs. Runs starting from left: X14, X16, X15, X12 & X13

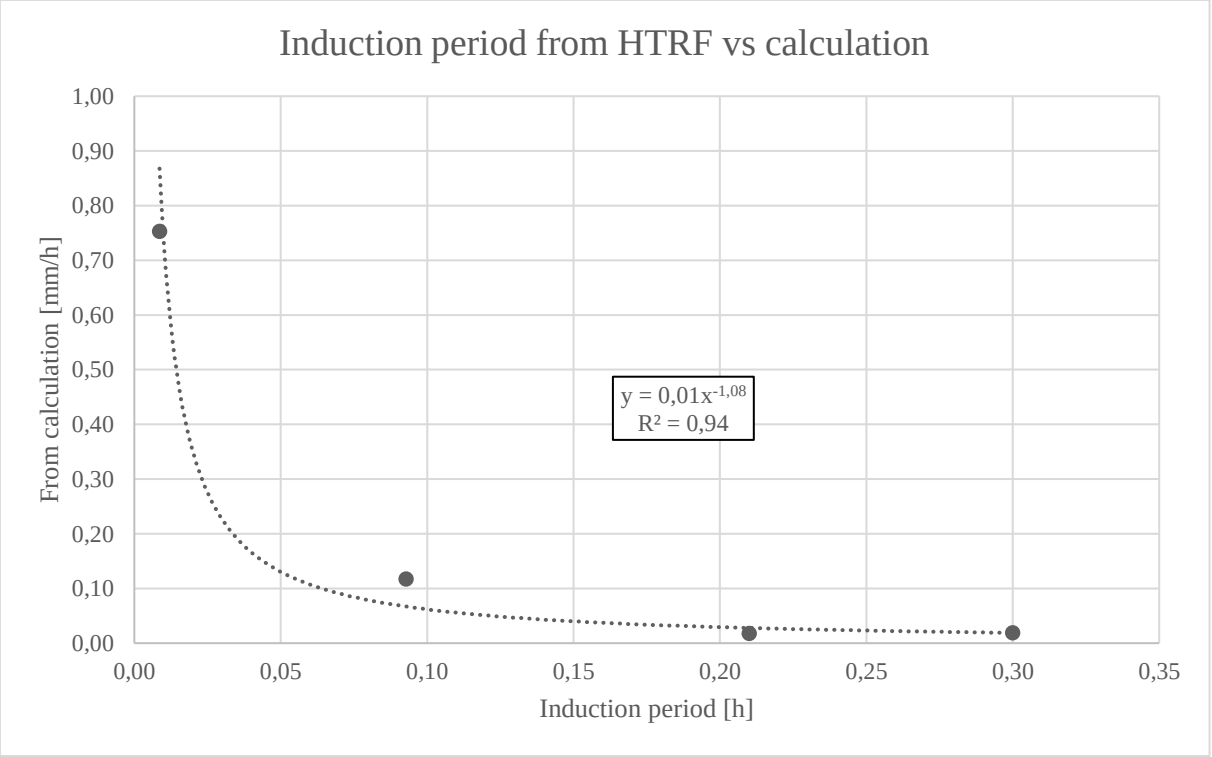

Figure 9.4. The defined induction period from the HTRF method versus the calculated fouling rate for the high level oxygen runs. Runs starting from left: X10, X07, X11 & X08.

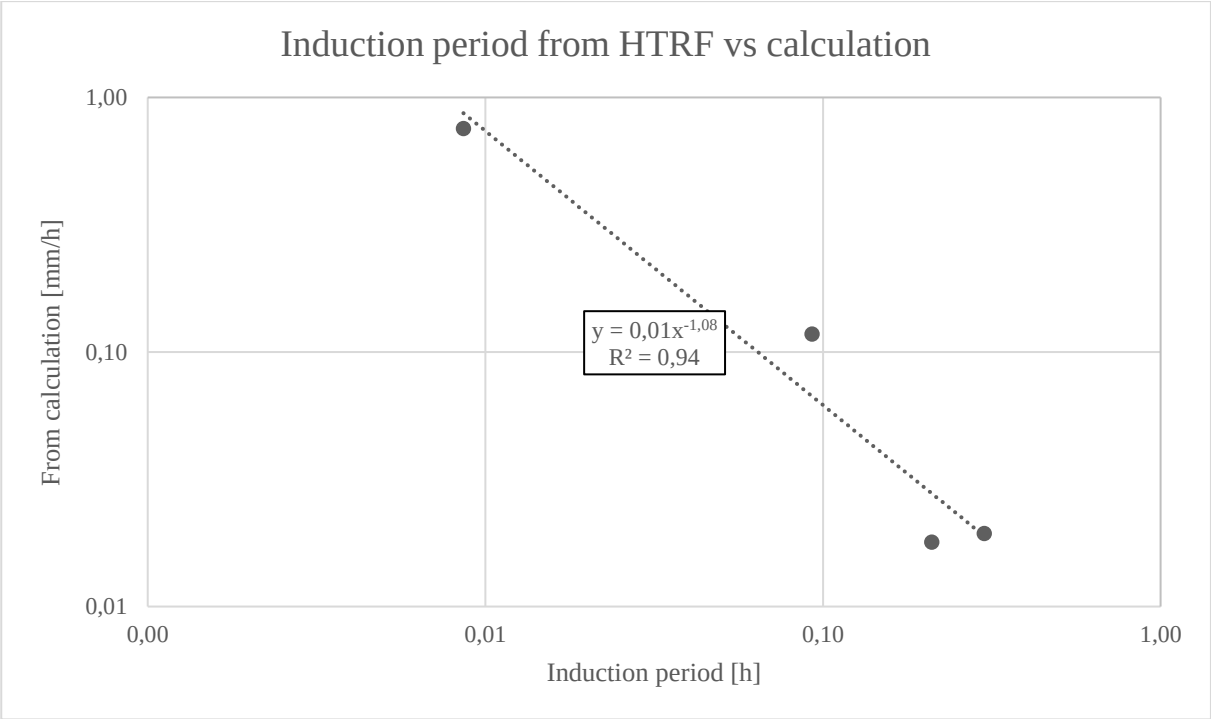

Figure 9.5. The defined induction period from the HTRF method versus the calculated fouling rate for the high level oxygen runs, with logarithmic scale on the axes. Runs starting from left: X10, X07, X11 & X08.

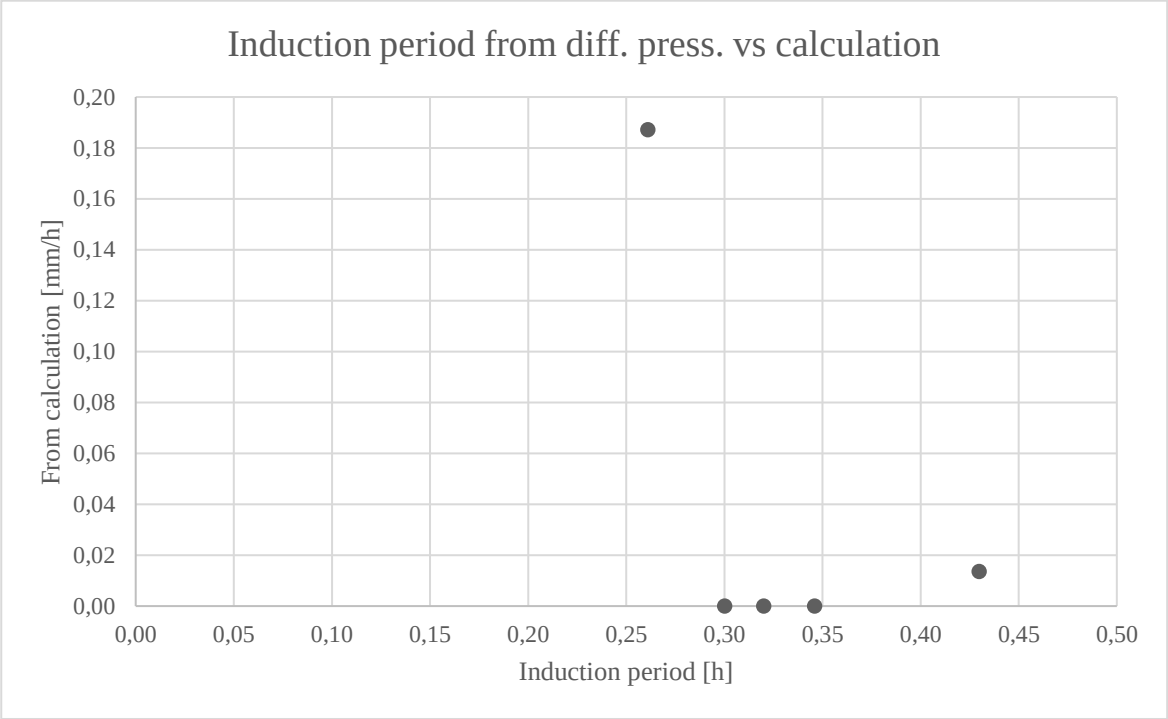

Figure 9.6. The defined induction period from the differential pressure method versus the calculated fouling rate for the low level oxygen runs. Runs starting from left: X14, X16, X15, X13 & X12.

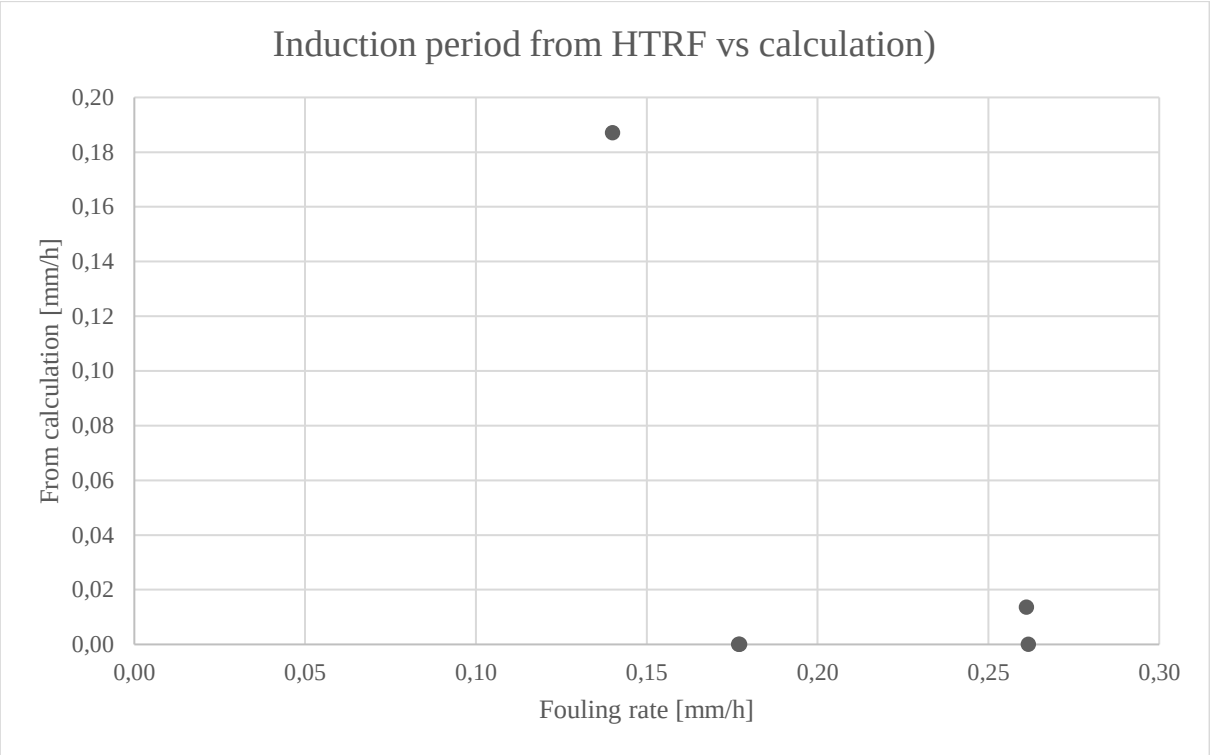

Figure 9.7. The defined induction period from the HTRF method versus the calculated fouling rate for the low level oxygen runs. Runs starting from left: X14, X15 & X13 (same position), X12 & X16.

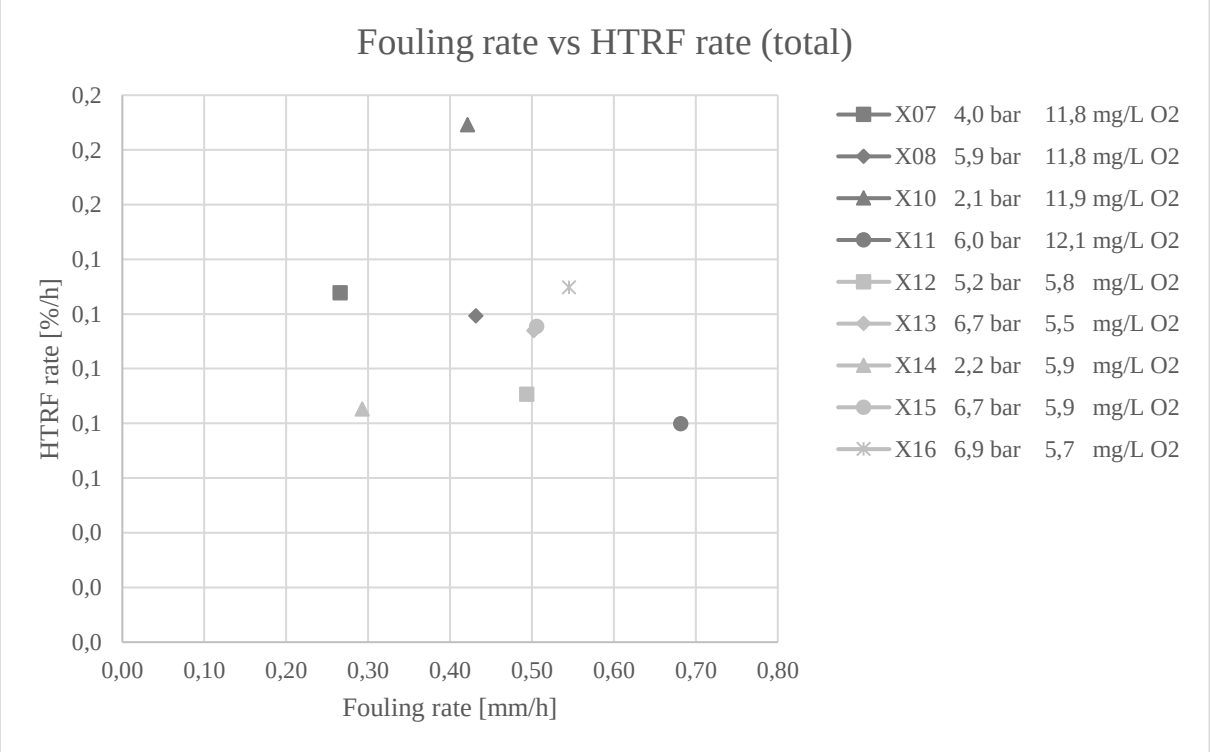

Figure 9.8. The correlation between the total experimental fouling rate and experimental HTRF rate.